Displacement Ventilation

theory and design

Nielsen, Peter Vilhelm

Publication date:
1993

Document Version
Publisher's PDF, also known as Version of record

DISPLACEMENT VENTILATION

- theory and design

Peter V. Nielsen
Aalborg University

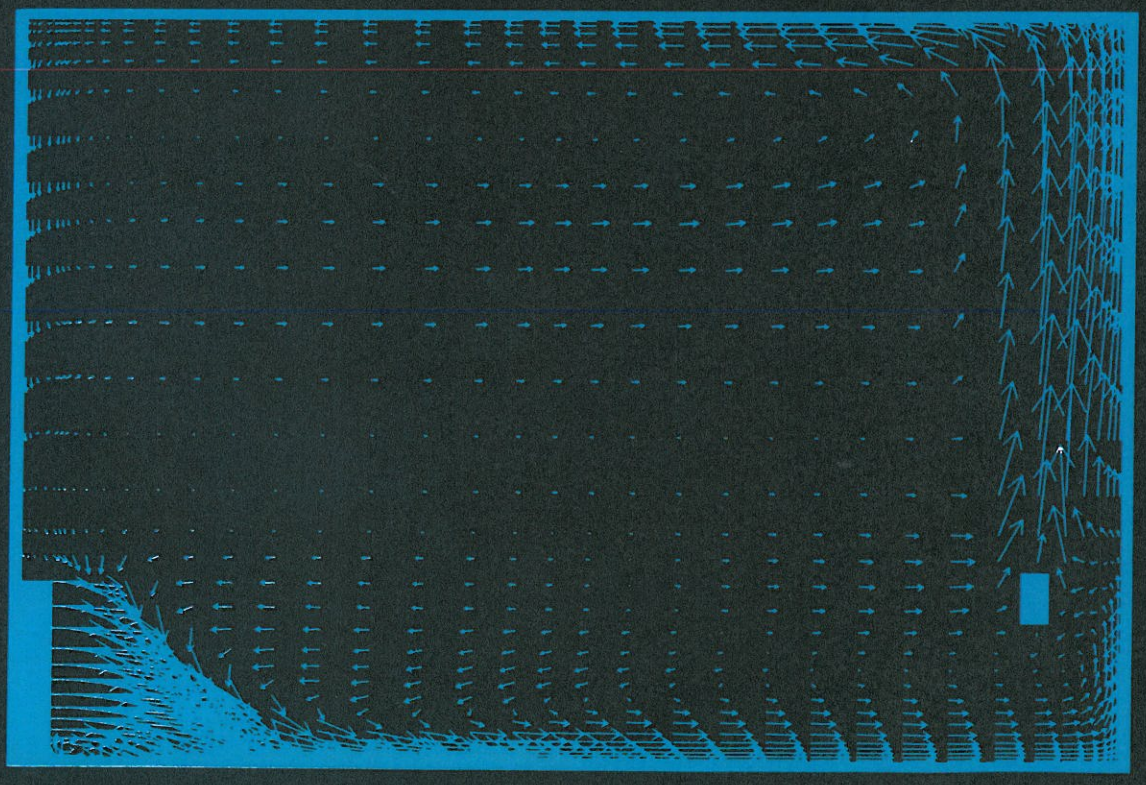

DISPLACEMENT VENTILATION
- theory and design

Peter V. Nielsen

Department of Building Technology and Structural Engineering, Aalborg University

August 1993

ISSN 0902-8002 U9306

PREFACE

Displacement ventilation is an interesting new type of air distribution principle which should be considered in connection with design of comfort ventilation in both small and large spaces.

Research activities on displacement ventilation are large all over the world and new knowledge of design methods appears continuously. This book gives an easy introduction to the basis of displacement ventilation and the chapters are written in the order which is used in a design procedure. The main text is extended by five appendices which show some of the new research activities taking place at Aalborg University.

The book has arisen from a short course of postgraduate lectures delivered by the author at Aalborg University. It is written for students as well as for engineers for example within system design and product development.

I will like to thank Peter Kofoed and Torsten V. Jacobsen for their support as co-authors of two appendices, Ingrid Christensen for the preparation of drawings and Bente Kjærgaard for the typing of the text.

Peter V. Nielsen

Aalborg University
August 1993

CONTENTS

1. INTRODUCTION

For many years buoyancy driven displacement ventilation has been used in industrial areas with high thermal load as for example in hot process buildings in the steel industry. The displacement ventilation system has also grown popular during the last ten years as comfort ventilation in rooms with low thermal loads as e.g. in offices. Some main features of displacement ventilation are the possibility of creating both high temperature effectiveness and high ventilation effectiveness. The supply openings are located at a low level in case of displacement ventilation and the air flows direct into the occupied zone. Free convection from heat sources creates a vertical air movement in the room and the heated air is removed by return openings located in the ceiling or just below the ceiling. It is thus the free convection or the buoyancy which controls the flow in the room while the momentum flux from the diffusers is low and without any practical importance for the general flow in the room.

A vertical temperature gradient will arise in a room with displacement ventilation due to the vertical flow of heat to the ceiling region. It is therefore possible to remove exhaust air from the room with temperatures which are several degrees above the temperature in the occupied zone. This allows an efficient use of energy because the supply temperature can be higher than the supply temperature in case of mixing ventilation. It is, on the other hand, necessary to use a higher air flow rate in displacement ventilation to obtain a large volume in the occupied zone with fresh air and to avoid too low temperatures in the occupied zone. This will lead to a duct system which is slightly larger than the duct system used in connection with mixing ventilation.

Displacement ventilation is only used in case of cooling. It can be used as a fresh air supply system combined with a radiator heating system in cases with heating demand.

A displacement ventilation system can have high ventilation effectiveness if the sources are both heat and contaminant sources. The vertical temperature gradient implies that fresh and contaminant air are separated and the most contaminated air can be found above the occupied zone.

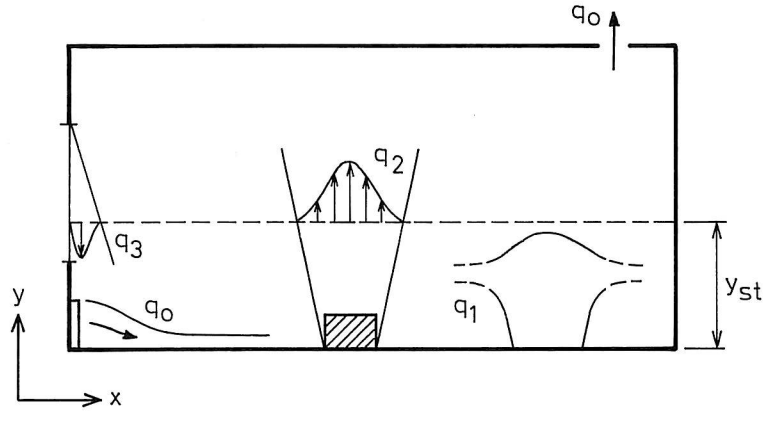

Figure 1. Room with displacement flow and natural convection.

Figure 1 shows the main principle of displacement ventilation. The airflow q_o is supplied direct into the occupied zone at low velocity from a wall-mounted diffuser. The plumes from hot surfaces, from equipment and from persons entrain air from the surroundings in an upward movement, and cold downdraft may transport air down into the occupied zone. A stratification will take place in a height where the flow $q_2 - q_3$ is equal to q_o in the situation shown in figure 1.

The design of a displacement ventilation system involves the calculation of the vertical flow in plumes from different heat sources. The stratification height is determined from the supply flow rate and the generated height of fresh air should be comparable with the height of the occupied zone. It is possible to estimate the vertical temperature gradient in the room. This gradient is important for thermal comfort due to the temperature difference between height of the legs and height of the head and due to radiation from the ceiling.

The diffuser can either be a wall-mounted low velocity diffuser or it can be floor-mounted diffusers. The flow from a wall-mounted diffuser moves downward to the floor due to gravity and it flows through the room in a thin layer which is typical of stratified flow, see figure 1. The flow along the floor is the only air movement which influences the comfort of the occupants and it is therefore important to have a design procedure which can support the selection of diffusers. Floor-mounted diffusers generate a high entrainment close to the openings. They should therefore mainly be distributed in secondary areas of the occupied zone.

The following chapters are arranged in the order which is used in a practical design procedure:

2. Free convection flow

3. Stratification height and concentration distribution

4. Temperature distribution

5. Velocity distribution in the occupied zone

Thermal flow from heat sources and cold surfaces can be treated independent of other flows in the room. The flow is for example independent of the stratified flow along the floor and it is often supposed to be independent of the vertical temperature gradient, although some influence is present as shown in the next chapter. A practical design procedure for displacement ventilation is often based on this simplified theory. A detailed description of the air distribution can only be achieved by full-scale experiments /1/ or by numerical prediction of the air movement as shown in references /2 and 3/.

The primary flow in a room with displacement ventilation expresses the similarity which is typical of fully turbulent flow. Vertical temperature gradients, velocity level in stratified flow at the floor, stratification level and ventilation effectiveness can all be described by an Archimedes' number independent of the velocity level in the room /4/. The Archimedes number is defined as

$$Ar = \frac{\beta g H \Delta T_o}{u_o^2} \tag{1}$$

where β, g and ΔT_o are volume expansion coefficient, gravitational acceleration and temperature difference between return and supply flows, respectively. u_o is the supply velocity and H is a characteristic height which e.g. can be the room height or the height of the wall-mounted air terminal device.

2. FREE CONVECTION FLOW

The driving force in free convection is the buoyancy effect on heated air in the room. Figure 1 shows as examples a plume from a concentrated heat source and a plume from a solar heated floor area as well as cold downdraft from a cold window surface.

2.1 Thermal Plumes from Heat Sources

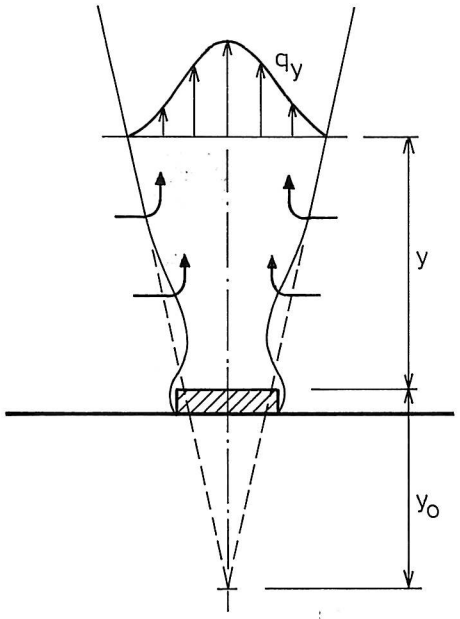

Figure 2. Free convection flow from a heat source.

Figure 2 shows the vertical flow above a heat source. The buoyancy generates a jetlike flow with a maximum velocity just above the source where the flow may expect to have a reduced diameter. Air is entrained into the plume and the width and the volume flow increase with the height.

A concentrated heat source will create a circular flow which can be expressed by

$$q_y = 0.005\ \phi_K^{1/3}\ (y + y_o)^{5/3} \qquad (2)$$

where $y + y_o$ is height above a virtual origin of the flow. q_y and ϕ_K are volume flow in the height y and the convective heat emission from the source, respectively, /5/.

Equation (2) is strictly valid for $y >> d$ where d is the hydraulic diameter of the source but practice shows that the equation can be used down to a height of $y \sim 2d - 3d$, see reference /6/, which is important because the size of a heat source often can be comparable to the height of the occupied zone.

The convective heat emission ϕ_K can be estimated from the energy consumption of the heat

source ϕ

$$\phi_K = k\phi \tag{3}$$

The level of the coefficient k is 0.7 - 0.9 for pipes and channels, 0.4 - 0.6 for smaller components and 0.3 - 0.5 for larger machines and components.

It can in practice be difficult to judge the location of the virtual origin but it is often assumed that $y_o \sim 2d$ for a concentrated source. The surface temperature distribution close to lighting or heating equipment may indicate rather large sources due to the radiation from the components.

A line source will create a two-dimensional flow which can be expressed by

$$q_y = 0.014(\frac{\phi_K}{l})^{1/3} (y + y_o)l \tag{4}$$

where l is the length of the source /7/. y_o corresponds to 1 - 2 times the width of the heat source.

A heat source in the occupied zone may also be the contaminant source in the room. Typical examples are printers in offices, welding plumes in industrial areas and people in general. The volume flow q_y is therefore the contaminated part of the flow in the room and the concentration distribution across the flow is distributed in a similar manner as in the velocity profiles indicated in figure 1.

Equations (2) and (4) are only strictly valid for homogeneous surroundings. The flow in surroundings with a vertical temperature gradient will show a decreasing velocity level compared to homogeneous surroundings because the temperature gradient will diminish the buoyancy force.

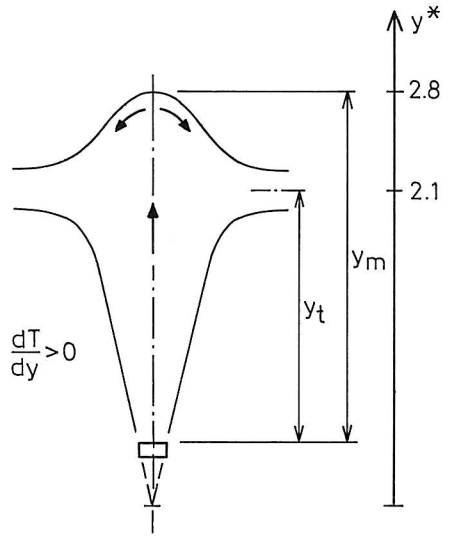

Figure 3. Vertical plume in a room with temperature gradients and stratification.

Figure 3 shows the flow from a heat source in a room with a strong temperature gradient. The flow will be buoyancy neutral in the height y_t but it will continue to the height y_m due to the momentum in the plume. The flow will finally terminate in a stratified layer at y_t.

The convective flow can be calculated from the following model given by Morton et al. /8/ and addressed by Mundt in /9/.

A dimensionless height y^* is calculated for different heights y above the source

$$y^* = 2.86(y + y_o)\frac{dT}{dy}^{3/8} \phi_K^{-1/4} \tag{5}$$

where dT/dy is the vertical temperature gradient. Figure 3 shows that only y^* values less than 2.1 are relevant to further calculations. A dimensionless parameter m is given by

$$m = 0.004 + 0.039y^* + 0.380y^{*2} - 0.062y^{*3} \tag{6}$$

and the volume flow rate in the height y^* is given by

$$q_y = 2.38 \cdot 10^{-3} \cdot m \cdot \phi_K^{3/4} \cdot \left(\frac{dT}{dy}\right)^{-5/8} \tag{7}$$

The maximum height y_m is given by equation (5) for $y^* = 2.8$

$$y_m = 0.98\phi_K^{1/4} \left(\frac{dT}{dy}\right)^{-3/8} - y_o \tag{8}$$

and the height for neutral buoyancy and stratification of the plume is given by

$$y_t = 0.74\ \phi_K^{1/4} \left(\frac{dT}{dy}\right)^{-3/8} - y_o \tag{9}$$

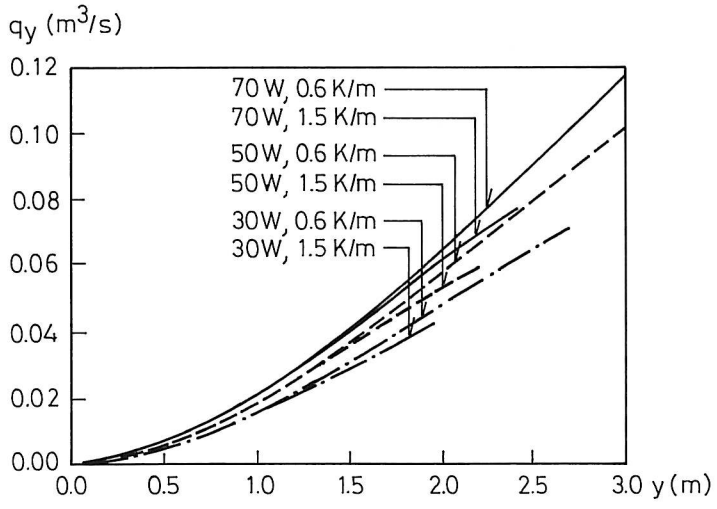

Figure 4. Free convection flow above a heat source of 30, 50 and 70 W in a room with different gradients. Reference /9/.

Figure 4 shows the flow in plumes from different sources. It is obvious that the flow rate is only moderately influenced by the temperature gradient while the maximum height y_m is strongly influenced by the temperature gradient. This is an important aspect in e.g. a workshop with welding because the welding fume will be concentrated in height y_t in case of a temperature gradient. It can therefore be concluded that the temperature gradient dT/dy should be small but, on the other hand, sufficient to create the stratification which is the background for displacement ventilation and for a clean occupied zone.

2.2 Flow above People and Components

Many practical heat sources are large compared to room dimensions and it is difficult to estimate the type of plume (circular or plane). Furthermore, it is difficult to judge the convective heat emission ϕ_K and the distance to the virtual origin y_o and it may be difficult to use the equations (2), (4) and (7) close to the equipment. A logical conclusion is to measure the volume flow above a number of typical sources in rooms as e.g. a person, office equipment, lighting equipment and catering equipment as described in the following.

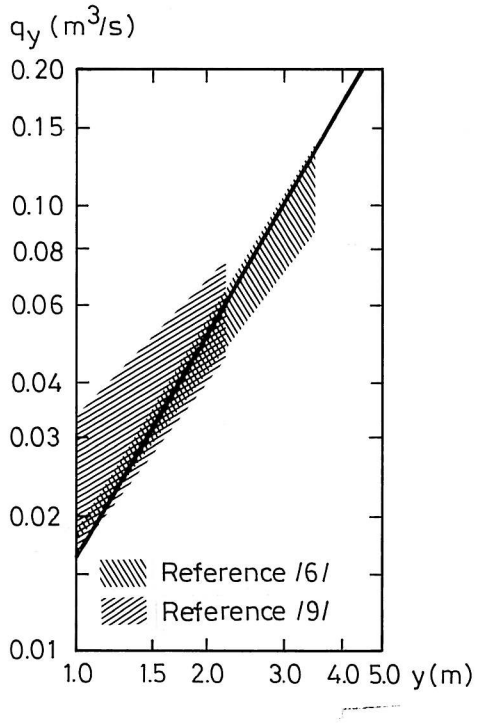

Figure 5. Free convection flow above a sedentary person. ϕ = 100 W. The height y is measured from floor level.

Figure 5 shows the flow above a source simulating a sedentary person. Measurements by Kofoed and Nielsen /6/ show influence from the vertical temperature gradient. Measurements in the upper part of the shaded area correspond to 0.09 K/m while the lower part of the area corresponds to 0.3 K/m. The measurements discussed by Mundt /9/ are a joint project between a number of manufacturers in the Scandinavian countries. The measurements are made for temperature gradients between 0.6 K/m and 1.5 K/m which are typical levels for displacement ventilation. The full-drawn line on figure 5 shows the volume flow according

to equation (2) for $k = 1/3$, $y_o = 0$ and y measured from floor level. Measurements by Fitzner /10/ show similar results as well as a strong decrease in entrainment at increasing temperature gradient. This effect is especially pronounced in heights close to neutral buoyancy.

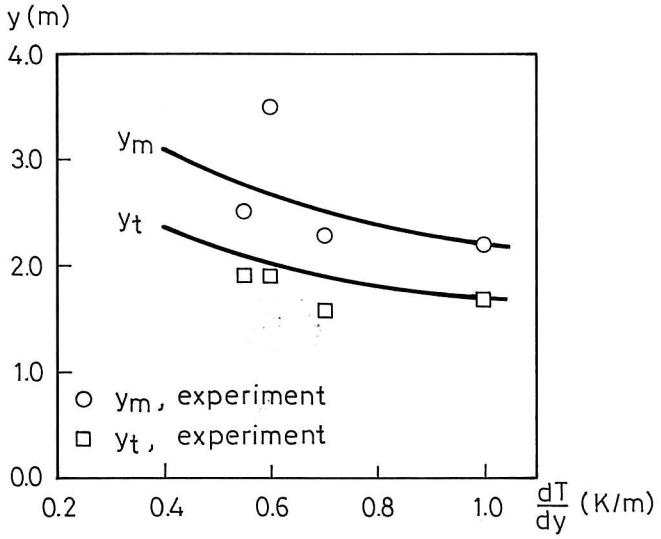

Figure 6. Maximum height and height to neutral buoyancy in a plume above a sedentary person. $\phi = 75$ W. The height y is measured from floor level $y_o = 0$ and $k = 1/3$.

Figure 6 shows measurements of maximum height and height to neutral buoyancy in a plume above a source simulating a sedentary person. y_m and y_t are also given according to equations (8) and (9).

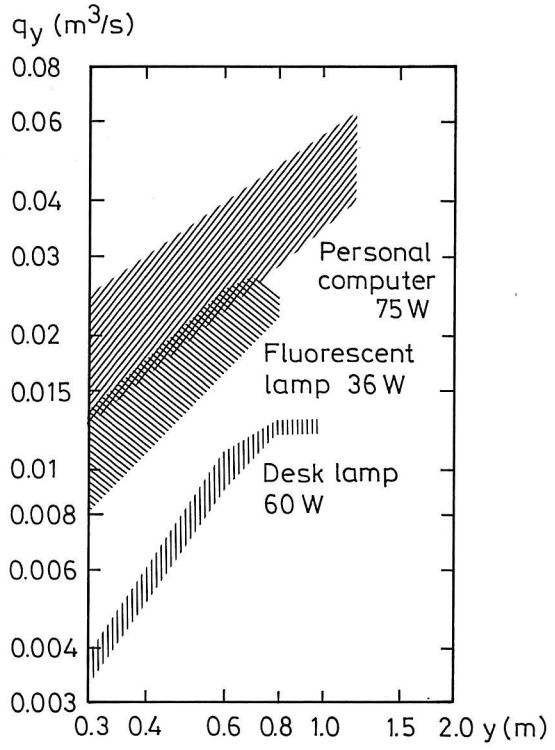

Figure 7. Free convection flow above a PC and different lamps.

Figure 7 shows the measurements given by Mundt /9/. It should be noticed that there is a large difference between the volume flow from the computer and the flow from a desk lamp, although the energy consumption ϕ is at the same level. The shaded areas show the distribution of the measurements for different temperature gradients. The height to neutral buoyancy must be found from equation (9).

2.3 Interaction between Thermal Plumes and Influence from Walls

The plume from a heat source located close to a wall may be attached to the wall due to the Coanda-effect, see figure 8A. The entrainment will be reduced compared to the entrainment in a free plume and this will influence the location of the stratification height in the room.

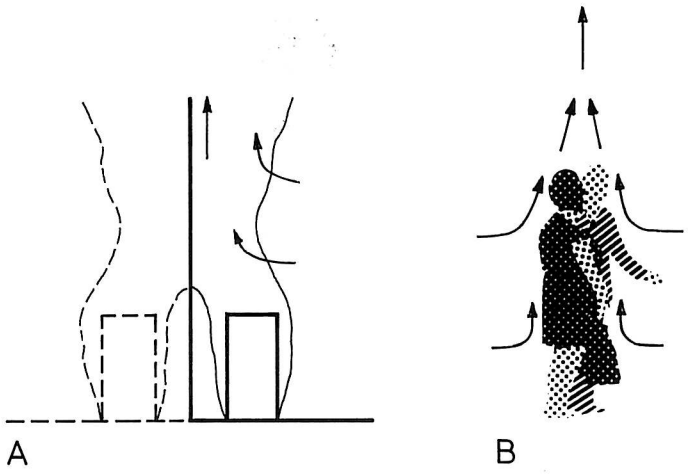

Figure 8. A) Thermal plume attached to a wall. B) Interaction between two thermal plumes.

The flow in a plume close to a wall is similar to one half of the flow in a free plume with a convective heat emission of 2 ϕ_K as indicated on the figure. The flow in the boundary layer close to the wall has a minor influence on the general air movement, and the volume flow q_{yw} in the actual plume is given from equation (2) for the heat emission of 2 ϕ_K and an entrainment of 2 q_{yw}.

$$q_{yw} = 0.0032\phi_K^{1/3}(y + y_o)^{5/3} \tag{10}$$

The equation shows that the flow rate is 63% of the flow in a free plume.

It can be shown that the flow is reduced to 40% of the flow in a free plume if the heat source is located close to a corner in the room. The flow rate q_{yc} in the plume is given from equation (2) for the heat emission of $4\phi_K$ and an entrainment of $4q_{yc}$

$$q_{yc} = 0.002\phi_K^{1/3}(y + y_o)^{5/3} \tag{11}$$

The thermal flows above a number of sources may be absorbed into one plume due to the Coanda-effect if the sources are located close to each other. The flow q_{yN} from N identical sources is given by

$$q_{yN} = N^{1/3}\, q_y \tag{12}$$

where q_y is the flow in a plume from one of the sources. The flow above the two persons on figure 8 B will therefore be 1.26 times the flow above a single person at equivalent heights. It is obvious from the equation that the flow in a merged plume from a high number of heat sources is small compared to the flow in individual plumes with sufficient space for entrainment.

Measurements in plumes close to a wall or a corner are reported by Kofoed and Nielsen /11/ and they support the assumption behind equation (10) and (11).

2.4 Thermal Flow and Cold Downdraft from Vertical Surfaces

A thermal flow will be generated close to a surface if the surface temperature is different from the air temperature.

A cold downdraft will take place at a cold surface. The air close to the surface will be cooled and it will obtain an increased density which will move the air downward due to the gravity force. Any heat loss through a vertical surface in areas with low velocities is connected with cold downdraft.

The volume flow in a cold downdraft or in a rising thermal flow close to a warm surface is given by the following equation, reference /12/

$$q_y = 2.8 \cdot 10^{-3}\, |\Delta T|^{2/5}\, y^{6/5}\, l \tag{13}$$

where q_y is the flow in the turbulent free convection boundary layer of the height y measured from the upper edge or lower edge of the surface. ΔT is the temperature difference between room temperature and surface temperature and l is the horizontal width of the surface.

Figure 1 shows a cold downdraft at a window. It appears that the volume flow q_3 will help to increase the stratification height. The flow in cold downdraft will also transport contaminant from upper zone down into the lower zone which is a problem in cases where the displacement ventilation is used for contaminant control.

The flow from cold downdraft may continue through the occupied zone causing discomfort due to the velocity of the flow. This effect will be discussed in the chapter on velocity distribution in the occupied zone.

Displacement ventilation is often connected to a large vertical temperature gradient. Heat losses may therefore take place in the upper part of the room and heat gains make likewise take place in the lower part of the room. A downward boundary layer flow will be generated in the upper part of the room and an upward flow will be generated in the lower part of the room, all with velocity levels dependent on the actual level of the heat fluxes.

3. STRATIFICATION HEIGHT AND CONCENTRATION DISTRIBUTION

It is necessary to consider both air quality and thermal comfort in a room with displacement ventilation. Air quality is an important aspect in case of contaminant emission in the room and thermal comfort is a general aspect in connection with design of a system. The air quality aspect will be considered in this chapter in connection with determination of stratification height, concentration distribution and ventilation effectiveness, and thermal comfort aspects will be considered in the last two chapters in connection with the determination of temperature distribution in the room and velocity distribution in the occupied zone.

3.1 Stratification Height

The volume flow to a room is calculated from the stratification height as explained on figure 1.

The heat source in the room in figure 1 will generate a plume. This plume will entrain a flow of q_2 up to the stratification height y_{st} which corresponds to the supply flow q_o and the cold downdraft q_3. The plume will continue above the stratification height and the entrainment in the upper zone will mix the air in this area.

The heat source in the room can also be a contaminant source. The contamination will move upward in the plume and it will mix in the upper zone. The stratification height is therefore the height of a lower zone which mainly contain fresh air from the supply system.

The supply flow rate q_o is connected to q_2 and q_3 via

$$q_o = q_2 - q_3 \tag{14}$$

where the flows q_2 and q_3 are obtained as described in the last chapter for a height which corresponds to the design value of y_{st}.

The thermal flow q_1 on figure 1 will not have any influence on the stratification height because the height to neutral buoyancy is smaller than y_{st}.

The statification height is influenced by the flow rate q_o. An increase in q_o will increase the height y_{st} because there will be more primary air in the occupied zone for entrainment into the plume. An increase of the supply air q_o will also decrease the temperature difference $T_R - T_o$ between the return and supply temperature and it is important that this difference is sufficient for the maintenance of stratification in the room.

The cold downdraft shown in figure 1 will increase the stratification height and it will also make a transport of contaminant from the upper zone into the room down into the lower zone.

Displacement ventilation requires a height volume flow rate to the room. Figure 5 indicates that the basic ventilation requirement of 0.01 m^3/s per person will maintain a stratification level of about 0.75 m and this height is hardly sufficient if the effect of a lower zone with

fresh air is the main feature in the design of the system.

A stratification height of minimum 1.1 m can be recommended in rooms where the occupants mainly have a sedentary working position. Figure 9 shows that the free convection around a person will generate a flow of clean air in the breathing zone although the stratification height is smaller than the height to the breathing zone in undisturbed surroundings. The measurements shown in figure 9 are made by Stymne et al. /13/ and they indicate that the lower zone can be locally displaced approximately 0.2 m upward around heated bodies.

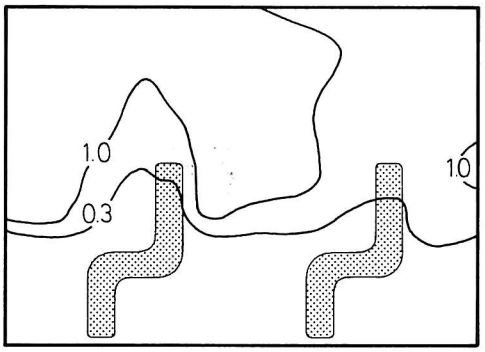

Figure 9. Normalized concentration distribution c/c_R around two persons. The ventilation rate is 0.011 (m^3/s, person) and the source of tracer gas is located in the upper zone close to the ceiling.

The air movement in the upper zone is often rather well mixed which means that the normalized concentration c/c_R, where c_R is the concentration in the return opening, is close to 1.0. A normalized concentration distribution of 1.0 is the concentration distribution which can be obtained by a mixing air distribution system and it can therefore be concluded that even cases with 1.0 concentration in the breathing zone should be acceptable in certain situations.

The stratification height in an industrial environment must be higher than the height of the occupied zone if the sources are combined heat and contaminant sources, and if the contaminant constitutes any health risk. Only measurements in the workers' breathing zone can demonstrate if the system works properly with respect to air quality.

3.2 Concentration Distribution

Figure 10 shows the vertical concentration distribution in a room where the heat source also works as a contaminant source. The location of the stratification height is clearly indicated by the measurements and both the lower and the upper zone have a well mixed concentation distribution. The tracer gas concentration in the upper zone is close to the concentration in the return opening, c_R, and the concentration in the lower zone is 0.1 to 0.3 times c_R which is typical of many situtations in highly loaded rooms.

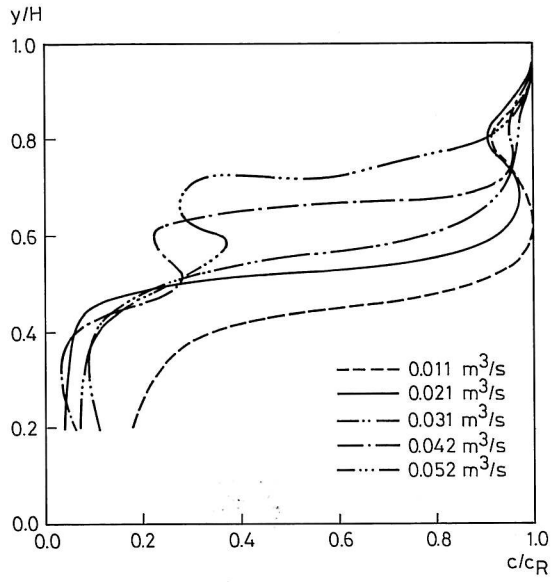

Figure 10. Vertical concentration distribution in a room with a combined heat and contaminant source versus volume flow rate to the room. Reference /14/.

The figure shows that the stratification height y_{st} is a function of the volume flow rate q_o to the room. This is also obvious from equation (2) which indicated that y_{st} is proportional to $q_o^{3/5}$ at constant heat load. It is further possible to show that the stratification height is a unique function of the Archimedes number and proportional to $Ar^{-1/5}$ in a geometry with concentrated heat sources.

Two of the concentration profiles on figure 10 show a small concentration peak just below the main stratification height. This increase is generated by cold downdraft at the wall which has a neutral buoyancy in the height $y/H \sim 0.5$.

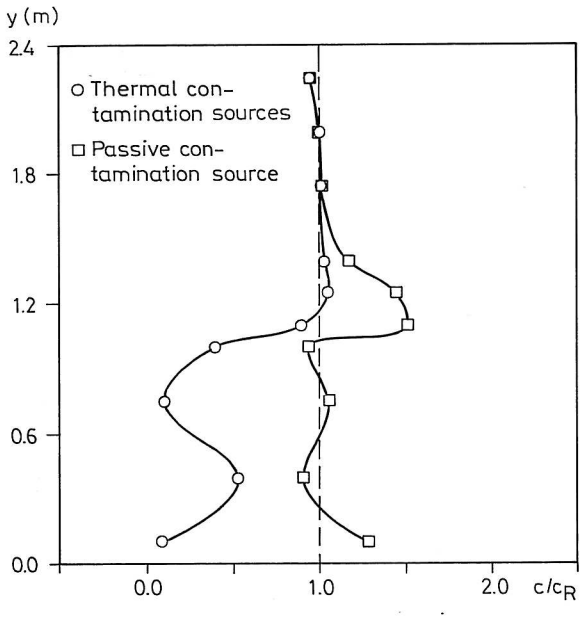

Figure 11. Vertical contaminant distribution in a room with displacement ventilation and two locations of the contaminant source, reference /1/.

The relative concentration distribution given on figure 11 shows in one example a stratification with a high concentration in the upper area of the room and a low concentration in the lower part of the room. The heat load consists of four thermal manikins and the tracer gas is released in the plumes from the manikins. The average value of the concentration in the lower part of the room is 0.25 c_R. The situation is different when the contaminant source is passive and located outside the plumes below the stratification height. The figure shows a high level of concentration in the room height corresponding to the height of the source. Very high concentrations may be obtained in this situation because the air movement is small in the area around the source and the contaminant is stabilized in a horizontal layer due to the temperature gradient.

The low velocity level and the vertical temperature gradient in a room with displacement ventilation will relaminarize the air movement. The consequence for a passive contaminant source is a high concentration level as indicated on figure 11. The free convection flow around a person may protect the breathing zone from surrounding contamination at the head level as shown on figure 9, but it may also attract contaminant from a passive source with a vertical location in the room below the breathing zone of the person. This process has been measured by Holmberg et al. /15/ and it is indicated on figure 12.

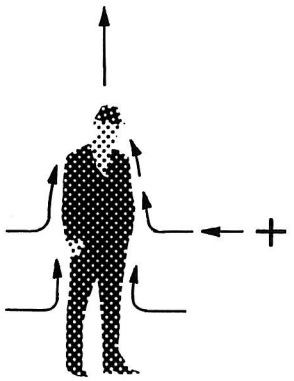

Figure 12. Contaminant transport from a passive source to the breathing zone of a person.

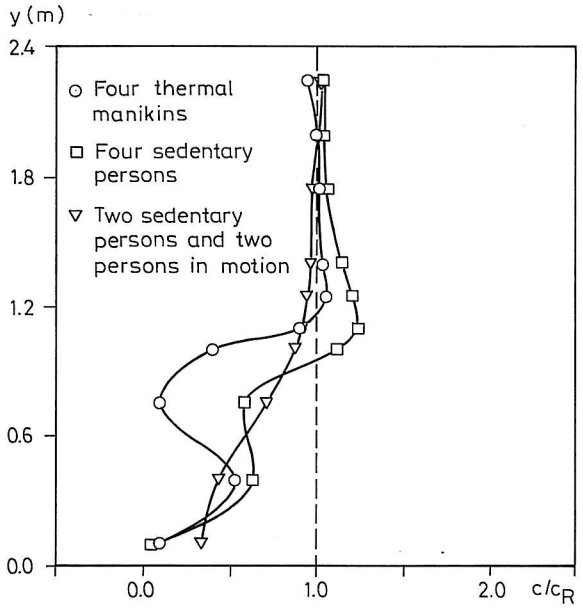

Figure 13. Concentration distribution in a room with thermal manikins, sedentary persons and persons in motion, reference /1/.

It is important to preserve the stratification in the room when persons are present and in motion. Figure 13 shows the vertical concentration distribution with four thermal manikins. A CO_2 tracer gas is released in the plumes above the manikins. The relative concentration distribution for four persons is also shown and the CO_2 concentration is, in this case, the values obtained from the presence of persons in the room. It is shown that two persons in motion are able to smooth the vertical gradient slightly, but it is in all situations possible to observe a stratification of CO_2.

3.3 Ventilation Effectiveness

The air quality and the efficient use of air are as important as thermal comfort. Different definitions of effectiveness for the evaluation of an air distribution system have therefore been commonly used during recent years.

The ventilation effectiveness shows how fast contaminant is removed from a room. It is defined as the ratio of concentration of the contaminant in the return opening to the concentration of contaminant in areas of the ventilated room.

The ventilation effectiveness ε_{oc} of the occupied zone is given by

$$\varepsilon_{oc} = \frac{c_R}{c_{oc}} \tag{15}$$

where c_R and c_{oc} are concentration in return opening and mean concentration in the occupied zone, respectively.

A local ventilation index ε_P is defined as

$$\varepsilon_P = \frac{c_R}{c_P} \tag{16}$$

where c_P is the concentration in a point of the room, e.g. the breathing zone of a person. ε_P is also the reciprocal of the normalized concentration in the point P.

A mean ventilation effectiveness $\bar{\varepsilon}$ is given by

$$\bar{\varepsilon} = \frac{c_R}{\bar{c}} \tag{17}$$

where $\bar{c}$ is the mean concentration in the whole room including areas outside the occupied zone.

Equations (15) to (17) assume that the supply flow is uncontaminated and it is also assumed that both the contaminant process and the flow are steady.

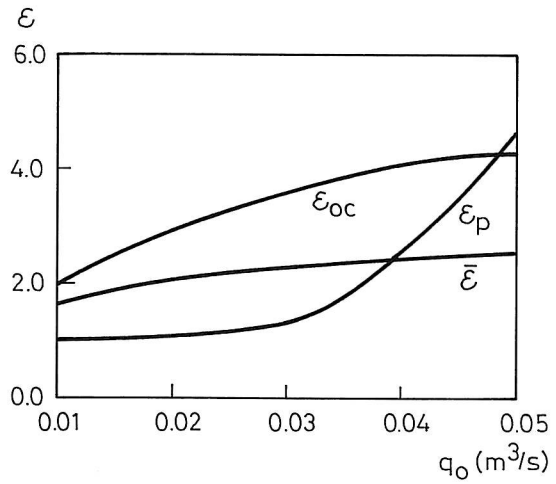

Figure 14. The ventilation effectiveness $\bar{\varepsilon}$ and ε_{oc} as well as the ventilation index ε_P for the measurements shown on figure 10.

Figure 14 shows the level of information which can be obtained from measurements of different versions of the ventilation effectiveness. The mean ventilation effectiveness $\bar{\varepsilon}$ indicates a low level at all air flow rates and the level is strongly influenced by the contaminant in the upper zone of the room. The ventilation effectiveness of the occupied zone ε_{oc} has a higher level because c_{oc} is calculated up to the height $y/H = 0.72$ which excludes the influence of a large part of the upper zone. The local ventilation index is measured in the height $y/H = 0.6$ in the case shown in figure 14. This index is very sensitive to the flow rate to the room because the height of the stratification crosses the measuring area at the actual flow rate.

It is typical that the ventilation effectiveness is larger than 1.0 in many practical situations with displacement ventilation and this is different from the situation in a room with conventional mixing ventilation.

It is easy to measure the mean ventilation effectiveness $\bar{\varepsilon}$ in small rooms because, in principle, it can be made by two concentration measurements. The tracer gas concentration in the return opening c_R is measured during the steady state of an experiment. The mean concentration $\bar{c}$ of the room is measured by mixing the room air by a fan immediately after shut down of ventilation system and tracer gas emission. The measurements of the ventilation effectiveness ε_{op} are more demanding because it is necessary to have a number of measuring points in the occupied zone to obtain the mean concentration in that area. It is of course easy to measure the ventilation index ε_P because it only involves two measurements in a steady state condition in the room.

The ventilation effectiveness can be defined from the height of the stratification y_{st} due to the presence of stratified flow.

$$\bar{\varepsilon} = \frac{H}{H + y_{st}\,(c_1/c_R - 1)} \tag{18}$$

It is assumed that the air in the lower and the upper zone is well mixed separately with a concentration of c_1 in the lower zone and a concentration in the upper zone which is equivalent to c_R

The ventilation effectiveness ε_{oc} of the occupied zone is given by

$$\varepsilon_{oc} = \frac{c_R}{c_1} \quad \text{for} \quad y_{oc} \leq y_{st} \tag{19}$$

and

$$\varepsilon_{oc} = \frac{y_{oc}}{y_{oc} + y_{st}\,(c_1/c_R - 1)} \quad \text{for} \quad y_{oc} > y_{st} \tag{20}$$

where y_{oc} is the height of the occupied zone.

4. TEMPERATURE DISTRIBUTION

A displacement ventilation system has an efficient use of energy because it is possible to remove exhaust air from the room where the temperature is several degrees above the temperature in the occupied zone which will allow a higher air inlet temperature at the same load.

The temperature distribution will also influence the thermal comfort in the room. It is therefore necessary to consider the consequences of a temperature gradient in the occupied zone as well as the asymmetric radiation from the ceiling.

4.1 Vertical Temperature Gradient for Different Types of Thermal Loads

The vertical temperature gradient is very characteristic of a room with displacement ventilation. Heat from heat sources is supplied to the room as convection and radiation. Free convection will raise the ceiling temperature compared to the surroundings, and radiation from the ceiling will then increase the temperature of the floor which, on the other hand, is cooled by the cold supply flow from the diffuser. The total effect is a vertical temperature gradient which is rather similar at different locations due to the stratification in the room.

The temperature gradient can be given with advantage in a dimensionless form. Figure 15 shows that the gradient has a limited variation compared with the variations which will be found for gradients in a dimensioned form.

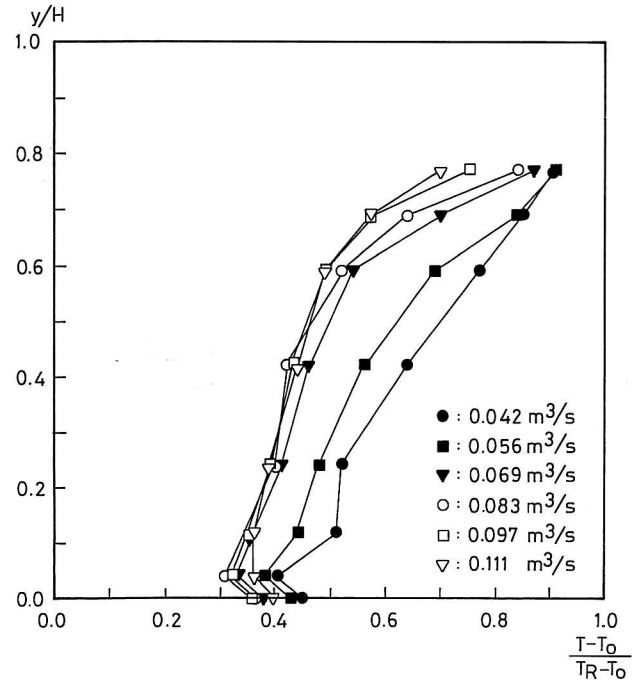

Figure 15. Vertical temperature distribution for different air flow rates, reference /16/.

The measurements shown on figure 15 are all made at constant heat load from a concentrated heat source. A closer examination of the measurements shows that an increasing Archimedes' number will decrease the normalized gradient slightly, while the dimensioned gradient will increase at increasing Archimedes' number. The dimensionless temperature gradient is a unique function of the Archimedes number when the flow is a high turbulent flow and

experiment in /4/ indicates this assumption in practice although some areas of a room may have an air movement with relaminarization.

The vertical temperature gradient is independent of the location of the heat load in the room as long as the elevation of the source is constant. The gradient is, on the other hand, strongly influenced by variation in elevation and the most energy efficient layout is a design with a high location of the heat sources. The ultimate use of this principle is to combine the ceiling lighting with the exhaust openings.

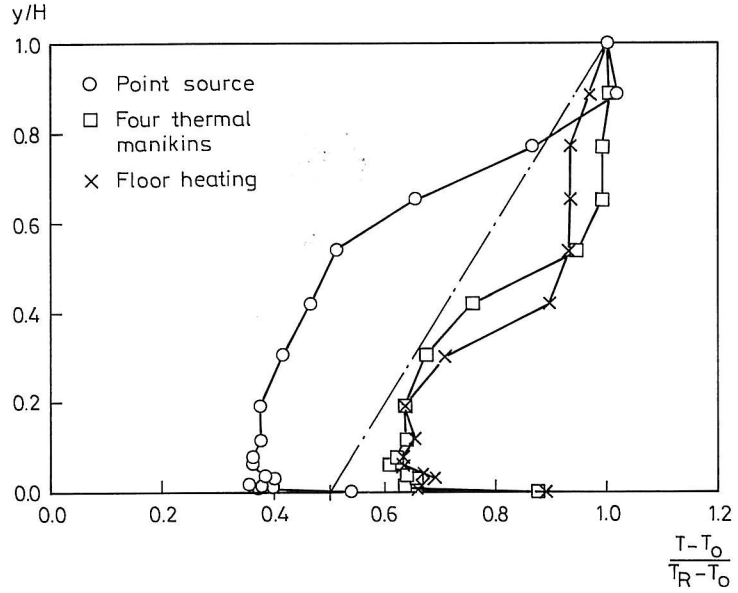

Figure 16. Vertical temperature gradients in a room with different heat sources at equal Archimedes' number /1/.

Figure 16 shows the vertical temperature gradient for different heat sources. The concentrated heat source is a small cylindrical heater with open heating elements, $0.3 \times 0.1^{\phi}$ m. The thermal manikin is a black painted cylinder with the dimensions $1.0 \times 0.4^{\phi}$ m. The floor heating consists of more electrical heating carpets covering a large part of the floor surface.

The location of the normalized temperature gradient on figure 16 depends on geometrical extension and temperature of the heat source. A heat source as the concentrated source will give a temperature distribution with high system effectiveness, while four thermal manikins will generate a temperature distribution with lower effectiveness. Floor heating shows a bad utilization of displacement flow. It is likely that the ratio between radiation and convection is an important parameter. A high level of this ratio will displace the curves to the right side on figure 16 because it will increase the amount of heat supplied to the floor. Experiments with four thermal manikins covered with aluminium foil support this theory because the vertical temperature profile in this situation is displaced to the left side on figure 16.

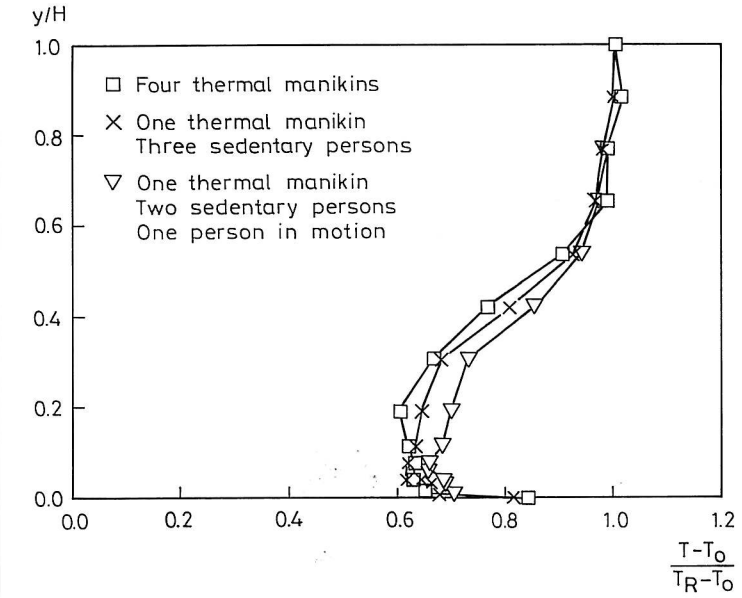

Figure 17. Vertical temperature gradients in a room with thermal manikins, sedentary persons and persons in motion /1/.

Figure 17 shows the vertical temperature distribution in a room with thermal manikins and persons. The manikins seem to give a sufficient thermal description of a person. It is especially important to see that a person in motion is unable to spoil the stratification, and the measurements show only a slight reduction in the effectiveness of the system. Other measurements with heavy activity and an open door to the test room do also confirm the large stability of the stratified flow in the room.

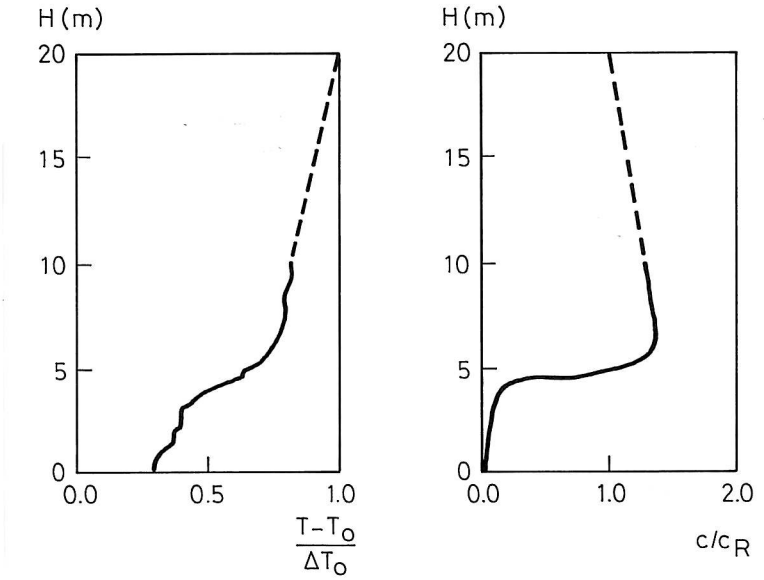

Figure 18. Temperature and concentration distribution in an industrial building.

The profiles shown on the figures 15 to 17 are made in a room of conventional size (H ~ 2.5 m). Most of the experience with large rooms comes from measurements in industrial areas and figure 18 shows the temperature distribution and the concentration distribution measured in a silicon carbide furnace room, Skistad /17/.

The figure shows a moderate change in temperature gradient and a very steep change in concentration gradient in the stratification height. Both gradients behave more or less in the same way as found in smaller rooms.

The contaminant is carbon monoxide from the furnaces. It is seen that the air with the high concentration level must be a convection flow from parts of a furnace with a lower temperature level than the surface temperature which generates the maximum temperature below the ceiling.

It has to be considered that it is difficult to obtain steady state solutions when measurements are made in large areas due to the large air volume and thermal mass. It is possible to use this effect in ventilation of areas which have a high level of the loads in short periods during the day.

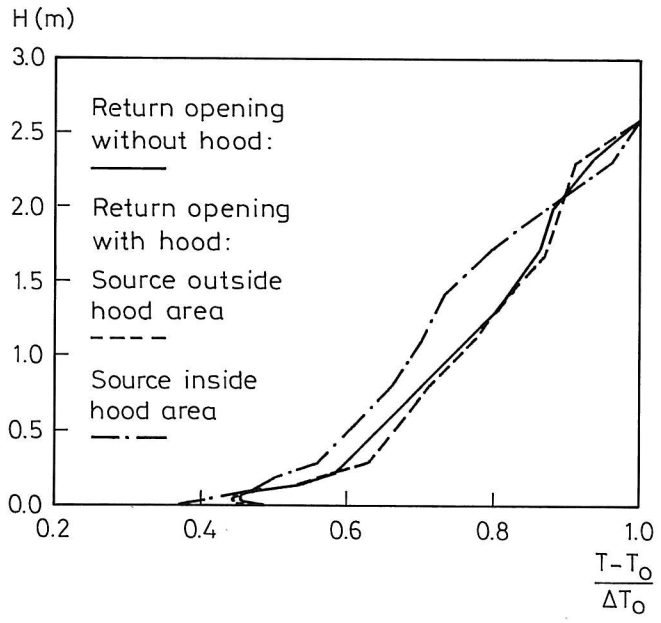

Figure 19. Experiments with return opening geometry.

It is generally assumed that the location of the return opening is of minor importance if it is located just below the ceiling or in the ceiling, because the air in the upper zone is almost fully mixed.

Experiments show that there is some influence from the details around the opening. A heat source with a plume which reaches the ceiling is ventilated in an efficient way if the opening is located above the source and if a small hood is located around the opening. Figure 19 shows some experiments with different location of heat source and return opening. A short hood or shield with a height of 0.6 m around the return opening will increase the efficiency of the opening and the measurements show that the return temperature will increase when the

plume reaches the ceiling with the centre line inside the hood. High flow rates in the room may destroy the effect.

4.2 Design Temperature Gradient

A design of a displacement ventilation system involves the prediction of the vertical temperature gradient. Knowing this gradient it is possible to calculate the thermal sensation of the temperature level, the thermal sensation of the temperature gradient and the thermal sensation of the asymmetric radiation from the ceiling.

Measurements indicate that it is possible to make the simplified assumption that the temperature varies linear with the height from a minimum temperature at floor level T_f to a maximum temperature at ceiling level which is equivalent to the return temperature T_R.

$$T = \frac{y}{H} (T_R - T_f) + T_f \tag{21}$$

Skistad /17/ assumed that $T_f - T_o$ is equivalent to 0.5 $(T_R - T_o)$ in all practical situations. Comparison with figure 15 shows that the minimum temperature T_f has a limited variation when it is given in a dimensionsless form and this may support the above-mentioned assumption. The dotted line on figure 16 shows the variation of T for $T_f - T_o = 0.5\ \Delta T_o$ and it can be argued that the line represents some mean assumption for gradients from different types of heat sources.

Figure 15 shows that $(T_f - T_o)/\Delta T_o$ varies slightly with the air flow rate. Mundt addresses this effect in /18/ and gives the following figure 20 for the variation as a function of the air flow rate per m^2 floor area. The figure summarize a large number of measurements in different rooms.

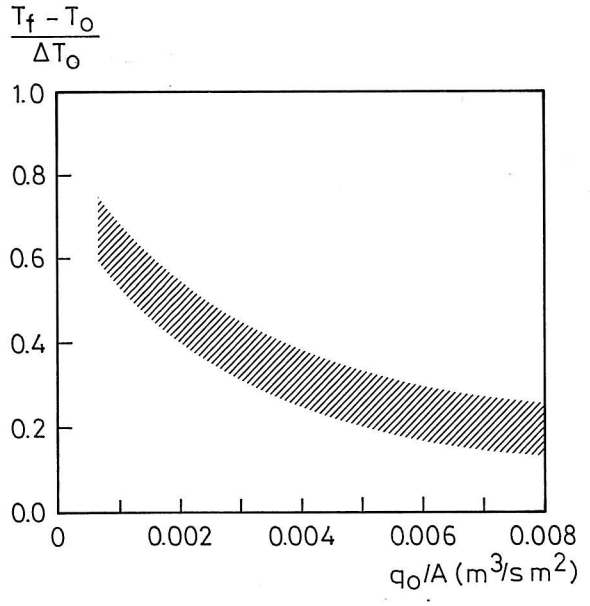

Figure 20. Minimum temperature at floor level T_f in a room with displacement ventilation versus air flow rate per square meter floor area.

4.3 Temperature Effectiveness

The efficient use of air in a ventilation system can be studied by the temperature effectiveness ε_T of the occupied zone.

$$\varepsilon_T = \frac{T_R - T_o}{T_{oc} - T_o} \tag{22}$$

where T_R, T_o and T_{oc} are temperature in return opening, temperature in supply opening and mean temperature in the occupied zone, respectively.

It is possible to express the temperature effectiveness ε_T by

$$\varepsilon_T = \Delta T_o \Big/ \left(\frac{y_{oc}}{2H} (T_R - T_f) + T_f - T_o \right) \tag{23}$$

if it is assumed that the vertical temperature distribution in the room is linear.

Figure 21 shows the variation of the temperature effectiveness as a function of the Archimedes number. The measurements are given on figure 15 and it is obvious that the temperature effectiveness is a unique function of the Archimedes number independent of flow rate and heat load. Two different types of diffusers are used in the experiments and the figure shows that the temperature effectiveness seems to be uninfluenced by the type of diffuser selected.

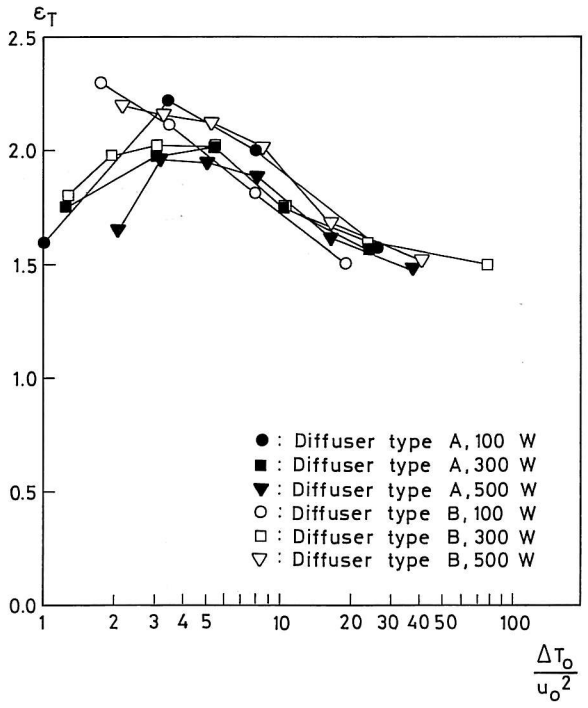

Figure 21. Temperature effectiveness versus the Archimedes number. The Archimedes number is expressed as $\Delta T_o/u_o^2$ (Ks^2/m^2) and the height of the occupied zone is measured to $y_{oc}/H = 0.81$.

The effectiveness of the air distribution system can also be expressed by a load factor. If, for example, the heat is generated below the ceiling it will contribute with a small load on the air conditioning system compared to heat generated in the occupied zone and this effect can be expressed by the following load factor

$$\mu_T = \frac{T_{oc} - T_o}{T_R - T_o} \tag{24}$$

The load factor μ_T is the reciprocal of the temperature effectiveness ε_T.

Figure 22 shows load factors for different locations of heat sources for ventilation in a room with a number of vertical jets in the floor. It is shown that a heat source at the floor, as for example solar radiation, results in a temperature in the occupied zone close to the return temperature which gives a high load factor. Load from people and equipment at table level and solar radiation on a wall will give a small load factor, while heat sources at higher level, as lighting in the ceiling, result in a reduction of the load on the air conditioning system, see Detzer and Jungbäck /19/. The lighting will heat the surfaces in the room due to radiation and this will limit the possibility of making reductions in the load factor below certain limits.

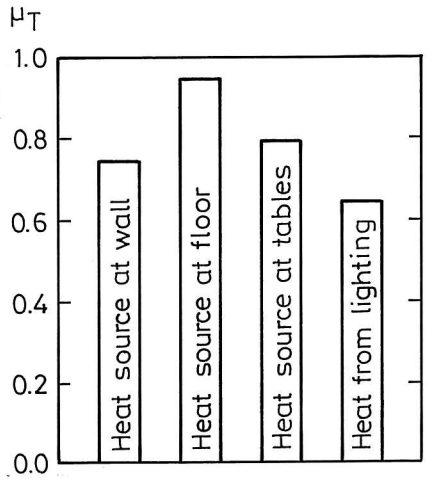

Figure 22. Load factors for different locations of heat sources in a room with floor-mounted diffusers.

5. VELOCITY DISTRIBUTION IN THE OCCUPIED ZONE

The air terminal devices for displacement ventilation are located in the lower part of the room. The airflow is supplied direct into the occupied zone and it is therefore important to have a design method which can predict the velocity distribution close to the floor. The velocity level outside the floor areas is very small due to the stratification and the sensation of draft is therefore primarily connected to the flow at floor level.

5.1 Velocity Distribution in the Flow from a Wall-Mounted Diffuser

Figure 23 shows the velocity distribution in front of a wall-mounted low velocity diffuser. The flow has a radial distribution when it leaves the diffuser and it will accelerate towards the floor due to the gravity effect on the cold air. The velocity contour for the 0.2 m/s velocity indicates an area close to the diffuser where the velocity is too high for a sedentary person.

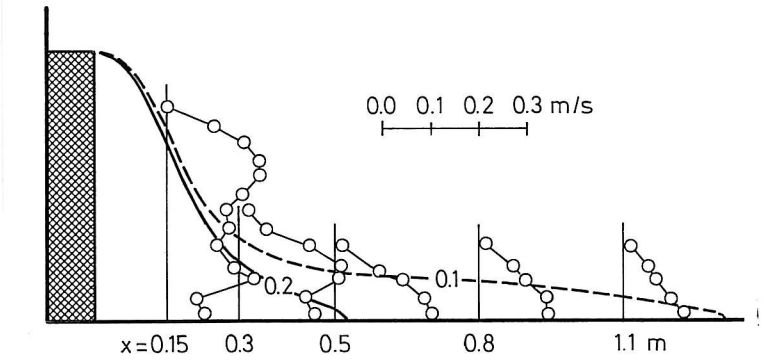

Figure 23. Velocity profiles and velocity contours in front of a wall-mounted low velocity diffuser type G. q_o = 0.029 m^3/s and $T_{oc} - T_o = 6\ ^oC$.

The design of a displacement ventilation system with a wall-mounted diffuser involves the determination of a length l_n which is the distance from the diffuser to the 0.2 m/s velocity contour measured along the centre line of the flow. The distance l_n is a function of the flow rate from the diffuser and it is a function of the temperature difference $T_{oc} - T_o$. It is important that l_n is small compared to the length of the room because it corresponds to an area which may be strongly influenced by draft.

Figure 23 shows that l_n is 0.5 m at the given conditions. Some producers are defining l_n as the distance to the 0.2 m/s velocity contour in a height of 0.1 m above the floor. This will give an l_n of 0.35 m in the situation on the figure.

The velocity distribution downstream from three different wall-mounted diffusers is shown on figure 24. The maximum velocity u_x close to the floor (1 - 4 cm above the floor) is given as a function of the distance x from the diffuser.

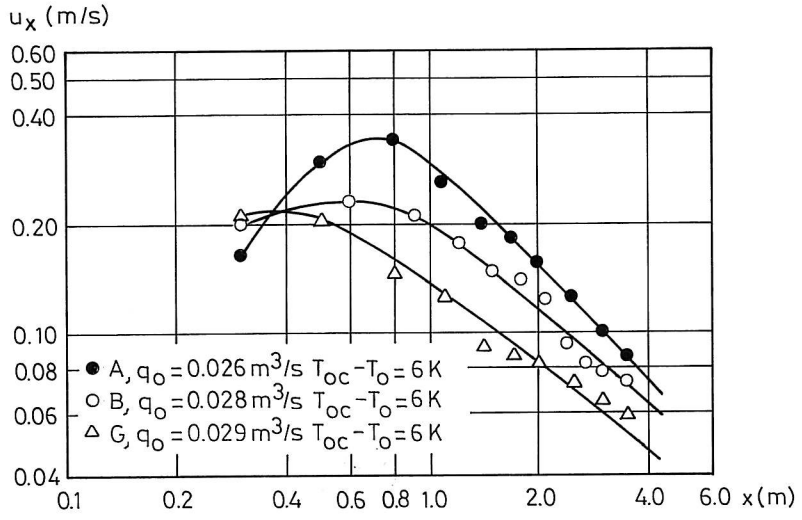

Figure 24. Maximum velocity close to the floor versus distance x. Reference /20/.

The cold air from supply opening A has a high initial acceleration due to buoyancy effect and a velocity of 0.34 m/s is obtained in a distance of 0.8 m from the diffuser. Type B has a large diffusion of the supply flow and the gravity will only increase the velocity to 0.23 m/s. The diffuser type G shows an even smaller velocity level although the flow to the room is almost the same in all three situtations but this diffuser has a higher velocity level outside the centre line.

Figure 24 indicates that the maximum velocity in the symmetry plane is proportional to $(1/x)^{\alpha}$ where the exponent α is close to 1.0 as pointed out by Nielsen et al. /16/.

It is obvious from figure 24 that different diffuser designs generate a different velocity level at the same flow rate and heat load.

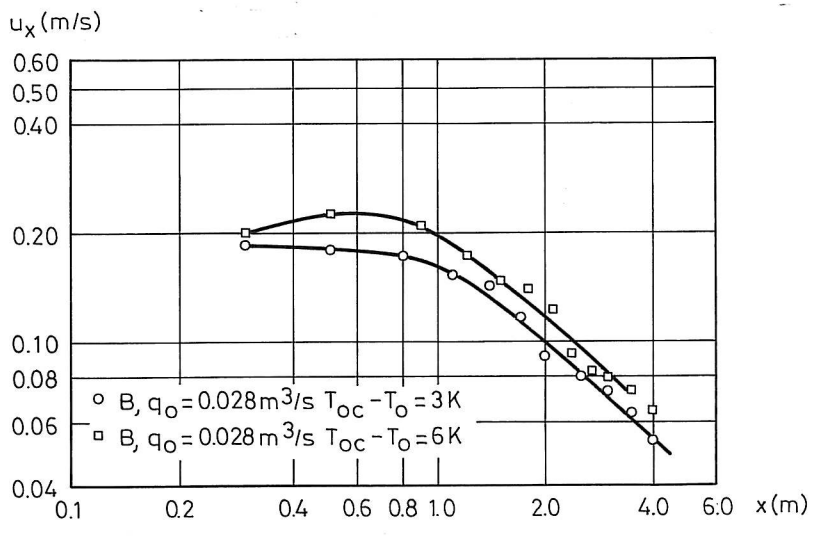

Figure 25. Velocity decay along the floor at different Archimedes' numbers. Reference /20/.

The velocity at the floor is not only influenced by the flow rate to the room and the type of diffuser. Figure 25 shows that the Archimedes number is an important parameter. A 3 °C increase in temperature difference will for example increase the velocity from 0.10 m/s to 0.12 m/s in a distance of 2 m from the diffuser. The figure shows that it is the gravity which accelerates the flow close to the diffuser resulting in a higher initial velocity level at higher Archimedes' numbers. This effect is very important for the flow in rooms with displacement ventilation and the outcome can be surprising. The velocity level in a room may for example be uninfluenced although the flow rate is reduced because the heat load in the room requires a reduction of the supply temperature and consequently an increase of the relative velocity level.

Profile measurements show that the flow in the vicinity of the floor can be characterized by a normalized velocity profile identical to the profile used for the description of wall jet flow, see reference /2/. The length scale δ in this profile is defined as the distance from the floor to the height where the velocity has a level which is half of the maximum velocity close to the floor, $u_x/2$.

Figure 26 shows the development in δ for three different Archimedes' numbers. (The characteristic temperature difference in the Archimedes number is in this chapter $T_{oc} - T_o$ where T_{oc} is the temperature in the height 1.1 m and the characteristic length is the height of the diffuser h). It can be seen that the height of the flow region is much smaller that the height of the diffuser, even at a distance of 0.5 m from the diffuser. The cold air from the diffuser accelerates towards the floor due to gravity and it behaves like a stratified flow in its further progress along the floor. δ is rather constant while it is proportional to x in a wall jet as indicated by the dotted line in figure 26. The length scale or thickness δ is slightly decreased at increasing Archimedes' number.

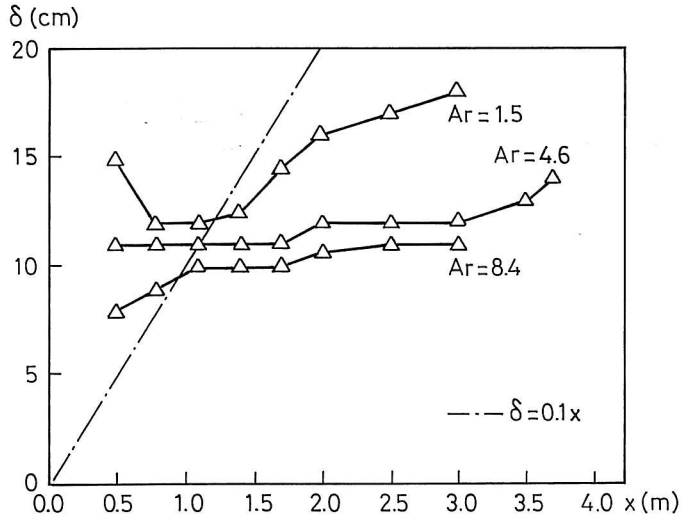

Figure 26. Length scale δ in the flow versus distance from the diffuser. Diffuser type G. Reference /20/.

The entrainment of air into the flow, or the turbulent mixing process, is diminishing when a vertical temperature gradient is present because the gravity will work against upward movement of heavy fluid and downward movement of light fluid. This is shown in hydraulics by for example Turner /21/ and it is shown for displacement ventilation by Jacobsen and Nielsen /2/.

The maximum velocity u_x in different distances from the opening x for a wall-mounted diffuser can be given by the following equation as shown by Nielsen /20/. The equation is based on stratified flow theory and it is confirmed by a number of measurements.

$$\frac{u_x}{u_f} = K_{dr} \frac{h}{x} \tag{25}$$

h is the height of the diffuser and u_f is the face velocity defined as flow rate q_o divided by the face area a_f of the diffuser. K_{dr} is a function of the Archimedes number as well as an individual function for different types of air terminal devices. Both x and u_x are measured in the centre plane of the flow. The development of equation (25) assumes a high Archimedes number but the structure is also valid for cases where the Archimedes number is very small. In this case the flow will be a part of a potential core or a part of a radial wall jet. The velocity will in both cases be proportional to $1/x$ and equation (25) will therefore be able to predict the velocity u_x when the K_{dr}-value is adjusted to the situation.

The variables in equation (25) are easy to measure for a given diffuser and the equation is therefore simple to use in a practical design procedure.

Equation (25) can only be used at some distance from the diffuser as it appears from the figures 24 and 25. This distance is 1.0 m to 1.5 m for most of the diffusers. The equation will in any case give a velocity equal to or higher than the actual velocity and therefore a value which is suitable for a design procedure.

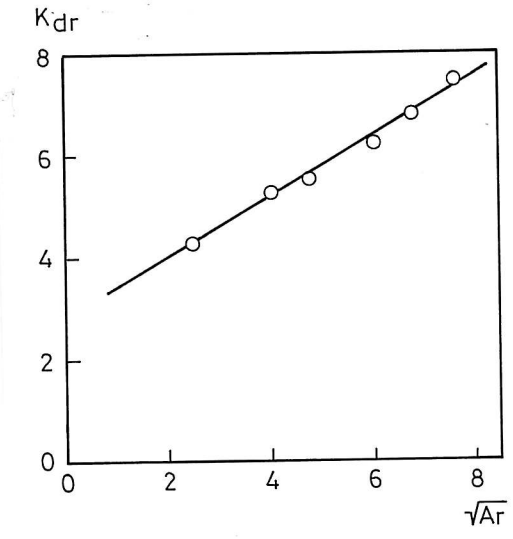

Figure 27. K_{dr} measured in the middle plane versus Archimedes' number for a wall-mounted air terminal device.

It is known from stratified flow in hydraulics that obstacles located downstream may influence the length scale δ of the flow, see reference /21/. Most of the measurements are made in test rooms of equal size so it is difficult to determine the influence from the end wall and the sidewalls, but practical experience indicates that room dimensions are of minor importance.

Figure 27 shows that K_{dr} increases with increasing Archimedes' number for the given diffuser. This is due to the fact that gravity will accelerate the vertical flow close to the opening and generate at stratified air movement in a relatively thin layer along the floor. Increased Archimedes' number will decrease δ and increase the maximum velocity in the layer. This effect is also shown on figure 25.

Mathisen /22/ has shown that the maximum velocity in the flow from a wall-mounted diffuser can be described as a linear function of $\sqrt{Ar}$. Figure 27 does confirm this assumption for large Archimedes' numbers, but deviations take place at smaller Archimedes' numbers for some products, reference /20/.

The flow from a single wall-mounted diffuser will be radial in the floor plane. The K_{dr}-values for different products will have different variations in directions outside the middle plane. It is typical that a new product has a small K_{dr} in the middle plane giving a small l_n, while older products have the largest K_{dr} in the middle plane, see /2/.

The flow from a number of diffusers placed close to each other on the wall will merge to a two-dimensional stratified flow. The velocity distribution can in certain areas be described by the equation

$$\frac{u_x}{u_f} = K_{dp} \tag{26}$$

if the Archimedes number is sufficiently large. It says that the velocity is independent of the distance but it is a function of flow rate, temperature difference and geometry around the diffusers. The same type of two-dimensional or plane flow will also take place in a narrow and a deep room with the diffuser located at the small end wall.

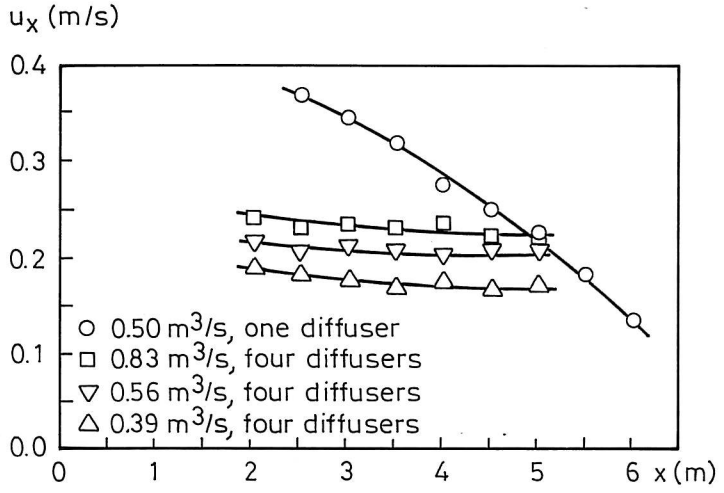

Figure 28. Velocity decay in radial flow from a single diffuser and velocity level in plane flow from a number of diffusers.

Nickel /23/ has measured the velocity distribution in the radial flow from a single diffuser. The diffuser is replaced by four diffusers located along one wall in a room with the width of 8 m. It is shown that two-dimensional flow gives the possibility to supply a high flow rate at a velocity level which is low compared to the velocity in the radial flow close to a single diffuser.

Velocity distribution in rooms with wall-mounted low velocity diffusers is also addressed by Mathisen /22/ and by Sandberg and Mattsson /24/. Fitzner /25/ shows full-scale measurements of stratified flow from sidewall-mounted diffusers and the interaction with a strong and a weak heat source in a typical office room.

5.2 Velocity Distribution from a Floor-Mounted Diffuser and from Diffusers Integrated into Furniture

Floor-mounted diffusers are often used in rooms with a high thermal load. The supply area is small and it is necessary with a supply velocity which is sufficient for a momentum driven flow in vertical direction (2 ~ 4 m/s).

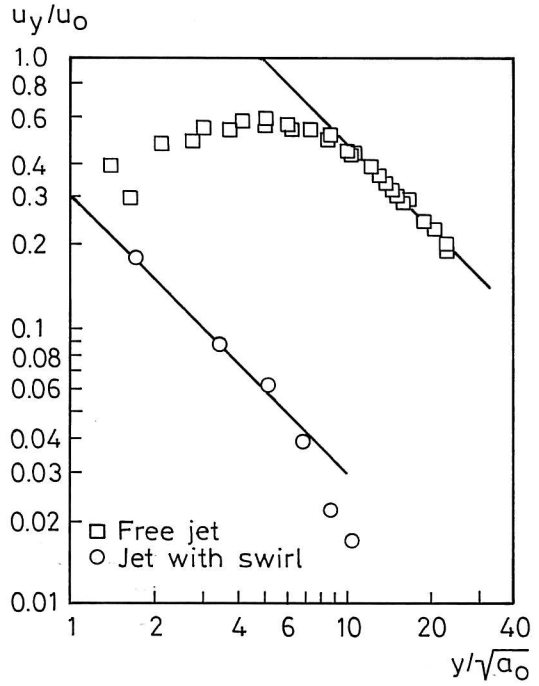

Figure 29. Velocity decay u_y/u_o in a free jet and in a jet with swirl versus the height y above the floor.

Figure 29 shows the velocity decay in free circular turbulent jet measured by Dittes and Mangelsdorf /26/. The openings can be located rather close in the floor dependent on the thermal load of the room. Entrainment into the jets will generate a recirculating flow above the opening and up to a height where the flow and temperature difference will dissolve the jets.

The velocity decay is given by the following equation for a free circular jet

$$\frac{u_y}{u_o} = \frac{K_a}{\sqrt{2}} \frac{\sqrt{a_o}}{y} \tag{27}$$

where u_y is the maximum velocity in distance y above the floor and a_o is the supply area of the diffuser. The K_a-value for the given diffuser is 6.8. A conventional air terminal device for the location in upper wall and ceiling in the case of mixing ventilation may have a K_a-value of the same level.

Figure 29 shows also measurements on a circular jet with swirl, reference /16/. It is convenient to compare the velocity decay in this jet with the velocity decay for a conventional free jet given by equation (27), and the velocity decay corresponds to a K_a-value of 0.42 which is about ten times smaller than the same value for a free jet. This is a surprising result and it shows that the swirl will generate a high entrainment and a very fast velocity decay. The diffuser if often used in a group of four within an area of 0.6 m × 0.6 m. The velocity level will in this case be higher than the velocity level from a single diffuser but both arrangements will have the same velocity level at a height of 0.8 m.

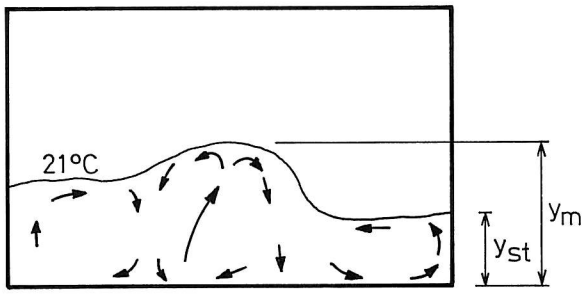

Figure 30. Flow in a room with a supply opening in the floor. Fitzner /10/.

The 21 °C isotherm in figure 30 indicates the boundary between lower and upper zones in a room with a floor-mounted supply opening. The recirculation around the cold jet generates a secondary flow in the lower part of the room with a movement towards the jet in a layer corresponding to the stratification height. The stratification height y_{st} is calculated from the entrainment into plumes in the room as discussed in chapter 3 and will not be influenced by the jet from the floor-mounted diffuser. The penetration height of the jet y_m is given by the following equation

$$\frac{y_m}{\sqrt{a_o}} = 3.33 \left(\frac{K_a u_o^2}{(T_{oc} - T_o)\sqrt{a_o}} \right)^{0.5} \tag{28}$$

when the supply temperature T_o is lower than the temperature in the occupied zone T_{oc}, reference /27/. y_m is the maximum penetration of the jet and this height is equivalent to the maximum penetration of a plume given by equation (8).

An integration of the supply opening in the furniture makes it possible to distribute the air efficiently in the occupied zone, especially in case of large rooms such as auditoria and lecture theatres. Figure 31 shows an air distribution system which is built into the seating structure. The conditioned primary air is fed from a pressure chamber accommodated in the chair mounting supports. Indoor air mixes with the primary air and the supply air emerges at the top of the back-rest, Rowlinson and Croome /28/.

The solution makes it possible to apply displacement ventilation in a large lecture theatre without having a draft risk. The recirculating room air flow that develops in downward systems is also avoided.

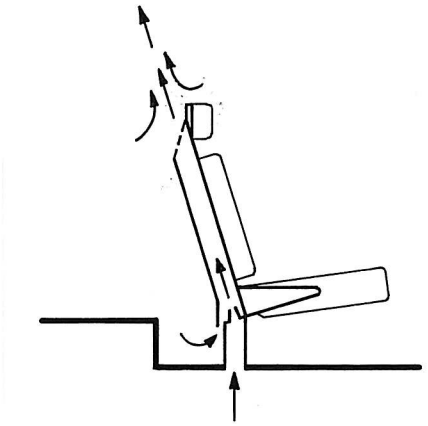

Figure 31. Seat with build-in supply system.

Typical system characteristics are a flow rate of 8 - 10 l/s per diffuser, a minimum supply temperature of 18 ^{0}C and a velocity of 1.5 - 2.5 m/s. The high location of the supply opening ensures a small temperature gradient in the occupied zone compared to the situation with supply openings at foot levels and the fresh air is supplied extremely close to the breathing zone of the people.

Supply openings can also be integrated into desks in an office. The supply system is connected via a double floor in the room. This system has the great advantage that it can be controlled partly by the individual users, reference /19/.

5.3 Flow between Obstacles in the Occupied Zone and Flow from Cold Downdraft

The flow in the vicinity of the floor may be influenced by furniture and by other obstacles in the occupied zone. The maximum velocity in the flow is located rather close to the floor (between 1 to 4 cm above the floor), and a great deal of the air movement will therefore take place in this region. Conventional furniture will only have a small influence on the air movement while obstacles placed direct on the floor will block the flow. An opening between this type of obstacles will work as new supply opening because the flow in the room is stratified. Figure 32 shows the flow between two obstacles where the cold air is supplied in the left side of the room and the heat sources are located in the right side of the room.

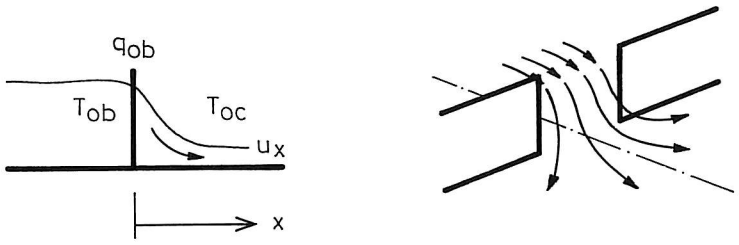

Figure 32. Radial stratified flow between obstacles.

Nielsen /20/ has shown that the flow from an opening between obstacles can be described as a semi-radial flow like the air movement from a wall-mounted supply opening. The velocity decay can be described by the equation

$$\frac{u_x}{q_{ob}} = K_{ob} \frac{1}{x} \tag{29}$$

where u_x is maximum velocity in distance x from the opening and q_{ob} is the excess air supplied on the upstream side. u_x is measured in the symmetry plane.

Figure 33 shows the measurements of K_{ob} in equation (29). The structure of equation (29) and the distribution of K_{ob}-values are equivalent to the structure of equation (25) and the distribution of K_{dr}-values in figure 27.

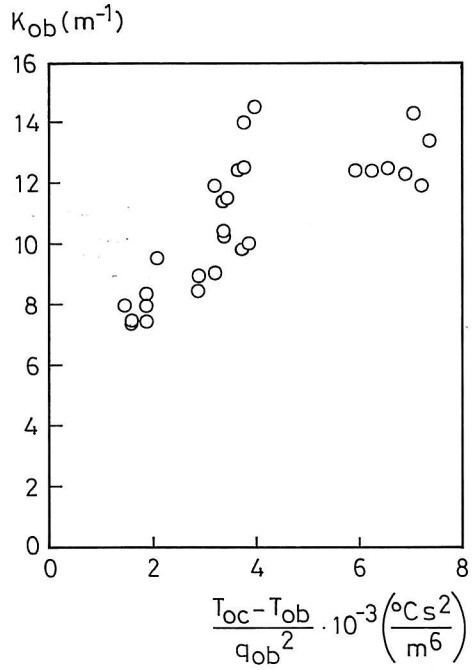

Figure 33. K_{ob} versus flow rate and temperature difference. Reference /20/.

The temperature difference $T_{oc} - T_{ob}$ is the difference between the temperature in the height 1.1 m in front of the opening and the lowest temperature in the opening between the obstacles. q_{ob} is the flow rate between the obstacles. The width of the opening is varying from 0.1 m to 1.5 m in the experiment on figure 33. The measurements show that the importance of the width is less obvious and results for different widths are given on the figure.

Cold downdraft from surfaces can be another reason for a velocity level in the occupied zone. The maximum velocity in a cold downdraft is given by /29/.

$$u_y = 0.055(y\Delta T)^{0.5} \tag{30}$$

where y is height of the cold surface and ΔT is the temperature difference between room temperature and surface temperature.

The cold downdraft will be deflected into the occupied zone at the floor and it will move as a stratified flow with a typical wall jet profile /29/. Two flow domains can be identified. One domain with growth of thickness (length-scale) which indicates entrainment of room air into the cold airflow and one with a constant thickness and a constant velocity which is typical of a plane stratified flow similar to the flow given by equation (26).

The maximum velocity in plane flow along the floor can be given by the folowing equation /29/.

$$u_x = 0.094 \frac{\sqrt{y\Delta T}}{x + 1.31} \qquad 0.4 \le x \le 2.0 \tag{31}$$

$$u_x = 0.028 \sqrt{y\Delta T} \qquad x > 2.0 \tag{32}$$

u_x is the maximum velocity close to the floor at distance x and y is the height of the cold surface. ΔT is temperature difference between room temperature and surface temperature. The measurements are made in rooms with a length of 3 to 7 m.

The flow along the floor will be radial if the cold surface is narrow compared to the width of the wall. The velocity will decrease rapidly from the level given by (30) in a velocity decay similar to the decay given in equation (25) and (29).

REFERENCES

1 Nielsen P.V., Air Distribution Systems - Room Air Movement and Ventilation Effectiveness, Proc. of the ISRACVE Conference, Tokyo, Society of Heating, Air-Conditioning and Sanitary Engineers of Japan, 1992.

2 Jacobsen T.V. and Nielsen P.V., Velocity and Temperature Distribution in Flow from an Inlet Device in Rooms with Displacement Ventilation, Proc. of the Third International Conference on Air Distribution in Rooms, ROOMVENT '92, ISBN 87-982652-6-1, Copenhagen, 1992.

3 Jacobsen T.V. and Nielsen P.V., Numerical Modelling of Thermal Environment in a Displacement-Ventilated Room, Proc. of the 6th International Conference on Indoor Air Quality and Climate, INDOOR AIR '93, Helsinki, 1993.

4 Nielsen P.V., Displacement Ventilation in a Room with Low-Level Diffusers, DKV-Tagungsbericht, ISBN 3-922-429-63-7, Deutscher Kälte- und Klimatechnischer Verein e.V., Stuttgart, 1988.

5 Baturin V.V., Fundamentals of Industrial Ventilation, Pergamon Press, 1972.

6 Kofoed P., Nielsen P.V., Thermal Plumes in Ventilated Rooms, Proc. of the International Conference on Engineering Aero- and Thermodynamics of Ventilated Room, ROOMVENT '90, Oslo, 1990.

7 Skåret E., Ventilation by Displacement - Characterization and Design Implications, Ventilation '85, edited by H.D. Goodfellow, Elsevier Science Publishers B.V., Amsterdam, 1986.

8 Morton B.R., Taylor G. and Turner J.S., Turbulent Gravitational Convection from Maintained and Instantaneous Sources, Proc. Royal Soc., Vol. 234 A, p. 1, 1956.

9 Mundt E., Convection Flows in Rooms with Temperature Gradients - Theory and Measurements, Proc. of the Third International Conference on Air Distribution in Rooms, ROOMVENT '92, ISBN 87-982652-6-1, Copenhagen,1992.

10 Fitzner K., Förderprofil einer Wärmequelle bei verschiedenen Temperaturgradienten und der Einfluss auf die Raumströmung bei Quellüftung, Ki Klima-Kälte-Heizung, Nr. 10, 1989.

11 Kofoed P. and Nielsen P.V., Auftriebsströmungen verschiedener Wärmequellen - Einfluss der umgebenden Wände auf den geförderten Volumenstrom, DKV-Tagungsbericht, Deutscher Kälte- und Klimatechnischer Verein e.V., Stuttgart, 1991.

12 Eckert E.R.G. Jackson T.W., Analysis of Turbulent Free-Convection Boundary Layer on Flat Plate, NACA Report No 1015, 1951.

13 Stymne H., Sandberg M. and Mattsson M., Dispersion Pattern of Contaminants in a Displacement Ventilated Room, Proc. of the 12th AIVC Conference. ISBN 0 946075 53 0, Warwick, 1991.

14 Heiselberg P. and Sandberg M., Convection from a Slender Cylinder in a Ventilated Room, Proc. of the International Conference on Engineering Aero- and Thermodynamics of Ventilated Room, ROOMVENT '90, Oslo, 1990.

15 Holmberg R.B., Folkesson K., Stenberg L.-G. and Jansson G., Experimental Analysis of Office Room Climate using Various Air Distribution Methods, Proc. of the First International Congress on Air Distribution in Ventilated Spaces, ROOMVENT '87, Stockholm, 1987.

16 Nielsen P.V., Hoff L. and Pedersen L.G., Displacement Ventilation by Different Types of Diffusers, Proc. of the 9th AIVC Conference, ISBN 0 946075 40 9, Warwick, 1988.

17 Skistad H., Fortrengningsventilasjon i komfortanlegg med lavimpuls lufttilførsel i oppholdssonene (In Norwegian), Norsk VVS Teknisk Forening, Oslo, 1989.

18 Mundt E., Convection Flows above Common Heat Sources in Rooms with Displacement Ventilation, Proc. of the International Conference on Engineering Aero- and Thermodynamics of Ventilated Room, ROOMVENT '90, Oslo, 1990.

19 Detzer R. and Jungbäck E., Bestimmung der Belastung des Aufenthaltsbereiches durch Wärme bei verschiedenen Luftführungen, Heizung Lüftung/Klima Haustechnik, Nr. 7, 1981.

20 Nielsen P.V., Velocity Distribution in the Flow from a Wall-Mounted Diffuser in Rooms with Displacement Ventilation, Proc. of the Third International Conference on Air Distribution in Rooms, ROOMVENT '92, ISBN 87-982652-6-1, Copenhagen, 1992.

21 Turner J.S., Buoyancy Effects in Fluids, Cambridge University Press, Cambridge, 1979.

22 Mathisen H.M. Analysis and Evaluation of Displacement Ventilation , Ph.D.-thesis, Technical University of Norway, 1989.

23 Nickel J., Air Distribution in Displacement Ventilation (In Danish), VVS, Teknisk Forlag A/S, Copenhagen, marts, 1990.

24 Sandberg M. and Mattsson M., The Mechanism of Spread of Negatively Buoyant Air from Low Velocity Air Terminals, IV Seminar on "Application of Fluid Mechanics in Environmental Protection 91", Gliwice, 1991.

25 Fitzner K., Impulsarme Luftzufuhr durch Quellüftung, Heizung Lüftung/-Klima Haustechnik, Nr. 4, 1988.

26 Dittes W. and Mangelsdorf R., Der Wärmetransport im Raum bei der Luftführung von unten nach oben, Heizung Lüftung/- Klima Haustechnik, Nr. 7, 1981.

27 Helander L., Yen S.M. and Crank R.E., Maximum Downward Travel of Heated Jets from Standard long Radius ASME Nozzles, ASHVE Transactions, Nr. 1475, 1953.

28 Rowlinson D. and Croome D., Supply Characteristics of Floor Mounted Diffusers, Proc. of the First International Conference on Air Distribution in Ventilated Spaces, ROOMVENT '87, Stockholm, 1987.

29 Heiselberg P., Draught Risk from Cold Vertical Surfaces, Proc. of the 6th International Conference on Indoor Air Quality and Climate INDOOR AIR '93, Helsinki, 1993.

LISTS OF SYMBOLS

Ar	Archimedes' number	
a_f	Face area	m^2
a_o	Diffuser supply area	m^2
c	Concentration	mg/m^3 or cm^3/m^3
c_{oc}	Mean concentration in occupied zone	mg/m^3 or cm^3/m^3
c_P	Concentration in point P	mg/m^3 or cm^3/m^3
c_R	Concentration in return opening	mg/m^3 or cm^3/m^3
$\bar{c}$	Mean concentration in the room	mg/m^3 or cm^3/m^3
c_1	Concentration in the lower zone	mg/m^3 or cm^3/m^3
d	Hydraulic diameter of heat source	m
g	Gravitational acceleration	m/s^2
H	Height of room	m
h	Height of wall-mounted diffuser	m
K_a	Constant for circular free jet	
K_{dp}	Coefficient for plane flow	
K_{dr}	Coefficient for radial flow	
K_{ob}	Coefficient for flow between obstacles	m^{-1}
k	Coefficient for convective heat emission	
l	Length of heat source. Width of surface	m
l_n	Length from diffuser to 0.2 m/s velocity contour	m
m	Dimensionless parameter	
N	Number of heat sources	
q_y	Volume flow in thermal plume or cold downdraft	m^3/s
q_{ob}	Volume flow between obstacles	m^3/s
q_{yN}	Volume flow from N heat sources	m^3/s
q_{yc}	Volume flow from a heat source located in a corner	m^3/s
q_{yw}	Volume flow from a heat source close to a wall	m^3/s
q_o	Volume flow supplied to the room or flow rate from a diffuser	m^3/s
q_1, q_2, q_3	Volume flows in plumes and downdraft	m^3/s
T	Temperature	°C
T_f	Minimum temperature close to floor	°C
T_{ob}	Minimum temperature in flow between obstacles	°C
T_{oc}	Mean temperature in occupied zone or temperature in the height of 1.1 m	°C
T_R	Return temperature	°C
T_o	Supply temperature	°C
u_f	Face velocity. Flow rate divided by face area	m/s
u_x	Maximum velocity at distance x	m/s

u_y	Maximum velocity at height y	m/s
u_o	Supply velocity	m/s
x	Coordinate and distance	m
y	Coordinate, distance and length of surface	m
y_m	Maximum height of a plume and a cold jet	m
y_t	Height to buoyancy neutral flow	m
y_{oc}	Height of the occupied zone	m
y_{st}	Stratification height	m
y_o	Height from virtual origin to heat source reference level	m
y^*	Dimensionless height	
α	Exponent	
β	Volume expansion coefficient	K^{-1}
ΔT	Temperature difference between room temperature and surface temperature	K
ΔT_o	Temperature difference $T_R - T_o$	K
δ	Thickness or length scale of flow	m
ε_P	Ventilation index	
ε_T	Temperature effectiveness	
ε_{oc}	Ventilation effectiveness of the occupied zone	
$\overline{\varepsilon}$	Mean ventilation effectiveness of the room	
μ_T	Load factor	
ϕ	Heat emission	W
ϕ_K	Convective heat emission	W

Appendix A

Displacement Ventilation in a Room with Low-Level Diffusers

Peter V. Nielsen

DISPLACEMENT VENTILATION IN A ROOM WITH LOW-LEVEL DIFFUSERS

Peter V. Nielsen, University of Aalborg, Denmark

INTRODUCTION

Ventilation systems with vertical displacement flow have been used in industrial areas with high thermal loads for many years. Quite resently the vertical displacement flow systems have grown popular as comfort ventilation in rooms with thermal loads e.g. offices.

The air is supplied directly into the occupied zone at low velocities from wall mounted diffusers. The plumes from hot surfaces, from equipment and from persons entrain air into the occupied zone and create a natural convection flow upwards in the room, see figure 1.

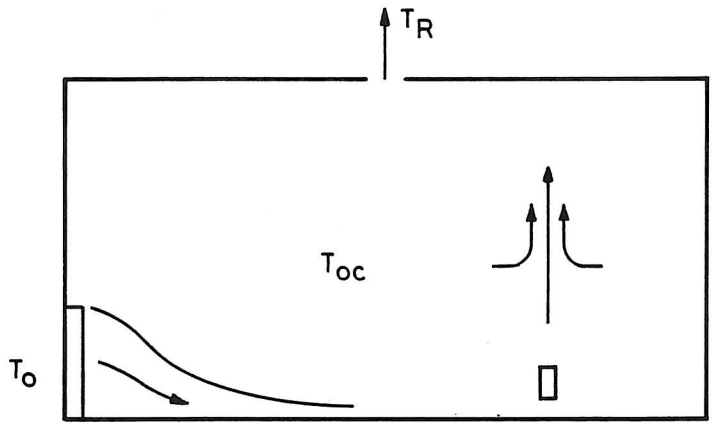

Fig. 1. Room with low-level diffuser, heat source and displacement flow.

The displacement flow systems have two advantages compared with traditional mixing systems.

- An efficient use of energy. It is possible to remove exhaust air from the room where the temperature is several degrees above the temperature in the occupied zone, which allows a higher air inlet temperature at the same load.
- An appropriate distribution of contaminant air. The vertical temperature gradient (or stratification) implies that fresh air and contaminant air are separated. The most contaminant air can be found above the occupied zone and the air flow rate can be reduced.

A general description of the displacement ventilation system has recently been given by Skåret [1] and by Fitzner [2]. Model experiments have been shown by Sandberg and Lindström [3], and measurements in plumes have been given by Kofoed and Nielsen [4]. The flow from different types of low-level diffusers has been described by Mathisen [5] and by Nielsen et al. [6].

The present paper will deal with the flow from different types of low-level diffusers. The main characteristics of the air movement which takes place in the room will be shown. The air movement is expressed by the velocity distribution along the floor, temperature efficiency and stratification level. Special emphasis will be put on an analysis of the velocity and temperature distribution at different Reynolds' numbers and the general importance of the Archimedes number.

FLOW FROM LOW-LEVEL DIFFUSERS

Figure 2 shows two different diffusers used in the experiments. The diffusers of types A and B are both low-level diffusers giving a horizontal air flow directly into the occupied zone. They both have a height of about 500 mm, but a different design. The diffuser A has a supply velocity profile which is very constant over the entire supply area, while the diffuser of type B has a supply velocity with a large variation over the supply area, see figure 3. This

variation applies to velocity level as well as to direction, and it means that the local entrainment - or diffusion - is very high close to the opening.

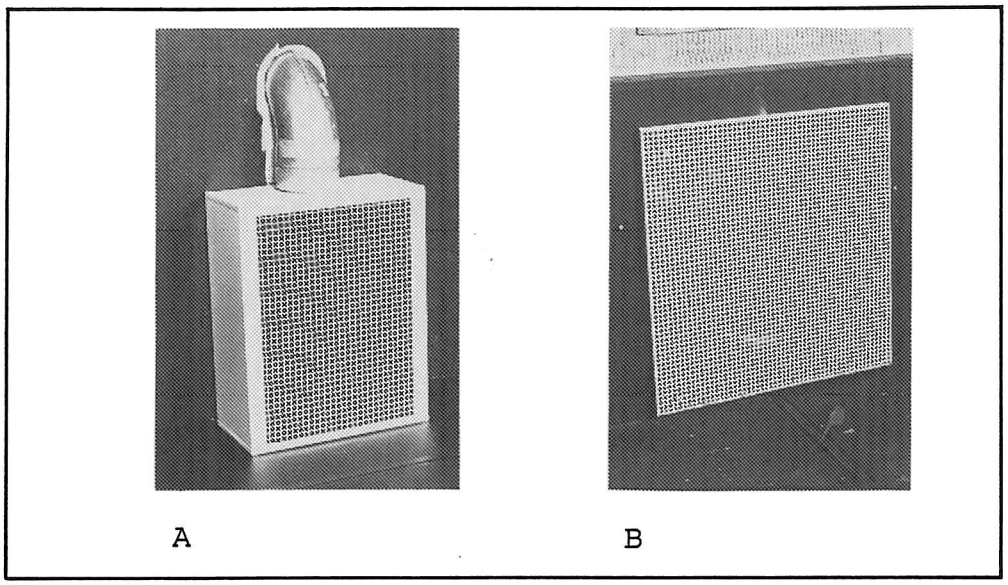

Fig. 2. Two low-level diffusers, type A and type B.

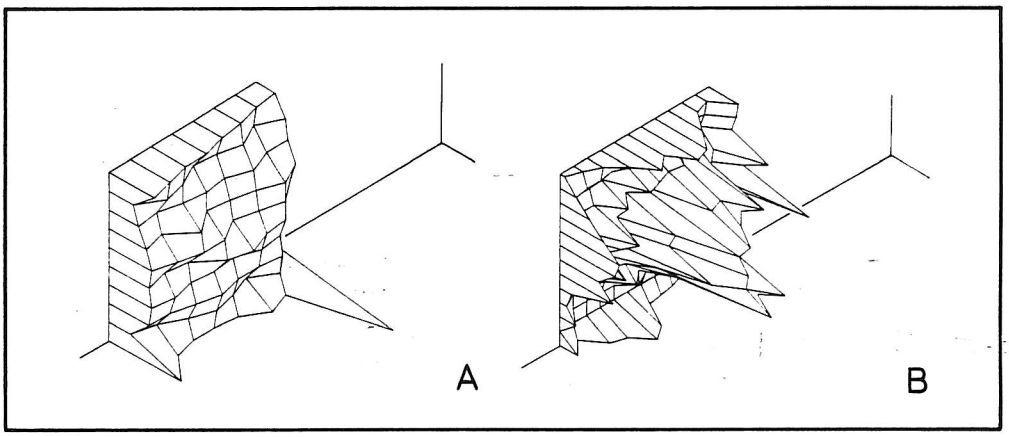

Fig. 3. Supply velocity profiles for diffusers A and B.

The experiments take place in a test room of the dimensions L × W × H = 5.4 × 3.6 × 2.6 m. The diffusers are mounted in the middle of the short end wall. The heat source is installed in the middle plane at a distance of 0.75 × L from the diffuser. The return opening is in the middle of the ceiling.

The flow pattern close to the openings and the local entrainment of room air influence the air movement in the room. Smoke experiments show that the flow from diffuser A spreads out within a 90° area downstream along the floor. Large temperature differences ($T_{oc} - T_o \sim 12$ K) will increase the angle and small temperature differences will decrease the angle giving a flow of a three-dimensional wall jet type for $T_{oc} - T_o \sim 0$ K.

Smoke experiments with diffuser B show that this diffuser spreads the flow over the whole floor area (180°) at all temperature differences.

It is obvious that the two different low-level supply openings - with various initial diffusion - will give a different air movement in the room. Figure 4 shows the velocity decay in the air movement along the floor for both supply openings. The figure indicates that the maximum velocity u_x along the floor is proportional to $1/x^n$ where the exponent n is about 1. The low diffusion in supply opening A results in a high initial acceleration of the air movement due to buoyancy effect on the cold supply air. The velocity level obtained, results in a high velocity in the whole flow along the floor.

The flow from diffuser B is also dependent on buoyancy but the acceleration close to the supply opening is smaller due to the high initial entrainment of room air.

The height of the flow along the floor is typically 0.2 - 0.25 m and the maximum velocity is located 0.03 - 0.04 m above the floor surface independently of the distance from the diffuser.

It is shown by the experiments that the flow is dependent on diffuser type and diffuser location in the room, as well as room width, implying that it is difficult to separate the influence of diffuser design from the influence of room geometry, see reference [6].

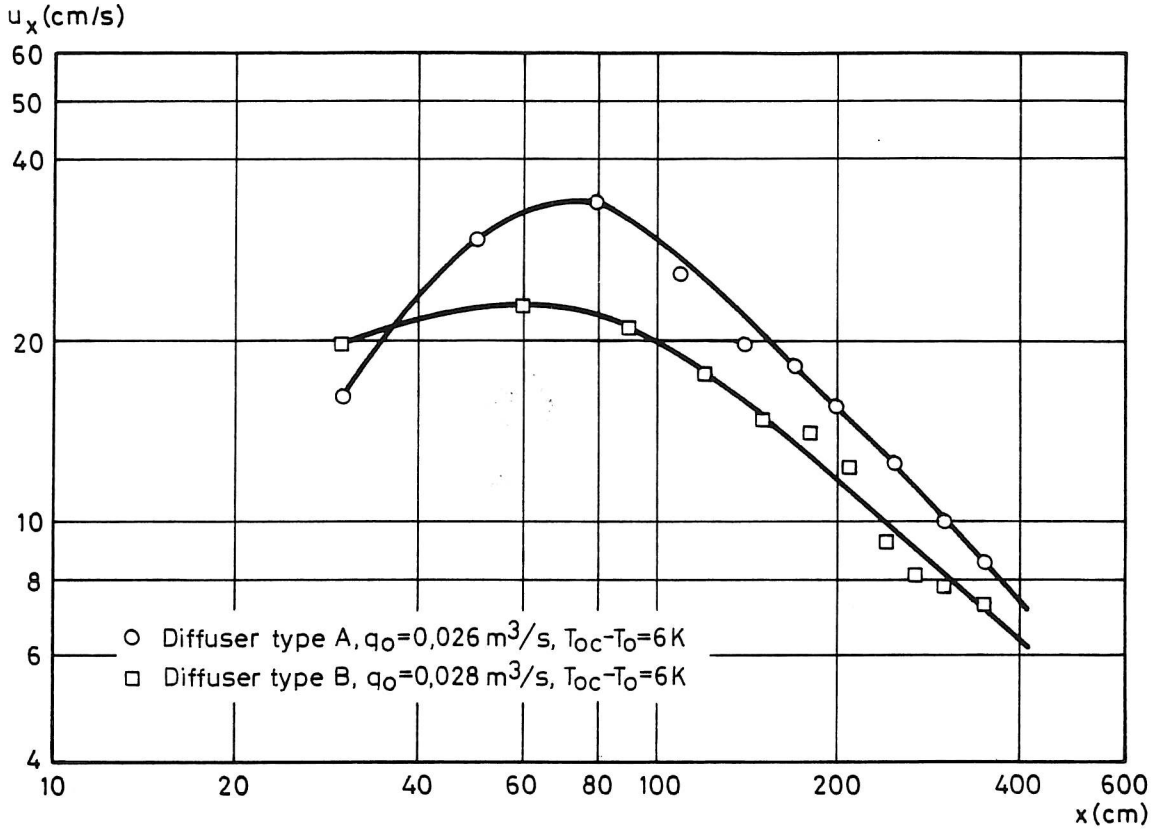

Fig. 4. Maximum velocity in the flow versus distance from diffuser.

It is important that the diffuser used for displacement ventilation is able to generate good thermal conditions in the occupied zone of the room. It is also important that the ventilation system - including the diffusers - is able to generate a high ventilation efficiency, which will be discussed in the following.

The ventilation efficiency based on temperature is given by the equation

$$\varepsilon_T = \frac{T_R - T_o}{T_{oc} - T_o} \qquad (1)$$

where T_{oc} is defined as the average temperature of the occupied zone measured at 24 points up to a height of 2.1 m.

Figure 5 shows the ventilation efficiency for diffusers A and B. The efficiency varies between 1.5 and 2.3 dependent

on the flow rate and it seems to obtain the same level rather independently of the type of diffuser.

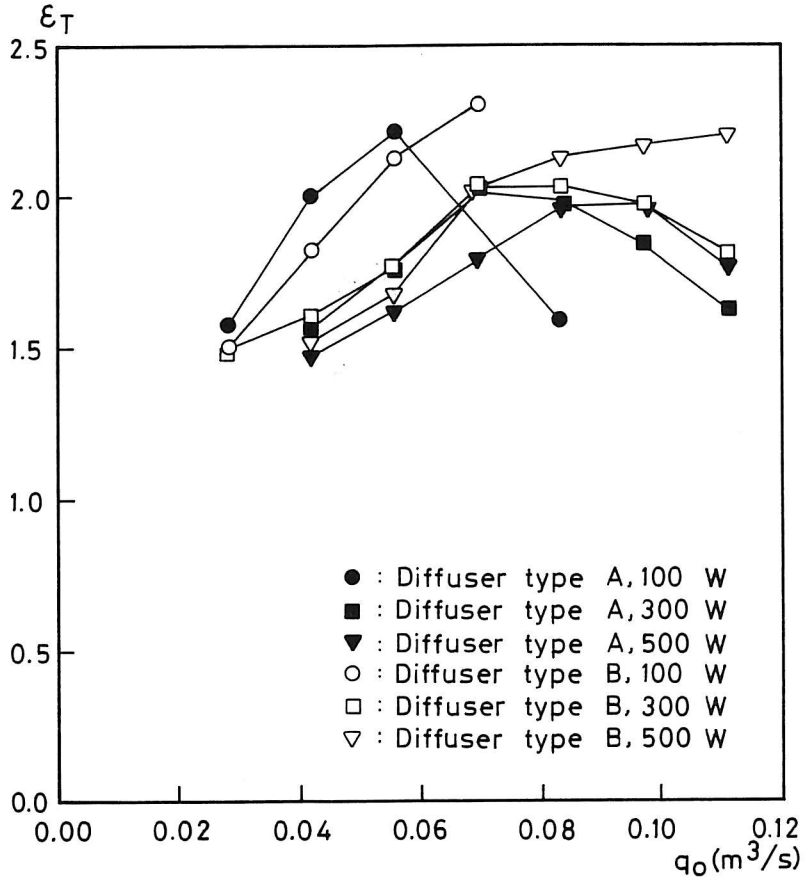

Fig. 5. Ventilation efficiency for diffusers A and B for different flow rates. Measurements by Andersen et al. [7].

THE ARCHIMEDES NUMBER AND THE FLOW

It is possible to describe the flow in a room by a set of dimensionless transport equations as demonstrated in reference [8]. All lengths involved are for example normalized with room height H, velocities with supply velocity u_o and temperatures T with ΔT_o, so they are given as $(T - T_o)/\Delta T_o$, where ΔT_o is the difference between the return temperature T_R and the suppply temperature T_o.

The following dimensionless numbers will appear in the transport equations

$$Re = \frac{u_o H \rho}{\mu} \tag{2}$$

$$Ar = \frac{\beta g H \Delta T_o}{u_o^2} \tag{3}$$

$$Pr = \frac{\mu c_p}{\lambda} \tag{4}$$

where μ, ρ, β are viscosity, density and volume expansion coefficient, respectively, and g, c_p and λ are gravitational acceleration, specific heat and thermal conductivity of the air.

The flow in the room is governed by the transport equations and the boundary conditions. This means that the air flow in the room will be uniquely described by the Reynolds number (2) and the Archimedes number (3), see reference [8].

Experiments show that the high turbulence level in a ventilated room generates a flow which is more or less self-similar and thus independent of the Reynolds number as shown for example by Müllejans [9] for the jet trajectory in a room with jet ventilation. It may also be shown that some details in the flow are dependent on the Reynolds number at low - but realistic - air flow rates, as for example the maximum velocity in the occupied zone of a room with jet-ventilation, see [10].

Assumption of self-similar flow (Reynolds' number independent) simplifies full-scale experiments as well as model experiments, and it is a useful tool in the formulation of simple design procedures. This chapter will show some examples of self-semilar flow where the Archimedes number is the only important parameter.

Figure 6 shows the results of three experiments with similar Archimedes' number and different Reynolds' number. In practice a flow is independent of the Reynolds number. It may be concluded that the air movement has a sufficient turbulence -

level for q_o > 0.023 m^3/s to obtain some self-similarity in the velocity decay along the floor. Other details in this flow may still be dependent on the Reynolds number.

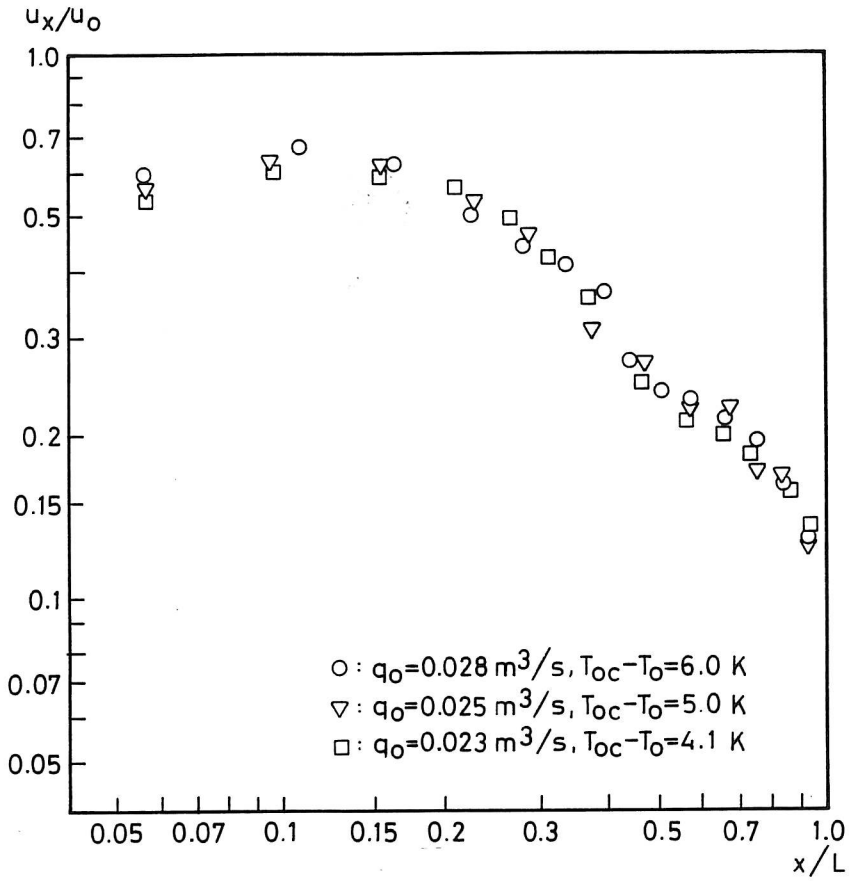

Fig. 6. Velocity decay versus distance measured for identical Archimedes' numbers for three different Reynolds' numbers. Diffuser type B. Reference [6].

Figure 7 shows vertical temperature profiles in the room for three different experiments with the same Archimedes' number. The dimensionless profiles are rather similar although the vertical profiles involve areas with a low turbulence level.

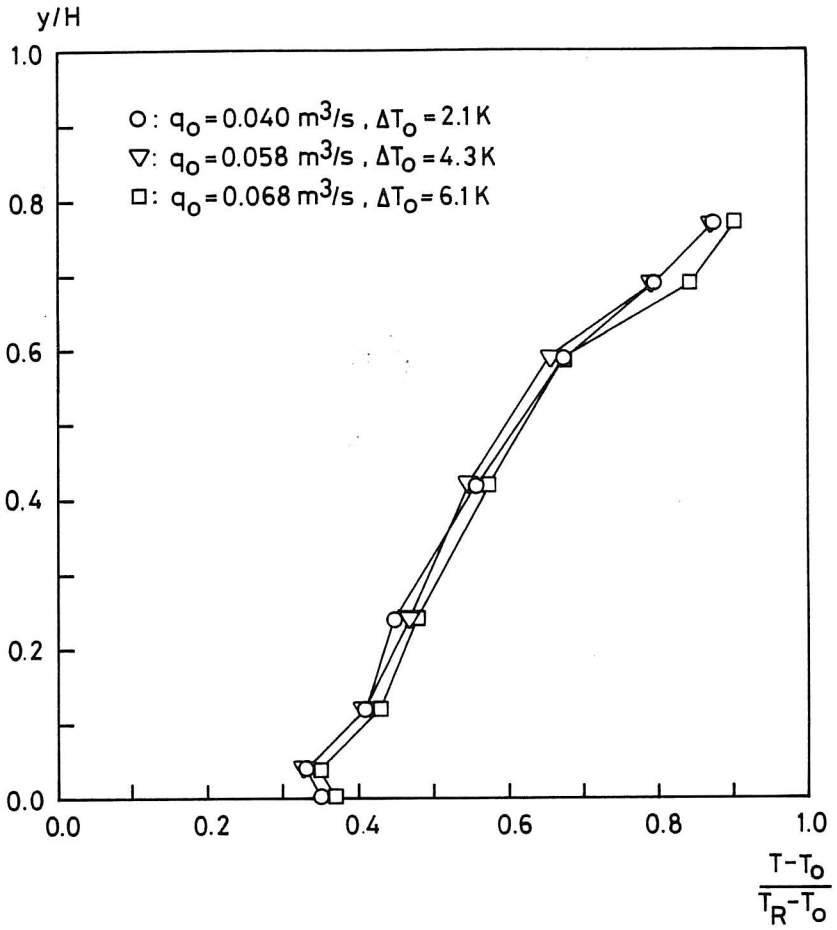

Fig. 7. Vertical temperature profile in the room for three different experiments with identical Archimedes' number. Diffuser type A. Reference [7].

The temperature efficiency is the inverted value of the dimensionless mean temperature in the occupied zone. The results in figure 7 indicate that this temperature efficiency may be a function of the Archimedes number more or less independent of the Reynolds number. It is therefore interesting to rearrange the measurements of ε_T in figure 5 so they are given as a function of Ar. Figure 8 shows this rearrangement and it is obvious that the measurements of ε_T show a fair dependence on the Archimedes number. An identical level of ε_T for the two diffusers A and B at the same Archimedes number implies that the temperature efficiency is rather

independent of the diffuser design and the local induction close to the diffuser. It is probably more dependent on other parameters which are constant in the experiments, such as heat source location and room geometry. ε_T is a function of Ar and thus a function of heat emission and air flow rate. ε_T is also influenced by the surface temperature and therefore influenced by the conductions through the walls, floor and ceiling.

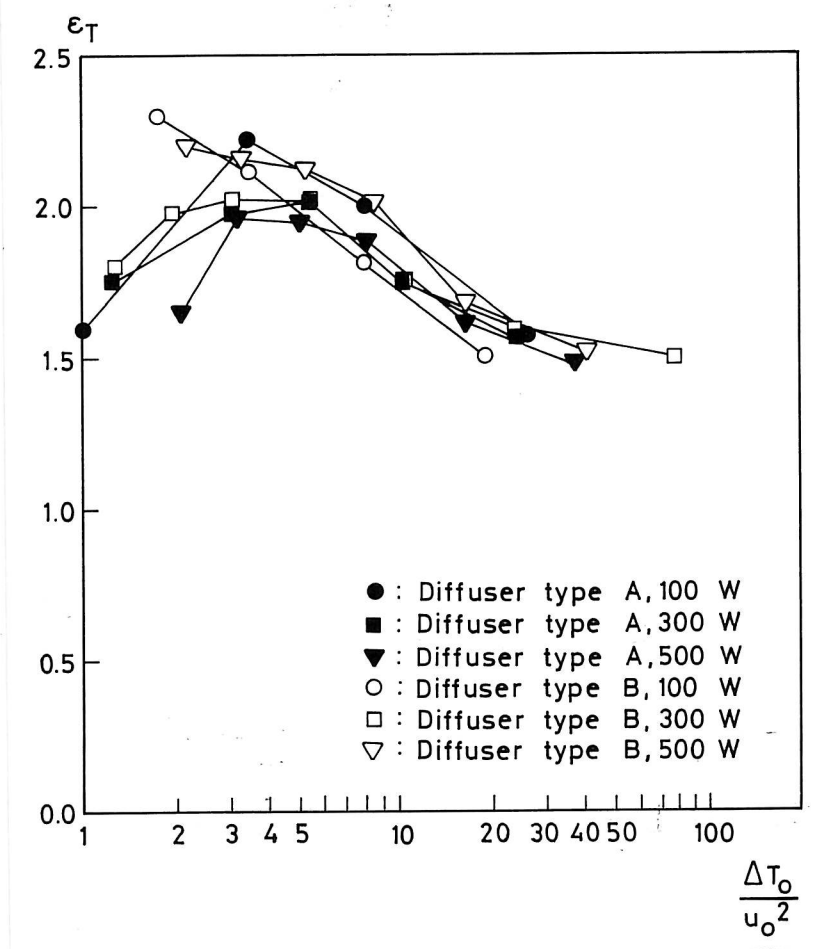

Fig. 8. Temperature efficiency ε_T versus the Archimedes number. The Archimedes number is given as $\Delta T_o/u_o^2$ $^oCs^2/m^2$.

Figure 8 shows a maximum value of the temperature efficiency of $\varepsilon_T \sim 2.0$ for an Archimedes' number of $\Delta T_o/u_o^2 \sim 4.0$ $^oCs^2/m^2$. This situation corresponds for example to the values $(\Delta T_o, u_o) \sim (2^oC, 0.71$ m/s) or (4^oC, 1.0 m/s). The flow rates for

u_o = 0.71 m/s are 0.059 m^3/s and it is 0.084 m^3/s for u_o = 1.0 m/s.

Part of the energy transport in the room takes place as radiation. This radiation is governed by other equations than the flow equations. This will influence the results in figure 7 and in figure 8 in a way which is described by other parameters than the Reynolds numbers and the Archimedes number.

DISPLACEMENT FLOW AND STRATIFICATION LEVEL

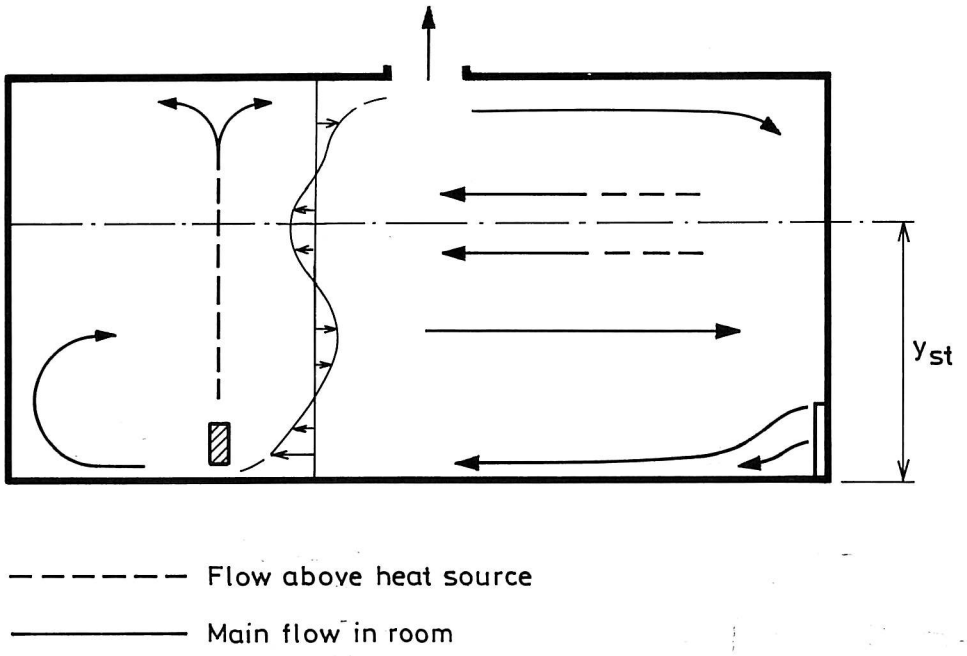

Fig. 9. Air movement and stratification level in a room with displacement flow. Diffuser type B, q_o = 0.069 m^3/s, Q = 500 W and y_{st} = 1.70 m.

Figure 9 shows the air movement in a room with displacement flow. The flow from the diffuser follows the floor along the whole room as described in connection with figure 4. There is an air movement backwards in the room at a very low

velocity above the supply flow, and it is possible to identify a second flow with a direction parallel to the supply flow. The horizontal flow in the room is connected to the vertical temperature gradient in such a way that a higher level of air movement corresponds to a higher temperature.

The heat source generates a vertical thermal plume as shown by the dotted lines in figure 9. The volume flow in this plume is given by

$$q_y = 0.005 \cdot Q^{1/3}(y + d)^{5/3} \qquad (m^3/s) \qquad (5)$$

where Q, d and y are the convective heat emission, diameter of the heat source and the vertical height, respectively, see reference [11].

The thermal plume will entrain the supply air flow q_o in the lower part of the room. The entrainment in the upper part of the room will be recirculated hot air from the plume. The stratification height y_{st} is defined as the height in the thermal plume where q_y is equal to q_o. It is possible to observe a temperature stratification at this height in rooms with a high thermal load, while it is not so easy to observe in normally loaded rooms.

The stratification height can be found by flow visualization. Smoke is added to the plume at the heat source and it will follow the thermal plume and fill the upper part of the room down to the height y_{st}. The stratification height y_{st} in figure 9 is 1.70 m.

The flow in the upper part of the room is especially characterized by a radial flow below the ceiling from the thermal plume. It is possible to observe another air movement at a lower level which is parallel to the flow in the lower part of the room.

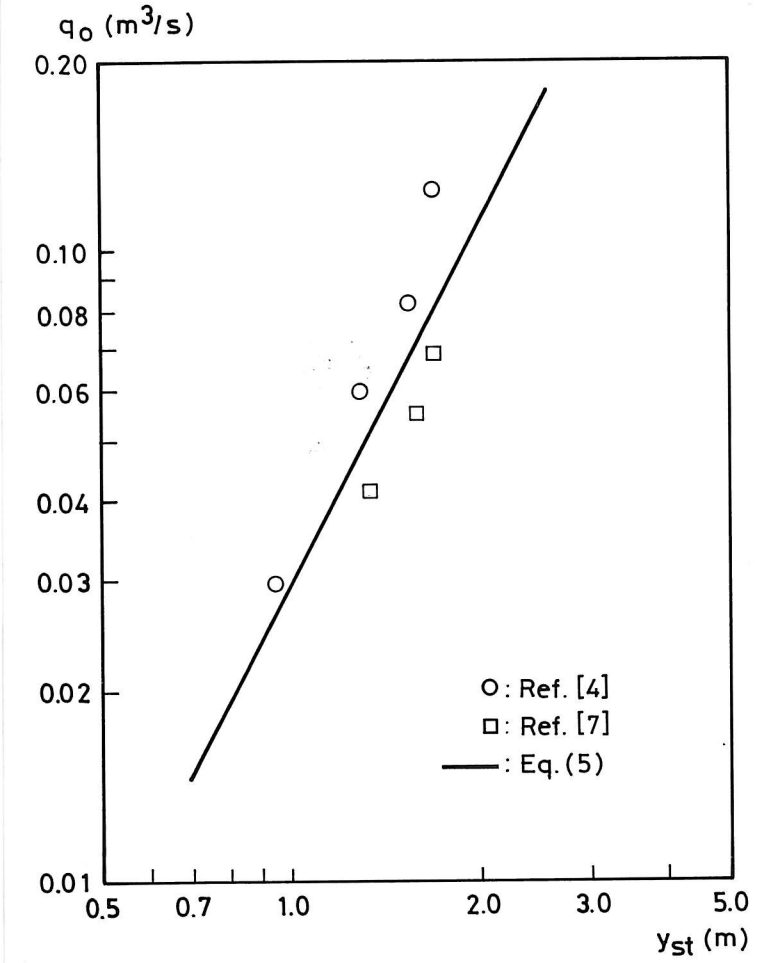

Fig. 10. Stratification height y_{st} as a function of measured supply air flow q_o or flow in plume q_y. Q = 500 W.

Theoretically it should be possible to calculate the stratification height from equation (5) for $q_o = q_y$. Figure 10 shows this calculated stratification height and measured values by flow visualizations in two different full-scale rooms. It is obvious that the measurements show the same relations between q_o and y_{st} as equation (5), but there are different levels of flow. The deviation could be explained by a natural convection along the walls in the rooms or by other disturbances. Figure 11 shows, as an example, a room with a cold downdraught which increases the stratification height, and it is obvious that a hot surface will reduce the stratification height compared to the value calculated from equation (5) for $q_y = q_o$.

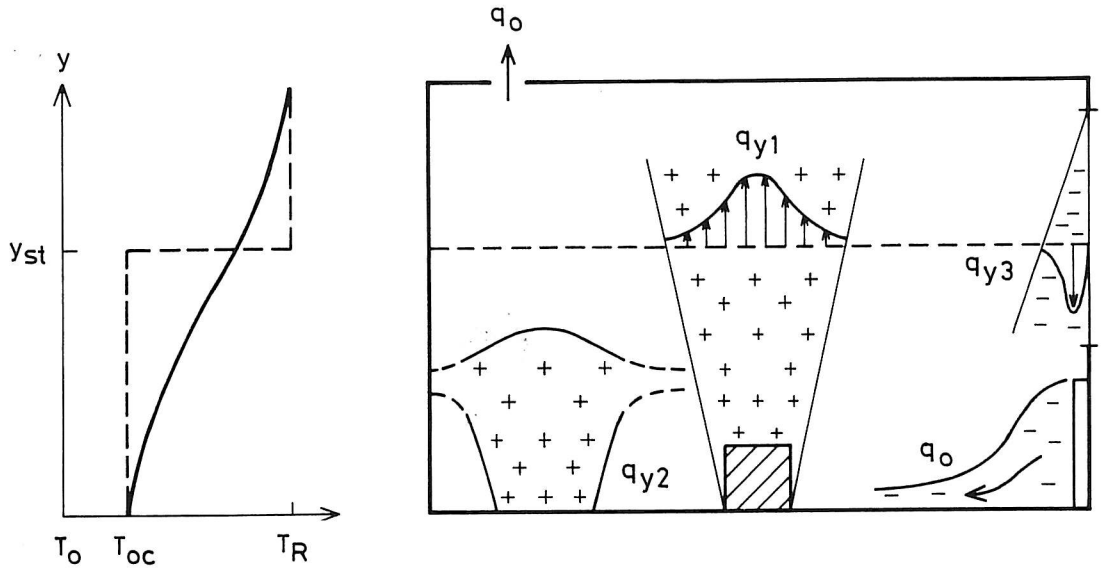

Fig. 11. Room with displacement flow and natural convection.

The stratification level in figure 11 is established at the height where $q_{y1} = q_o + q_{y3}$. The vertical temperature distribution shown in the left hand side of figure 11 is maintained by the combined effect of radiation between the surfaces, the low temperature of the supply flow, which is gradually heated by the movement in the occupied zone - see figure 9 - and by the warm flow below the ceiling. Cold downdraught and plumes from heat sources with low heat emission density - as q_{y2} - will dissolve at a height where the temperatures correspond to the ambient temperatures, and all in all it will maintain a vertical temperature distribution as shown in left hand side of figure 11.

The vertical temperature gradient in the room may have an influence on the volume flow q_y in the plumes. Equation (5) assumes a small temperature gradient, but the equation is used in practice for larger temperature gradients if the heat source is concentrated and have a high intensity. Equation (5) cannot be used for sources with very low intensity, and it cannot be used in areas where the ambient temperature will begin dissolving the plume, reference [4].

The entrainment in the plume will depend on the location of the heat source. The entrainment will be reduced to 70% when the heat source is placed close to a single wall, and it is reduced to 60% when the heat source is placed in a corner, reference [4].

CONCLUSIONS

Measurements on two different low-level diffusers show that a high initial entrainment close to the diffuser will reduce the velocity in the flow along the floor. A low entrainment will increase the velocity along the floor due to an initial acceleration genereated by the buoyancy effect.

The velocity level and velocity decay in the flow along the floor are dependent on room geometry, and therefore, it is difficult to obtain a general description of the flow which is connected to the diffuser design.

The ventilation efficiency based on temperatures is given for the diffusers for different levels of air exchange rates and thermal loads. The ventilation efficiency varies between 1.5 and 2.3 and it is rather unaffected by the type of diffuser.

Examples show that the general flow and the temperature distribution can be described as self-similar and thus as a fully developed turbulent flow. This means that the air movement can be described by the boundary values and the Archimedes number rather independently of some variations in the Reynolds number. Measurements show a distinct connection between ventilation efficiency and Archimedes' number.

It may be difficult to identify a thermal stratification in a room with displacement ventilation. Flow from plumes and cold downdraught at different levels, as well as thermal radiation, will maintain a vertical temperature profile which is more or less linear.

LIST OF SYMBOLS

Ar	Archimedes' number	
c_p	Specific heat capacity	J/kgK
d	Diameter of heat souce	m
g	Gravitational acceleration	m/s^2
H	Height of room	m
L	Length of room	m
n	Exponent	
Pr	Prandtl's number	
Q	Heat emission	W
q_o	Volume flow supplied to the room	m^3/s
q_y	Volume flow in thermal plume	m^3/s
Re	Reynolds' number	
T	Temperature	^oC
T_o	Supply temperature	^oC
T_{oc}	Mean temperature in the occupied zone	^oC
T_R	Return temperature	^oC
u_o	Supply velocity	m/s
u_x	Maximum velocity along floor	m/s
W	Width of room	m
x	Coordinate	m
y	Coordinate	m
y_{st}	Stratification height	m
β	Volume expansion coefficient	K^{-1}
ΔT_o	Temperature difference T_R-T_o	K
ε_T	Ventilation (temperature) efficiency	
λ	Thermal conductivity	W/mK
μ	Dynamic viscosity	Ns/m^2
ρ	Density	kg/m^3

REFERENCES

[1] Skåret, E., Displacement Ventilation, Room Vent 87, International conference on air distribution in ventilated spaces, Stockholm, 1987.

[2] Fitzner, K., Impulsarme Luftzufuhr durch Quellüftung, HLH, Bd 39, 1988.

[3] Sandberg, M. and Lindström, S., A Model for Ventilation by Displacement, Room Vent 87, International conference on air distribution in ventilated spaces, Stockholm, 1987.

[4] Kofoed, P. and Nielsen, P.V., Thermal Plumes in Ventilated Rooms - An Experimental Research Work, III seminar on Application of Fluid Mechanics in Environmental Protection, Silezian Technical University, Gliwice, Poland, 1988.

[5] Mathisen, H.M., Air Motion in the Vicinity of Air-Supply Devices for Displacement Ventilation, "Effective ventilation", 9th AIVC Conference, Gent, Belgium, 1988.

[6] Nielsen, P.V., Hoff, L. and Pedersen, L.G., Displacement Ventilation by Different Types of Diffusers, "Effective Ventilation", 9th AIVC Conference, Gent, Belgium, 1988.

[7] Andersen, M., Hauervig, A., Hjortsøe, J., Mathiesen, P.M., Nielsen, A. and Pedersen, M., Private communication, University of Aalborg, 1988.

[8] Nielsen, P.V., Flow in Air-Conditioned Rooms (English translation of Ph.D. thesis from the Technical University of Denmark, 1974), Danfoss A/S, 1976.

[9] Müllejans, H., Über die Ähnlichkeit der nicht-isothermen Strömung und den Wärmeübergang in Räumen mit Strahllüftung, Diss., T.H. Aachen, 1963.

[10] Nielsen, P.V., Numerical Prediction of Air Distribution in Rooms - Status and Potentials, Annex 20 Kick-Off meeting, International Energy Agency, Winterthur,

1988, ISSN 0902-7513 R8823.

[11] Baturin, V.V., Fundamentals of Industrial Ventilation, Pergamon Press, 1972.

Appendix B

Thermal Plumes in Ventilated Rooms

Peter Kofoed and Peter V. Nielsen

THERMAL PLUMES IN VENTILATED ROOMS - Measurements in Stratified Surroundings and Analysis by use of an Extrapolation Method.

Peter Kofoed and Peter V. Nielsen
University of Aalborg
Aalborg, Denmark

Summary.

The design of a displacement ventilation system involves determination of the flow rate in the thermal plumes. The flow rate in the plumes and the vertical temperature gradient influence each other, and they are influenced by many factors. This paper shows some descriptions of these effects.
Free turbulent plumes from different heated bodies are investigated. The measurements have taken place in a full-scale test room where the vertical temperature gradient have been changed. The velocity and the temperature distribution in the plume are measured. Large scale plume axis wandering is taken into account and the temperature excess and the velocity distribution are calculated by use of an extrapolation method.
In the case with a concentrated heat source (dia 50mm, 343W) and nearly uniform surroundings the model of a plume above a point heat source is verified. It represents a borderline case with the smallest entrainment factor and the smallest angle of spread. Due to the measuring method and data processing the velocity and temperature excess profiles are observed more narrowly than those reported by previous authors.
In the case with an extensive heat source (dia 400mm, 100W) the model of a plume above a point heat source cannot be used. This is caused either by the way of generating the plume including a long intermediate region or by the environmental conditions where vertical temperature gradients are present. The flow has a larger angle of spread and the entrainment factor is greather than for a point heat source.
The exact knowledge of the vertical temperature gradient is essential to predict the flow propagation due to its influence on the entrainment, e.g. in an integral method of plume calculation . Since the flow from different heated bodies is individual full-scale measurements seem to be the only possible approach to obtain the volume flow in: thermal plumes in ventilated rooms.

Nomenclature.

Ar	Archimedes number, $Ar = \beta g \Delta T R / v^2$
c_p	specific heat at constant pressure
E	kinetic energy flux
F_0	buoyancy flux
G	air volume supplied
H	enthalpy flux
I	momentum flux
m	velocity distribution factor
n	air change rate in room
p	temperature distribution factor
r	radial distance from plume axis
R	profile width where 1/e of the maximum value is obtained
Q_0	convective heat from source
ΔT	mean temperature excess, $\Delta T = T - T_\infty$
x	vertical height above source
V	volume flux
v	vertical mean velocity
dT/dx	vertical temperature gradient
$-g\Delta\rho/\rho_\infty$	buoyancy in plume, $\Delta\rho = \rho - \rho_\infty$

Greek Symbols.

α	entrainment factor
β	thermal expansion coefficient
λ	ration between profile width, $\lambda = R_T/R_V$
ρ	local plume density

Subscripts.

0	source condition
F	floor
M	maximum value
∞	ambient condition
R	return
ST	stratification
T	temperature
V	velocity

1. Introduction.

1.1. Thermal Plumes in Ventilated Rooms.

During the last 10 years vertical displacement systems have grown popular as comfort ventilation in rooms with heat loads e.g. office rooms. The plumes from hot surfaces, from equipment located at different heights and from persons together with cold downdraught from cold surfaces make a rather complicated situation as shown in fig.1., ref. (17,18).

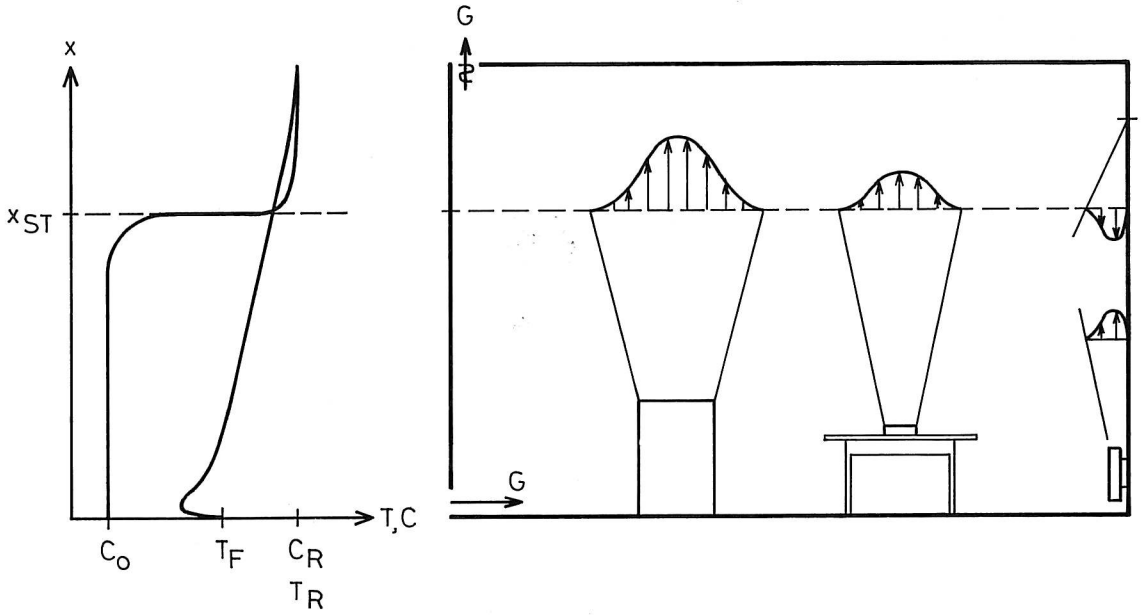

Fig.1. Vertical displacement flow in an office room. The primary air is supplied in the occupied zone and is entrained in the hot plumes from the heat sources and in the cold downdraught. Dependent on the air flow supplied G and the vertical air flow in the room there must be a height x_{ST} where the upward moving air flow is equal to the supplied air flow. This is experimentally shown by Heiselberg & Sandberg (4). The graphs to the left show: I. the vertical temperature gradient created by interaction between the different plumes and by radiation between the surfaces in the room and II. the contaminant distribution created only by the plumes.

The design of a displacement ventilation system involves determination of the flow rate in the thermal plumes so that a reasonable supply air quantity G can be chosen. In practice simple formula systems based on plume models above a point heat source have been used. However, the flow is much more complex and is influenced by many factors, e.g. vertical temperature gradients. Experiments and literature study show this, ref. (1,2,5,6,7,12, 17). At the present moment no satisfactory description of the flow is given. It is the purpose of this work to verify a possible approach.

1.2. Previous Works.

Turbulent buoyant axisymmetric plumes have been investigated for around 50 years. Turbulent plumes in a uniform environment are treated by Schmidt (16) in 1941. Schmidt makes basic assumptions about the flow from a point heat source extending Prandtl's mixing length theory. For the axial velocity and excess temperature and the width the results are:

$$(1) \qquad v \approx x^{-1/3}$$

$$(2) \qquad \Delta T \approx x^{-5/3}$$

$$(3) \qquad r \approx x$$

Rouse, Yih and Humphreys (15) in 1952 introduce a similarity hypothesis. The result is consistent with Schmidt's and the following expressions for volume flux V, momentum flux I and kinetic energy flux E are obtained:

$$(4) \qquad V = 2\pi \int_0^\infty vr\, dr \qquad \approx x^{5/3}$$

$$(5) \qquad I = 2\pi \int_0^\infty \rho v^2 r\, dr \qquad \approx x^{4/3}$$

$$(6) \qquad E = 2\pi \int_0^\infty \tfrac{1}{2}\rho v^3 r\, dr \qquad \approx x$$

Traditionally the dimensionless radial velocity and excess temperature distributions f_1 and f_2, respectively, are approximated by Guassian curves:

$$(7) \qquad f_1(r/x) = \exp(-m(r/x)^2)$$

$$(8) \qquad f_2(r/x) = \exp(-p(r/x)^2)$$

Popiolek (12) in 1981 gives an analysis of the plume above a heat source and also takes up the similarity hypothesis. The following functions for the velocity and buoyancy are obtained:

$$(9) \qquad v = \left(\frac{3}{2\pi}\right)^{1/3} \left(\frac{m^2}{p} + m\right)^{1/3} F_0^{1/3}\, x^{-1/3} \exp\left(-m\left(\frac{r}{x}\right)^2\right)$$

$$(10) \qquad \frac{-g\Delta\rho}{\rho_\infty} = \left(\frac{2}{3\pi^2}\right)^{1/3} \left(\frac{p(m+p)^2}{m}\right)^{1/3} F_0^{2/3}\, x^{-5/3} \exp\left(-p\left(\frac{r}{x}\right)^2\right)$$

where F_0 is the buoyancy flux connected with the convective heat output Q_0 from the source in the following way:

$$(11) \qquad F_0 = Q_0 ßg/c_p \rho$$

If equation 11 together with the values c_p=1005 J/kgK and ρ=1.205 kg/m^3 are assumed, Popiolek gets:

$$(12) \qquad v = 0.023 \left(\frac{m^2}{p} + m\right)^{1/3} Q_0^{1/3}\, x^{-1/3} \exp\left(-m\left(\frac{r}{x}\right)^2\right)$$

$$(13) \qquad \Delta T = 0.011 \left(\frac{p(m+p)^2}{m}\right)^{1/3} Q_0^{2/3}\, x^{-5/3} \exp\left(-p\left(\frac{r}{x}\right)^2\right)$$

Morton, Taylor and Turner (8) in 1956 consider plumes also in stratified surroundings. Integral forms of the continuity, momentum and buoyancy equations together with similarity variables for velocity and density are used. The problem is closed by adopting Taylor's entrainment assumption - simply that the entrainment is proportional to the mean centerline velocity:

$$(14) \qquad V_{ENTRAINMENT} = \alpha v$$

Fox (2) and Morton (9) in the beginning the 1970'es suggest some improvements of the entrainment assumption. Fox finds that the entrainment is a function of the Reynolds stresses α_1, form of the similarity profiles α_2 and the local Archimedes number Ar:

$$(15) \qquad \alpha = \alpha_1 + \alpha_2 Ar$$

Popiolek and Knapek (13) in 1982 analyse the integral method of plume calculation. Popiolek and Mierzwinski (14) present some calculations in 1984. The flow is strongly dependent on stratification, and the problem of the entrainment has not been completely solved yet.

In the 1970'es differential turbulence models are used to predict the flow in turbulent buoyant plumes. The level of sophistication is high and the drawback of this approach lies in the increased complexity of the formulation and consequent increased computer time required. A rewiev is given by Chen, ref. (1). The modelling of buoyant flows still presents uncertainties and additional work is necessary.

Many quantitative experiments are performed to confirm the theoretical predictions, ref. (1,3,5,6,7,8,11,12,15,16). The most cited experiment is Rouse et al. (15), where the velocity and temperature distribution factors in equation 9 & 10 are: m=96 and p=71 respectively.

2. Experimental Technique.

The measurements have taken place in a full-scale room - 8 x 6 x 4.6 m. A displacement ventilation system with 2 wall-mounted diffusers and 2 exhaust openings in the ceiling are installed, so that the room can be ventilated and different vertical temperature gradients created, if required. A picture of the room is given in fig.2.

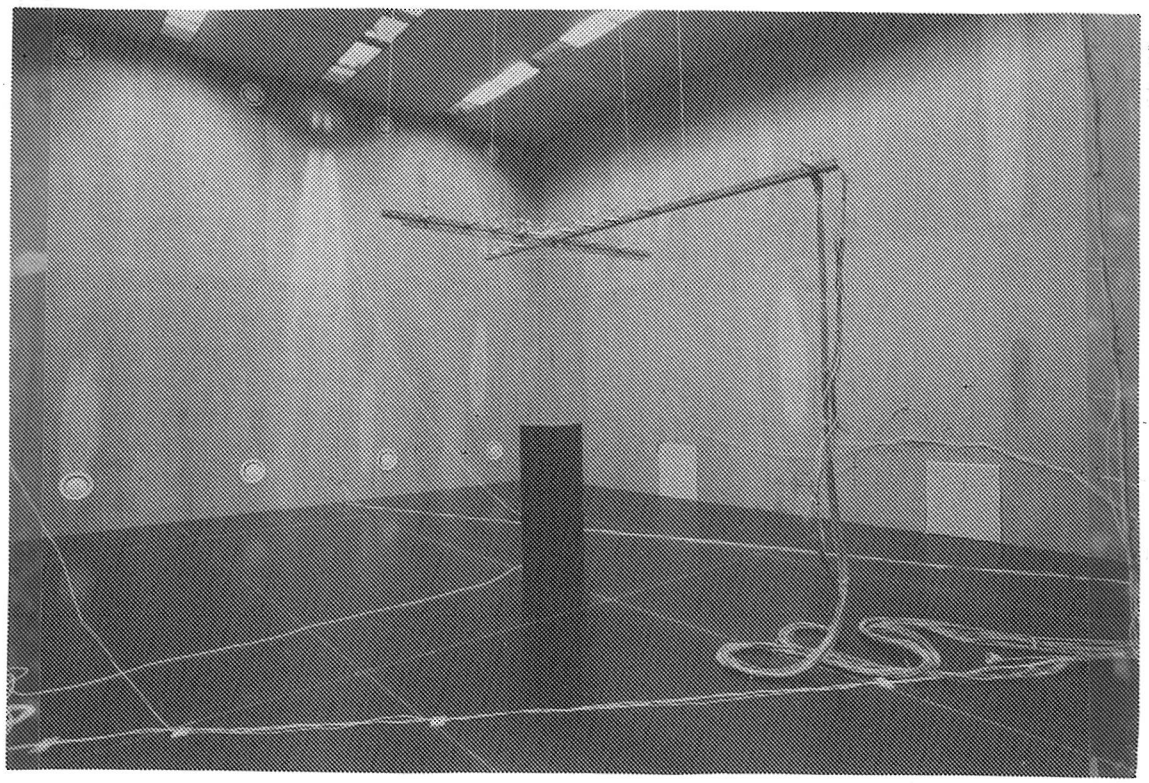

Fig.2. Full-scale room with wall mounted diffusers, heat source and measurement equipment.

The velocity measurements are carried out using a Dantec 54N10 low velocity multiflow analyser with Dantec 54R10 temperature compensated sphere probes. The temperature excess in the plume is measured with termocouples. 17 velocity probes and 17 termocouples are located in the flow. Additonal 33 thermocouples are used to get information about the surrondings.

2.2. Experimental Procedures.

In plume experiments large scale flow instability is often present. Rouse et al. (15) measurements show that the velocity and temperature profiles are symmetrical about the maximum. Rouse et al. (15) and Mierzwinski (6) observed that the maximum value often occurs at a point situated away from the vertical centerline to the source. Popiolek (12) presents a measuring method and data processing which take the plume axis wandering into account. In this paper it is called the extrapolation method:

The extrapolation method. The probes are placed in a coordinate system - in this work 9 velocity probes and 9 termocouples on each axis. The common probe or origin is located in the symmetry axis to the source. For each of the axes the temperature measurements are approximated by a Gaussian distribution curve. The symmetry axes of the 2 curves are found and thereby the position of the plume axis. Next the measuring points distances from the plume axis are calculated. On this basis it is possible to extrapolate the true temperature excess and velocity Gaussian curves.

The vertical temperature gradient in the room is held at different values by changing the inlet temperature. Measurements without mechanical ventilation also have taken place.

2.3. Calibration.

In general the flow velocity and temperature excess in thermal plumes are small - often less than 0.10 m/s and 0.5 K, respectively. **Velocity.** The effect of the natural convection around the hot sphere of the velocity probe has to be taken into account, therefore calibration in vertical flow is carried out. **Temperature.** To eliminate the accuracy of cold junction temperature stabilization as well as calibration accuracy the temperature excess in the plume are measured as a difference between temperatures in 2 points. Here the exact knowledge of the thermocouple sensitivity is essential.

3. Measurement Results and Discussion.

3.1. Preliminary Remarks.

The sampling time of measuring is 180 seconds. The treatment of the data is done using the extrapolation method. One single experiment has been performed several times to make sure the reproducibility of the data and constant values obtained. If account were not taken to the axis wandering the axial velocity v_M and temperature excess ΔT_M would be lower and the width of the profiles R_v & R_T greather. The plume axis wandering observed is of the order 25 % R_T.

3.2. Plume in Uniform Environment.

The aim of this measurement series is the experimental verification of the point heat source model. In general the flow in the plume above a heat source propagating in environment without a vertical temperature gradient (dT/dx=0) can be divided into 3 zones as shown in fig.3., ref (7). The model of a plume above a point heat source is characterized by flow in zone 3.

In ventilated rooms environment with zero stratification very seldom occurs. During this measurement series the vertical temperature gradient dT/dx is less than 0.05 K/m in the measuring zone 0.75 to 3.50 m above the floor - the closest to uniform environment that is obtained. The heat source is concentrated - a 343 W dia 50 mm vertical tube with heating coils. The source is placed in mineral wool and the air is sucked through the source from below. The measurement results are shown in table 1.

Vertical tube dia=50mm h=150mm Q=343W Recircl.flow G=0m^3/s n=0h^{-1} Ver.temp.grad. dT/dx=0.05 K/m												
Plume parameters	Height above source x m											Notice
	0.75	1.00	1.25	1.50	1.75	2.00	2.25	2.50	2.75	3.00	3.25	
vM m/s	.874	.607	.625	.624	.631	.615	.587	.572	.557	.535	.517	Gaussian fit by minimizing a sum of squares
Rv m	.106	.154	.186	.207	.231	.254	.284	.309	.331	.367	.391	
ΔT_M C	13.3	11.7	7.6	5.3	4.1	3.4	3.0	2.4	1.9	1.5	1.3	
RT m	.085	.099	.129	.164	.214	.241	.273	.284	.319	.354	.376	
H W	195	187	206	208	241	240	232	223	210	202	191	Integral plume parameter values
V m^3/s	.031	.045	.068	.084	.106	.125	.149	.172	.192	.226	.249	
I kgm/s^2	16	16	25	31	40	46	52	59	64	73	77	
Ar	.062	.162	.124	.095	.080	.076	.075	.075	.068	.066	.065	
λ	.80	.64	.69	.79	.93	.95	.96	.92	.96	.96	.96	
m	281	96	125	125	94	95	94	112	112	117	124	Local approximation by a model of a plume above a point source
p	440	233	261	200	110	105	102	134	121	126	134	
α	.050	.085	.074	.075	.086	.086	.086	.078	.078	.077	.075	

Table 1. Measurement results.

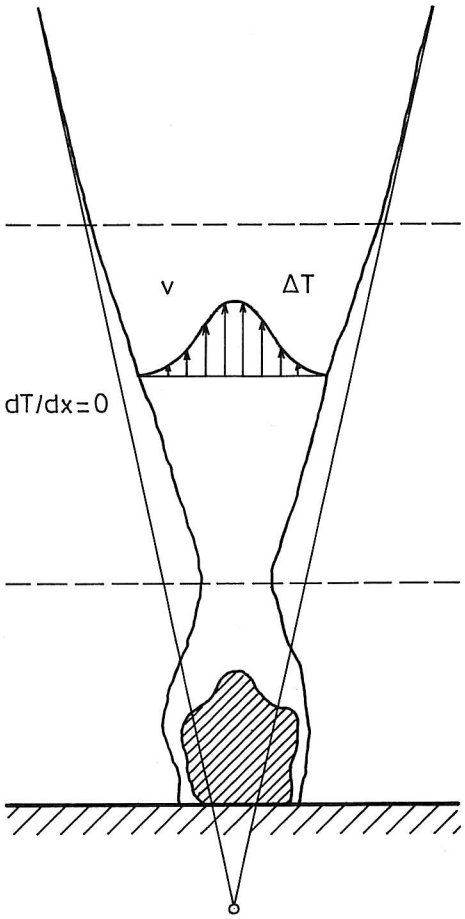

Zone 3, the zone of complete similarity: The flow is fully developed, the plume spreads linearly, the local Archimedes number Ar and the ratio of temperature and velocity profiles widths λ are constant.

$$\lambda = \left(\frac{m}{p} \right)^{1/2} \qquad Ar = \frac{2}{3} \frac{p}{m^{3/2}}$$

Zone 2, the intermediate zone: The plume is turbulent and axisymmetrical, the velocity and temperature distribution curves are of Gaussian type, the plume spreads non linearly, the local Archimedes number Ar and the ration of temperature and velocity profiles widths λ change.

$$\lambda = \frac{R_T}{R_V}$$

Zone 1, the boundary layer zone. Transition from boundary layer to a plume form, laminar flow becomes turbulent.

Fig.3. The flow regions in the plume above a heat source without vertical temperature gradient, dT/dx=0 K/m, ref. (7).

The flow in a plume above a point heat source is characterized by complete similarity. In the area x = 1.75 to 3.25 m constant ratio between the velocity and temperature excess widths is observed, the mean ratio is λ = 0.96. The velocity and temperature excess distribution factors in equation 12 and 13 are: m = 110 and p = 115. The mean enthalpy flux H which equals the convective heat supplied is Q_o = 221 W.

3.2.1. Axial Distribution.

Width. The axial increase of the width is shown i fig.4.

The measurements have taken place in: Zone 2, intermediate zone, where the plume spreads non-linearly and the ration λ of the temperature and velocity profiles changes. Zone 3, the region of complete flow similarity, where the plume spreads linearly and the ration λ between the velocity and temperature excess profiles is constant. The experimental temperature width values in zone 3 are reduced to a strait line by means of a least mean square method. Note that the widths do not become zero at the top of the heat source. In this case the virtual point of plume propagation is situated below the heat source, x_o = -0.22 m. The strait line representing the velocity width values is drawn through the virtual point. The excess temperatur width spreads with an angle of 7.6 degrees. The spread of the velocity width is greather.

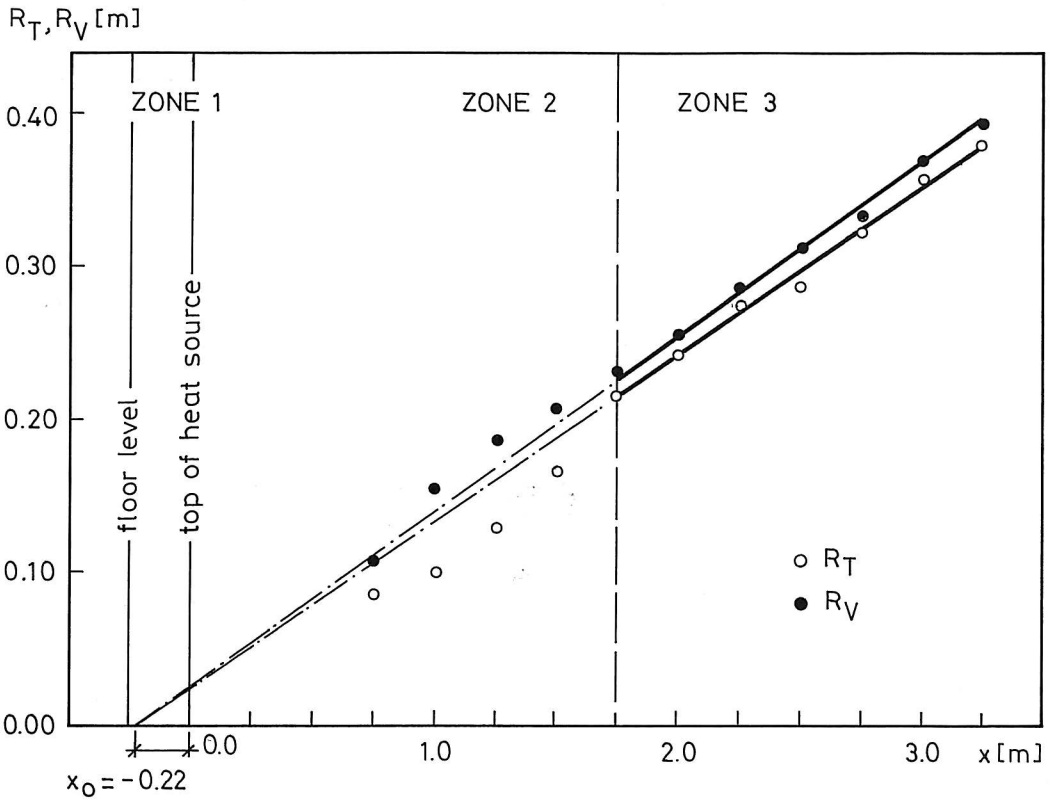

Fig.4. Increase of plume width R_T & R_V.

Velocity. The velocity measurements do also indicate that the flow can be divided in regions: Zone 2 with acceleration and zone 3 with a velocity decay of the type $v \approx (x-x_0)^k$ as shown in fig.5.

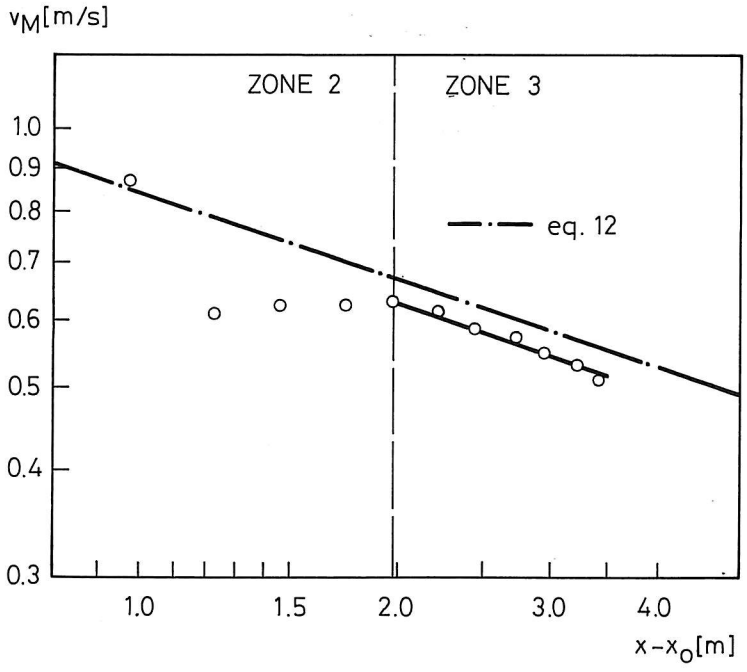

Fig.5. Distribution of maximum mean velocity v_M along the axis of the plume.

The power k = -1/3 as indicated in the similarity hypothesis is verified in zone 3. But the velocities are about 7 % lower than the values obtained by equation 12. The flow shows no disintegration tendencies. For the practical use it is worth mentioning that the flow up to x = 1.75 m (2.00m above the floor) still is in the intermediate zone, zone 2, where the flow cannot completely be described by the model of a plume above a point heat source.

Excess Temperature.

Fig.6. shows that the mesured temperatures are close to the values given by equation 13. They are below the values given by equation 13, and the power is numerically greather than -5/3 as given by the similarity hypothesis. This may indicate the influence of the vertical temperature gradient, though it is very little, and it is further indicated by the fall in heat flux H in table 1.

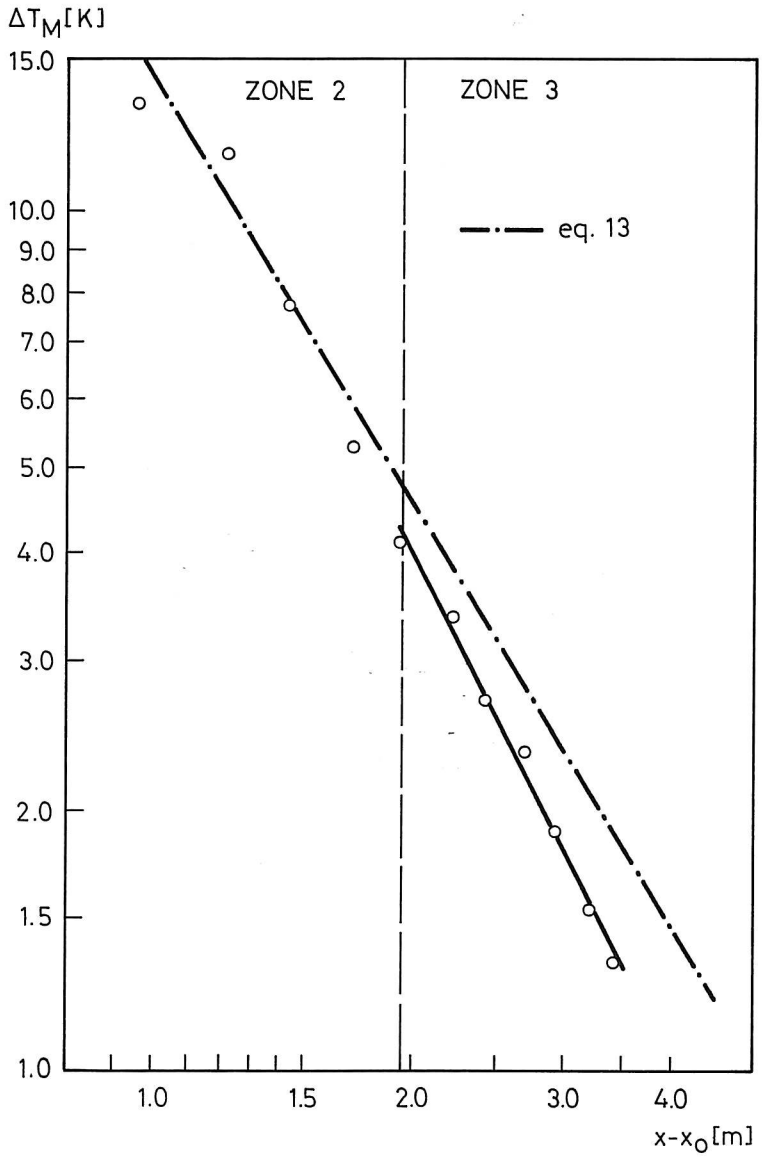

Fig.6. Distribution of maximum mean temperature excess ΔT_M along the axis of the plume.

Volume flux. The volume flux V in the plume is found as the volume of the rotation Gaussian distribution function. Eq. 4, 12, m = 110 & p = 115 give:

$$(16) \qquad V = 0.0051\ Q_0^{1/3}\ (x-x_0)^{5/3}$$

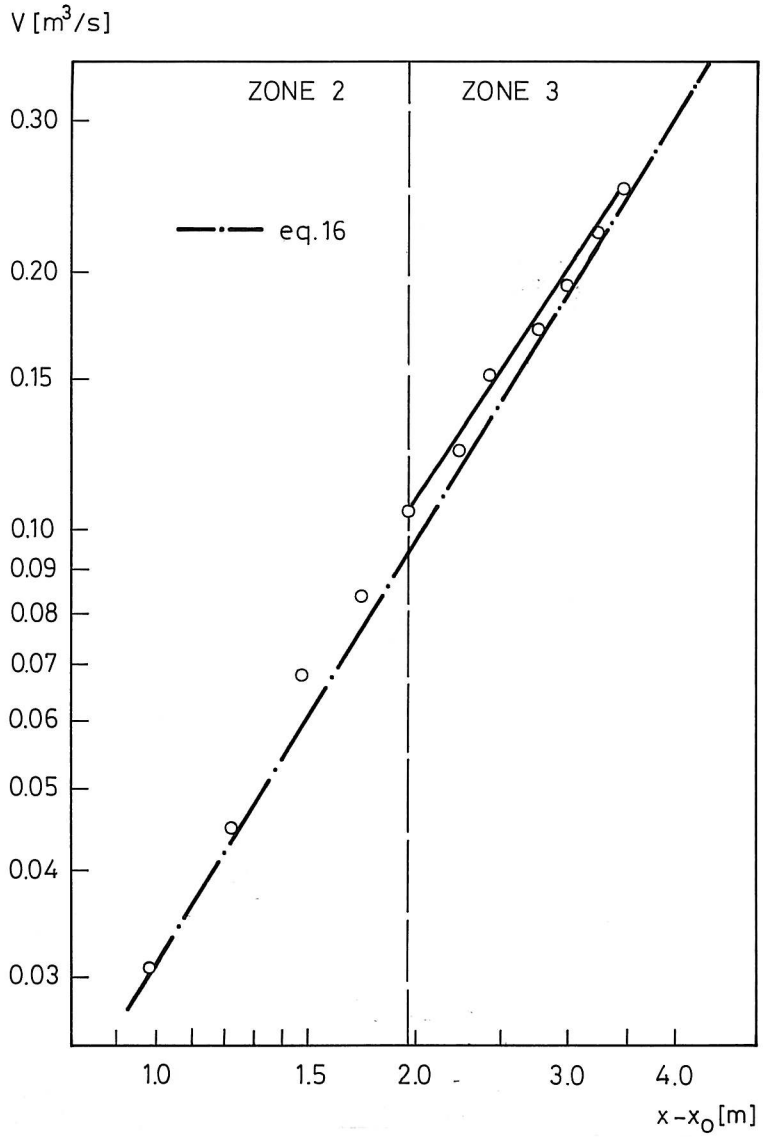

Fig.7. Distribution of volume flux $V = \pi v_M R_V^2$ along the plume axis.

The measurements show good aggrement with equation 16. The power 5/3 is observed in both zones, though the flow in zone 2 does not fulfil other elements of the flow in a plume above a point heat source. The explanation is that the width Rv of the velocity profile is greather than indicated by the strait line in fig.4, which compensates for the lower velocity v_M in fig.5.

Momentum Flux. Equation 5,12,13, m=110 & p=115 give the following formula for the momentum flux I:

$$(17) \qquad I = 0.00043\ Q_0^{2/3}\ (x-x_0)^{4/3}$$

The measurements show good aggrement with equation 17 in both zones. The explanation is the same as before. The slope in zone 3 is a litte smaller than 4/3.

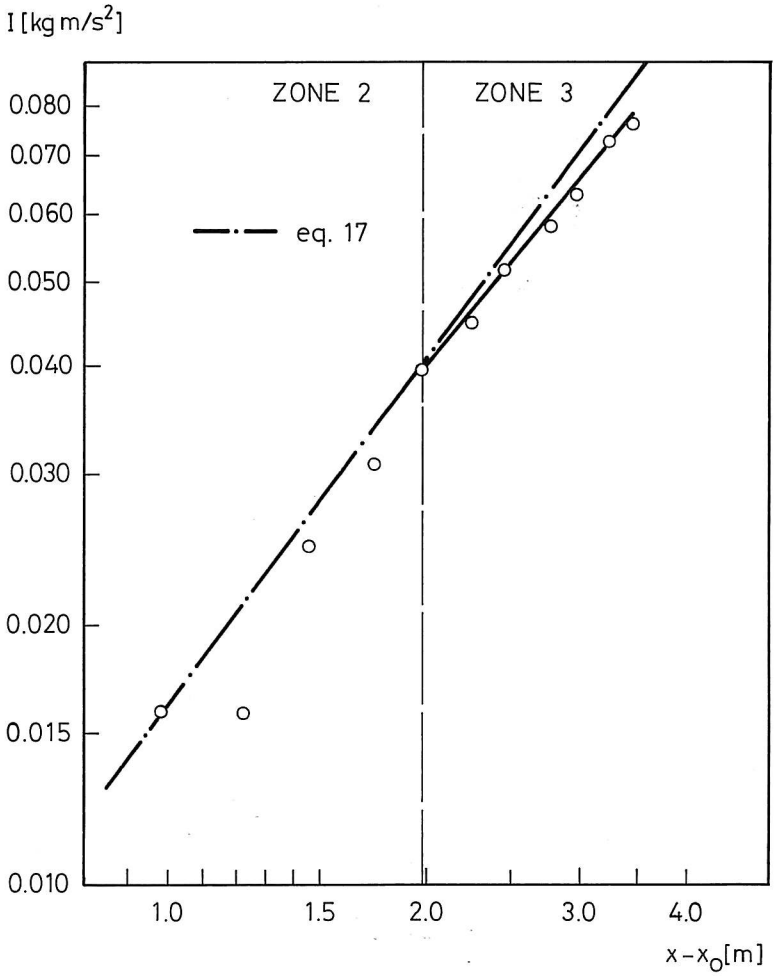

Fig.8. Distribution of momentum flux $I = \frac{1}{2}\pi\rho v_M^2 R_V^2$ along the plume axis.

3.2.2. Radial Distributions.

Mean velocity and temperature excess profiles. As mentioned before the similarity in mean profiles of velocity and temperature is reached at x = 1.75 m. The spread of the velocity profile is greather than that of the temperature, $\lambda = R_T/R_V = 0.96 < 1$. In table 2 the velocity and temperature distribution factors m and p from equation 7 & 8 are compared with the results from previous works.

Rouse et al. (15) indicate as the only author that the spread of buoyancy is greather than that of momentum, p = 71 < m = 96 and $\lambda = 1.16$. This result may be influenced by the fact that Rouse et al. used a wane anemometer (3 cm dia) with a lower limit of 6 cm/s. The accuracy of such an instrument is less than those reported here. In contrast the results of other authors are coincident with the present results. This means it is more likely that the spread af momentum is at least equal or wider than that of thermal energy, p > m and $\lambda < 1$. The profiles are compared in fig.9.

Velocity & temperature distribution factors and instrumentation			
m	p	Author	Instrumentation
45?	45	Schmidt 1941 (16)	1 HWA
55	65	George 1977 (3)	1 HWA & 1 RT
65	70	Nakagome 1976 (11)	1 HWA & 1 RT
80		Morton 1956 (8)	1 HWA
96	71	Rouse 1952 (15)	1 VA & 1 TC
110	115	Present work	17 HSA & 17 TC

Abbreviations:
HWA hot wire anemometer
VA vane anemoneter
HSA hot sphere anemometer
RT resistance thermometer
TC thermocouple

Table 2. Velocity and temperature distribution factors and instrumentation.

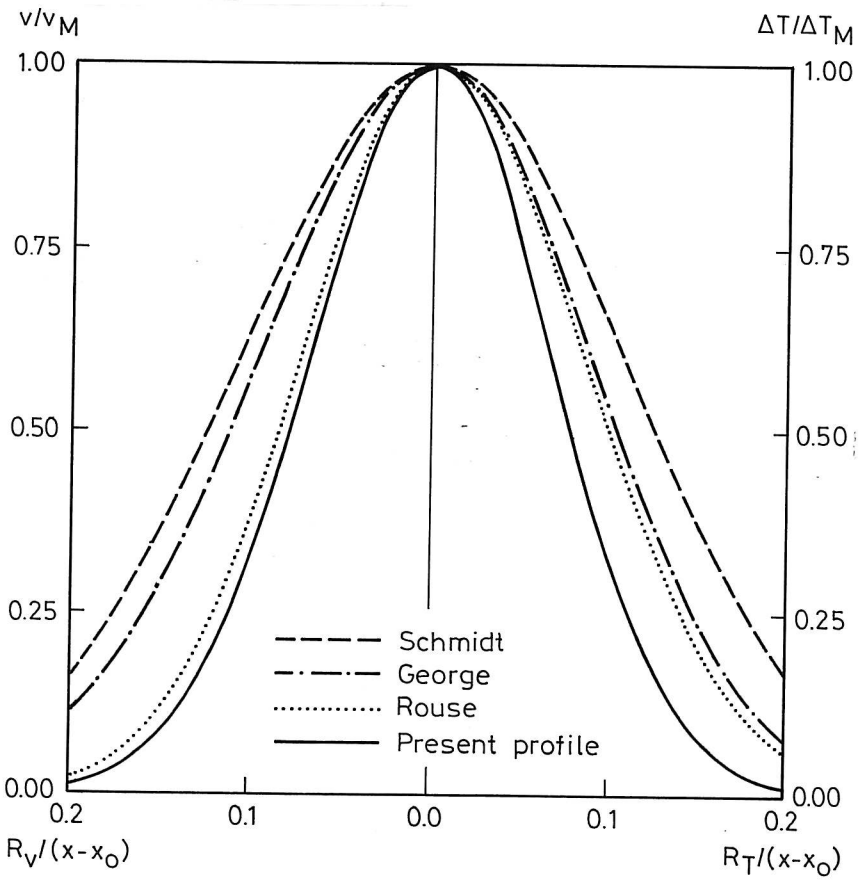

Fig.9. Distribution of dimensionless mean velocity v/v_M and mean temperature excess $\Delta T/\Delta T_M$ in a plume.

The results of the present work show more narrow profiles. The explanation is due to the measuring method and data processing, which take the plume axis wandering into account. George et al. (3) mention that the plume maybe has not reached a fully developed state resulting in a larger angle of spread. The same thing could be present in the results of Rouse et al. (15) because they use a gas burner as source giving a long intermediate zone.

3.2.3. Entrainment. The entrainment factor α based on a model of a plume above a point heat source is constant. In his similarity analysis Popiolek (12) presents the following formula:

$$(18) \qquad \alpha = \frac{5}{6} m^{-1/2}$$

The entrainment factor α calculated by Morton (8) using data of several authors are consistent with the data shown in table 3.

Entrainment factor: $\alpha = \frac{5}{6} m^{-1/2}$						
Author:	Schmidt	George	Nakago.	Morton	Rouse	Pr.Work
α :	0.124	0.112	0.103	0.093	0.085	0.080

Table 3. The constant entrainment factor α in the model of a plume above a point heat source calculated on the base of results from several authors.

The results are calculated using equation 18. The measuring method and data processing of the present work shows that the entrainment is smaller than previous assumptions. This is interesting, because the correct formulation of the entrainment factor is the closure of the integral method of plume calculation. More work has to be carried out in this field.

3.3. Plumes in stratified surroundings.

The measurements have been carried out to evalute the effect on the flow by vertical temperature gradients and by ventilation in a room. In ventilated rooms complex vertical convection flow from extensive heat sources such as human bodies will occur. Mierzwinski (6) has investigated the plume above a human body: The flow is too complex and influenced by too many factors to be described by the model of a plume about a point heat source, but quasi Gaussian profiles have been observed 0.5 m above the head. Kofoed and Nielsen (5) reported that the entrainment in a thermal plume can be influenced by the surrounding walls. And many author show the importance of vertical temperature gradients, ref. (1,2,5,6,7,12,13,14,17,18).

In general the flow in a plume above a heat source propagating in stratified surroundings is different from the one without stratification. A description af the flow is given in fig. 10., ref (7).

3.3.1. Measurements.

The source is a 1 m high black painted cylinder (dia 400mm) covered with plates in both ends directly placed on the floor as shown in fig.2. Inside the source 4 lamps are placed and the total power supplied is Q = 100 W. The source is equal to the one in Mundts project (10). The measurement results are shown in table 4,5 & 6. Table 4 represents a case without ventilation and a recirculation flow is present. Table 5 & 6 represent cases with displacement ventilation which could be expressed as a "co-flow" situation.

Vertical cylinder dia=400mm h=1000mm Q=100W Recircl.flow G=0m^3/s n=0h^{-1} Ver.temp.grad dT/dx=0.07 K/m												
Plume parameters	Height above source x m											Notice
	0.00	0.25	0.50	0.75	1.00	1.25	1.50	1.75	2.00	2.25	2.50	
vM m/s		.205	.247	.254	.258	.223	.203	.254	.236	.221	.202	Gaussian fit by minimizing a sum of squares
Rv m		.164	.202	.221	.253	.282	.326	.336	.351	.383	.431	
ΔT_M C		2.1	1.4	.95	.71	.50	.43	.36	.29	.25	.18	
RT m		.155	.212	.240	.288	.355	.388	.417	.460	.429	.432	
H W		21	27	24	25	21	21	24	20	17	13	Integral plume parameter values
V m^3/s		.017	.032	.039	.052	.056	.068	.090	.091	.102	.118	
I kgm/s^2		2.1	4.7	6.0	8.0	7.5	8.3	13.8	13.0	13.5	14.3	
Ar		.279	.150	.109	.091	.095	.115	.062	.060	.065	.064	
λ		.95	1.05	1.09	1.14	1.26	1.19	1.24	1.31	1.12	1.00	
m		7	16	27	32	20	17	49	42	66	108	Local approximation by a model of a plume above a point source
p		8	15	23	25	12	12	32	24	53	107	
α		.312	.206	.161	.147	.189	.203	.119	.129	.102	.080	

Table 4. Measurement results.

Vert.cyl. dia=400mm h=1000mm Q=100W "Co-flow" G=0.0042m^3/s n=0.7h^{-1} Ver.temp.grad. dT/dx= 0.09 K/m												
Plume parameters	Height above source x m											Notice
	0.00	0.25	0.50	0.75	1.00	1.25	1.50	1.75	2.00	2.25	2.50	
vM m/s		.180	.254	.203	.238	.233	.210	.208	.174	.187	.168	Gaussian fit by minimizing a sum of squares
Rv m		.214	.205	.259	.297	.296	.380	.380	.414	.472	.510	
Δ_{TM} C		2.0	1.6	.82	.74	.58	.43	.31	.26	.25	.20	
RT m		.198	.196	.305	.298	.336	.385	.564	.713	.781	.612	
H W		29	31	25	30	25	25	24	22	29	19	Integral plume parameter values
V m^3/s		.026	.034	.043	.066	.064	.095	.095	.094	.131	.137	
I kgm/s^2		2.8	5.1	5.2	9.4	9.0	12.0	12.0	9.8	14.8	13.8	
Ar		.446	.174	.172	.130	.106	.124	.090	.120	.115	.121	
λ		.93	.95	1.18	1.00	1.13	1.01	1.48	1.72	1.65	1.20	
m		3	18	8	26	24	27	11	4	5	15	Local approximation by a model of a plume above a point source
p		4	19	6	26	18	27	5	1	2	10	
α		.479	.198	.299	.164	.171	.247	.443	.393	.218	.080	

Table 5. Measurement results.

Vert.cyl. dia=400mm h=1000mm Q=100W "Co-flow" G=0.0042m^3/s n=0.7h^{-1} Ver.temp.grad. dT/dx= 0.30 K/m												
Plume parameters	Height above source x m											Notice
	0.00	0.25	0.50	0.75	1.00	1.25	1.50	1.75	2.00	2.25	2.50	
vM m/s		.180	.221	.226	.200	.192	.204	.164	.159	.158	.119	Gaussian fit by minimizing a sum of squares
Rv m		.203	.206	.215	.263	.292	.303	.360	.381	.363	.478	
ΔT_M C		1.6	1.1	.75	.54	.37	.29	.17	.16	.11	.10	
Rt m		.180	.204	.248	.319	.404	.347	.508	.567	.703	.840	
H W		20	20	17	17	15	12	9	10	7	8	Integral plume parameter values
V m^3/s		.023	.029	.033	.043	.052	.059	.067	.072	.065	.086	
I kgm/s^2		2.4	3.8	4.4	5.1	6.0	7.2	6.6	6.9	6.2	6.1	
Ar		.369	.160	.106	.118	.097	.071	.077	.081	.054	.111	
λ		.88	.99	1.15	1.21	1.38	1.15	1.41	1.49	1.94	1.76	
m		5	18	22	15	13	51	19	14	11	4	Local approximation by a model of a plume above a point source
p		7	18	17	10	7	39	9	6	3	1	
α		.361	.197	.177	.218	.232	.116	.193	.224	.252	.430	

Table 6. Measurement results.

The results show that the zone of complete similarity does not occur in any of the measurements independent of height. This is caused either by the way of generating the plume or by the environmental conditions. The velocity and temperature distribution factors m & p are below the values indicated in the model of a plume above a point heat source and the entrainment factor is larger. This means that the plume has a larger angle of spread and propagates with a lower velocity.

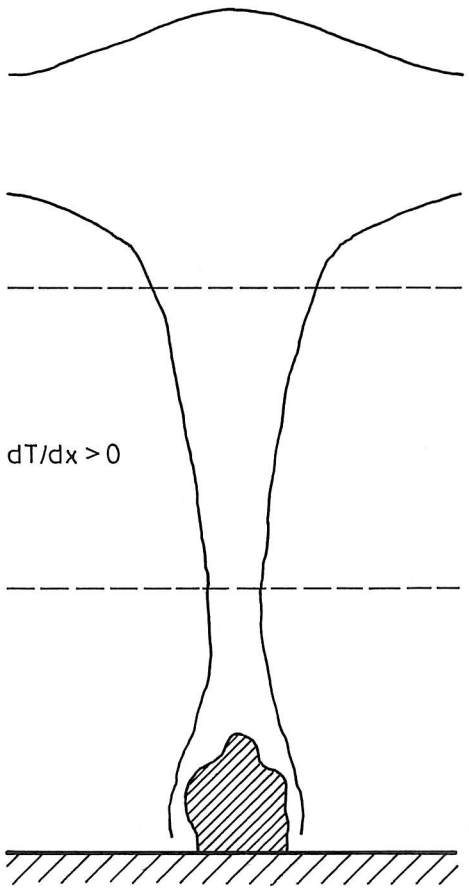

Zone 3, zone of maximum plume rise: The maximum elevation is reached, the air flows out horizontally as a stratified layer.

Zone 2, intermediate zone: As zone 2 in the case without stratification dT/dx=0, but the effect of stratification is significant.

Zone 1, the boundary layer zone: As zone 1 in the case without stratification dT/dx=0, the stratification affects the flow.

Fig.10. The flow regions in the plume above a heat source, with vertical temperature gradient, dT/dx > 0 K/m, ref. (7). (Compare with fig.3.).

In the case with little vertical temperature gradient dT/dx = 0.07 K/m and recirculating flow, table 4, it looks like the plume approaches the complete similarity at x = 2.50 m above the source (3.50 m above the floor), because the entrainment factor approaches the value α = 0.08 and the velocity and distribution factors are greather than 100. This indicates that the intermediate zone is long and extends the height of a normal office room.

In the case with the vertical temperature gradient dT/dx = 0.30 K/m and "co-flow" disintegration tendencies are shown, see table 6. The heat flux H and the temperature excess ΔT_M decrease fast. The velocity and temperature distribution factors m and p approach zero level and the entrainment factor α is often more than 2 times greather than the value α = 0.08. The results in table 5 show the same characteristics as in table 6. But it is not so clear because the vertical temperature gradient is less dT/dx = 0.09 K/m.

Fig.11. and fig.12. show the flow rate in the thermal plumes as a function of the distance from the top of the heat source. The characteristics reported are observed in more experiments with other heat source geometries, e.g. tubes and plates.

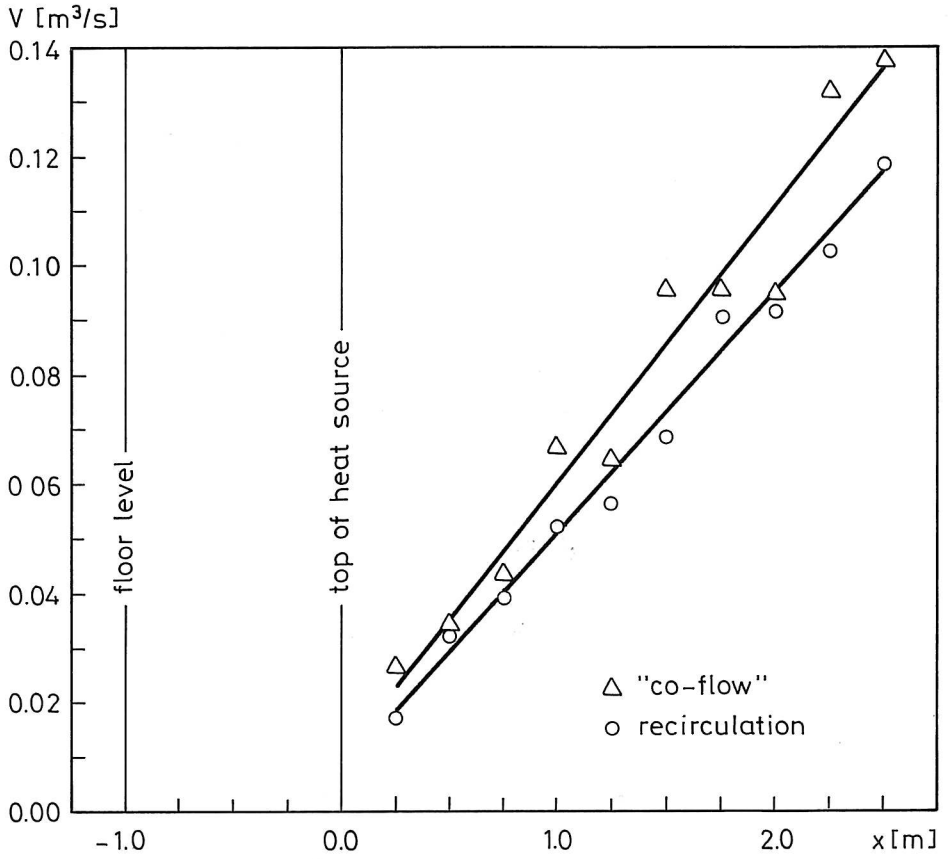

Fig.11. Distribution of volume flux $V = \pi v_M R_V^2$ along the plume axis. Recirculation flow and "co-flow" are compared. Table 4 & 5.

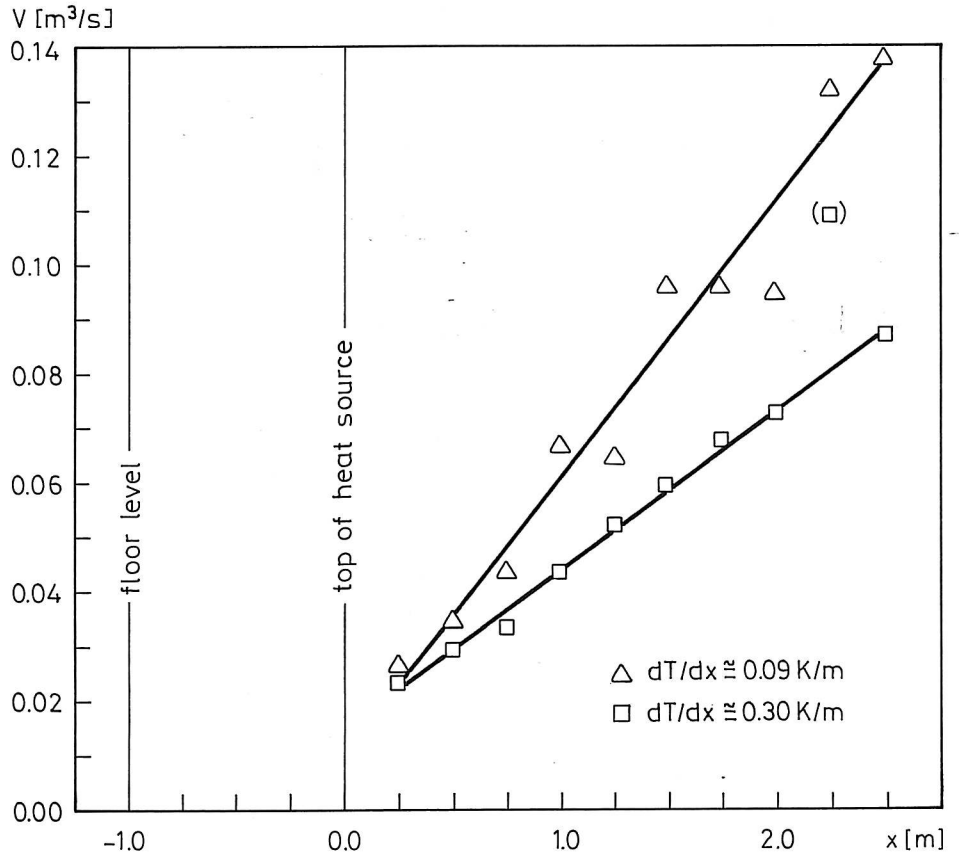

Fig.12. Distribution of volume flux $V = \pi v_M R_V^2$ along the plume axis. "Co-flow", the effect of vertical temperature gradient is shown. Table 5 & 6.

Fig.11. shows the effect of the flow from the diffusers. In the case with recirculation flow the buoyancy in the plume is the main driving force of the total flow in the room. This is not the case when the entrainment is supported with flow from the diffusers. The flow rate will increase in this case, which is called "co-flow" in the tables and figures.

The effect of the vertical temperature gradient dT/dx on the volume flux appears in fig.12. The flow rate V in the thermal plume decreases when the vertical temperature gradient dT/dx increases. It must be emphasized that it is important to relate the vertical temperature gradient to the zone where the flow takes place. For the purpose of buoyant plume calculation by means of an integral method the exact distribution of the vertical temperature distribution in the surroundings is essential. In other experiments than those reported here total disintegration tendencies and horizontal flow are observed. In this case it is difficult to describe the flow.

Conclusion.

The model of a plume above a point heat source has been verified as a borderline case which only takes place when the flow propagates in surroundings without a vertical temperature gradient. The zone of complete similarity where the modelling is possible is found above an intermediate region. The length of this region is dependent on the heat source geometry, and it is observed longer than the height of a normal office room. Due to the measuring method and data processing the width of the velocity and temperature excess profiles are found to be more narrowly than that observed by previous authors, and the entrainment factor is smaller.
Even very small vertical temperature gradients make the modelling impossible. The entrainment factor strongly depends on the vertical temperature gradient. In the intermediate region the entrainment factor is greater than observed in the case without a vertical temperature gradient. The exact knowledge of the vertical temperature gradient is essential to predict the flow propagation due to its influence on the entrainment, e.g. in an integral method of plume calculation.
Since the flow from different heated bodies is individual full-scale measurements seem to be the only possible approach to obtain the volume flow in: thermal plumes in ventilated rooms.
At the present moment the entrainment in thermal plumes influenced by enclosing walls is investigated.

References.

(1) Chen C.J. & W. Rodi: Vertical turbulent buoyant jets - a review of experimental data, HMT, vol.4, Pergamon Press, 1980.

(2) Fox D.G.: Forced plume in a stratified fluid, Journ. Geophys. Res., 75, pp.6818-6835, 1970.

(3) George W.K., R.L. Alpert & F. Tamini: Turbulence measurements in an axisymmetric plume, Int. J. Heat Mass Transfer, Vol.20, pp.1145-1154, 1977.

(4) Heiselberg P. & M. Sandberg: Convection from a slender cylinder in a ventilated room, Roomvent'90, International conference in Oslo, 1990.

(5) Kofoed P. & P.V. Nielsen: Thermal plumes in ventilated rooms - an experimental research work, Indoor Environmental Technology, paper no.7, ISSN 0902-7513 R8833, 1988.

(6) Mierzwinski S.: Air motion and temperature distribution above a human body in result of natural convection, A4-series no.45, Dept. of Heating and Ventilating, Royal Inst. of Technology, Stockholm, Sweden, 1981.

(7) Mierzwinski S. & Z. Popiolek: Experimental verification and possibilites of application af a plume model above a point heat source, A4-series no.58, Dept. of Heating and Ventilating, Royal Inst. of Technology, Stockholm, Sweden, 1982.

(8) Morton B.R., G.I Taylor & J.S. Turner: Turbulent gravitational convection from maintained and instantanous sources, Proc. Roy. Soc. London, A, 234, pp.1-23, 1956.

(9) Morton B.R.: The choise of conservation equations for plume models, journ. Geophys. Res., vol.76, no.30, pp.7409-7416, Okt.20, 1971.

(10) Mundt, E.: Convection flows above common heat sources in rooms with displacement ventilation, Roomvent'90, International conference in Oslo, 1990.

(11) Nakagome H. & M. Hirata: The structure of turbulent diffusion in an axisymmetrical thermal plume, ICHMT, vol.1-2, Dubrovnik, 1976.

(12) Popiolek Z.: Problems of testing and mathematical modelling of plumes above human body and other extensive heat sources, A4-series no.54, Dept. of Heating and Ventilating, Royal Inst. of Technology, Stockholm, Sweden, 1981.

(13) Popiolek Z. & P. Knapek: Analysis of the integral method of plume calculation, A4-series no.59, Dept. of Heating and Ventilating, Royal Inst. of Technology, Stockholm, Sweden, 1982.

(14) Popiolek Z. & S. Mierzwinski: Buoyant plume calculation by mean of the integral method, A4-series no.89, Dept. of Heating and Ventilating, Royal Inst. of Technology, Stockholm, Sweden, 1984.

(15) Rouse H., C.S. Yih & H.W. Humphreys: Gravitational convection from a boundary source, Tellus, 4, pp.201-210, 1952.

(16) Schmidt, W.: Turbulente Ausbreitung eines Stromes erhitzter Luft, Z. angw. Math. Mech., Bd.21, Nr.5 & 6, Okt. & Dez., 1941.

(17) Skistad, H.: Fortrengningsventilasjon i komfortanlegg med lavimpuls lufttilførsel i oppholdssonene, Norsk VVS Teknisk Forening, 1989.

(18) Skåret, E.: Displacement ventilation, Roomvent'87, International conference on air distribution in ventilated spaces, Stockholm, 1987.

Appendix C

Velocity Distribution in the Flow from a Wall-Mounted Diffuser in Rooms with Displacement Ventilation

Peter V. Nielsen

VELOCITY DISTRIBUTION IN THE FLOW FROM A WALL-MOUNTED DIFFUSER IN ROOMS WITH DISPLACEMENT VENTILATION

Peter V. Nielsen
Aalborg University, Denmark

INTRODUCTION

Ventilation systems with vertical displacement flow have been used in industrial areas with high thermal loads for many years. Quite recently the vertical displacement flow systems have grown popular as comfort ventilation in rooms with thermal loads, e.g. offices.

The air is supplied directly into the occupied zone at low velocity from wall-mounted diffusers. The plumes from hot surfaces, from equipment and from persons entrain air into the occupied zone and create a natural convection flow upwards in the room, see figure 1.

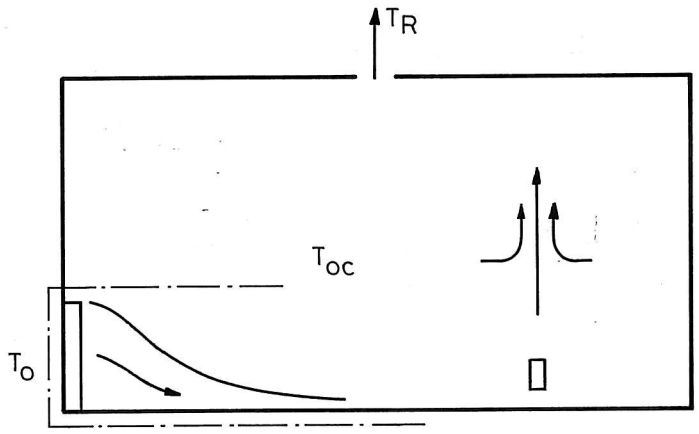

Figure 1. Room with low-level diffuser, heat source and displacement flow.

The displacement flow systems have two advantages compared with traditional mixing systems.

- An efficient use of energy. It is possible to remove exhaust air from the room where the temperature is several degrees above the temperature in the occupied zone which allows a higher air inlet temperature at the same load.

- An appropriate distribution of contaminated air. The vertical temperature gradient (or stratification) implies that fresh air and contaminated air are separated and the most contaminated air can be found above the occupied zone.

The design procedure for displacement ventilation deals with the velocity in front of a wall-mounted diffuser by defining the distance from the diffuser to an area where the velocity has decreased to 0.2 m/s (in many cases measured 0.1 m above the floor). The research described in this report is focused on the flow from wall-mounted low velocity air terminal devices. It is the aim of the work to obtain results which can simplify and improve the practical design procedure.

- It is important to examine the flow in front of an air terminal device and to investigate if this flow can be treated unconnected with parameters as room geometry (generally speaking), heat source location and location of exhaust opening, etc.

  The design procedure is simplified if the flow depends only on some main parameters as e.g. type of diffuser, obstacles on the floor, flow rate and Archimedes' number of the flow. It is especially a simplification if the influence of width and length of the horizontal section is small.

  The expectation of this simplification is indicated in figure 1 by the dotted line. An equivalent situation is known in mixing ventilation where the flow from air terminal devices can be described relatively independent of the recirculating flow in the room.

- Furthermore, it is important to obtain a quantitative description of the flow along the floor. The flow along the floor in a room with buoyancy driven ventilation is the only air movement which influences the comfort of the occupants. A description of this air movement will therefore make it possible to obtain a detailed picture of the thermal comfort of the room which is a valuable information compared to the knowledge of distance to the 0.2 m's velocity level.

- One of the main problems in connection with computational fluid dynamics used for the prediction of room air movement is to obtain a practical description of the boundary conditions at the supply opening. Experimental work on the flow from diffusers may give important information which can be used for the individual description of different supply openings.

Large parts of the experiments described in this report are based on a number of research activities made at Aalborg University in connection with the education of M.Sc. students. The research activities are dated back to 1987 and the participating

students are mentioned in the reference list. All the experimental work has been supervised and tied together by the author who wants to use this opportunity to express his thanks to all participants.

WALL-MOUNTED LOW VELOCITY DIFFUSER

Figure 2 shows the wall-mounted low velocity diffusers which are tested and discussed in this paper. They are different products and they are designed for flow rates of 50 - 300 m^3/h, except diffuser type F which is designed for a flow rate of 500 - 1400 m^3/h.

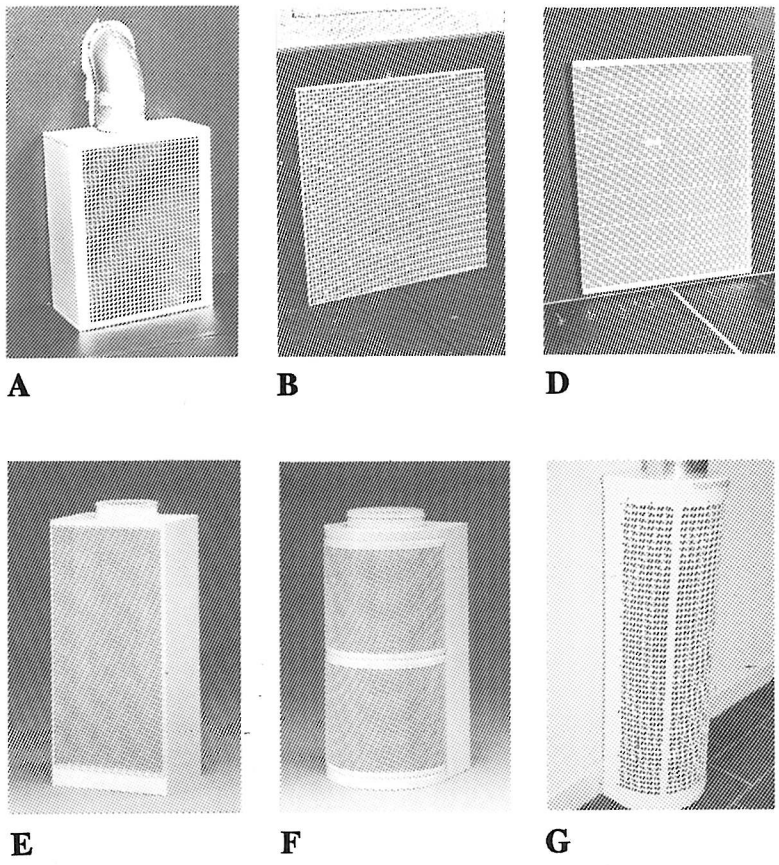

Figure 2. Six different wall-mounted low velocity diffusers for displacement ventilation.

Diffuser type A has a supply velocity profile which is very constant over the entire supply area, while diffuser type B has a supply velocity with a large variation over the supply area both in speed and in direction, see reference [1].

Diffuser type D can be adjusted to two different modes. It can either work as a traditional diffuser, D_1, or it can work with an internal induction unit, D_2, which increases the flow rate at the diffuser surface with a factor of 2.5 compared with the

supply flow q_o. The supply temperature T_o will be increased accordingly. The diffuser with the induction unit is especially used for displacement ventilation in systems generally designed for mixing ventilation (low flow rate and high temperature difference). The diffuser generates a semi-radial flow at the supply surface.

Diffuser type E is a conventional diffuser for displacement ventilation without any devices for the generation of radial flow at the supply surface.

The experiments with diffuser F are mainly made to test the influence of the diffuser size. The diffuser is designed for a flow q_o of 500 - 1400 m^3/h, but in this paper it is tested in the range of 100 - 200 m^3/h. The flow from the diffuser is radial.

Diffuser type G generates a radial flow at the supply surface. The velocity distribution is varying over the surface from 70% to 140%. The diffuser is selected for the displacement flow experiments in the International Energy Agency Annex 20 work.

The flow from the diffusers is either given by the flow rate q_o or by a face velocity u_f calculated from

$$u_f = \frac{q_o}{a_f} \tag{1}$$

where a_f is the surface area of the perforated part of the diffuser. u_f is easy to calculate but it is different from the supply velocity measured in the opening of the diffuser. (It is very time-consuming to find the supply velocity u_o based on measurements in a number of openings in the diffuser).

The height h of the different diffusers is an important parameter because the cold flow is influenced by vertical acceleration due to the gravity. The height and the area of the diffuser are given in table 1.

Diffuser	A	B	D_1	E	F	G
$a_f(m^2)$	0.159	0.306	0.437	0.267	1.293	0.188
h(m)	0.48	0.58	0.73	1.00	1.42	0.56

Table 1. Area a_f and height h of the six different low velocity diffusers.

The Archimedes number Ar for a flow is given by

$$Ar = \frac{\beta \cdot g \cdot h \cdot (T_{oc} - T_o)}{u_f^2} \qquad (2)$$

where β, g and $(T_{oc} - T_o)$ are volume expansion coefficient, gravitational acceleration and temperature difference between the temperature in the height 1.1 m and the supply temperature, respectively.

FLOW FROM A WALL-MOUNTED DIFFUSER

The flow from three different wall-mounted diffusers is shown in figure 3. The maximum velocity u_x close to the floor is given as a function of the distance x to the surface of the diffuser.

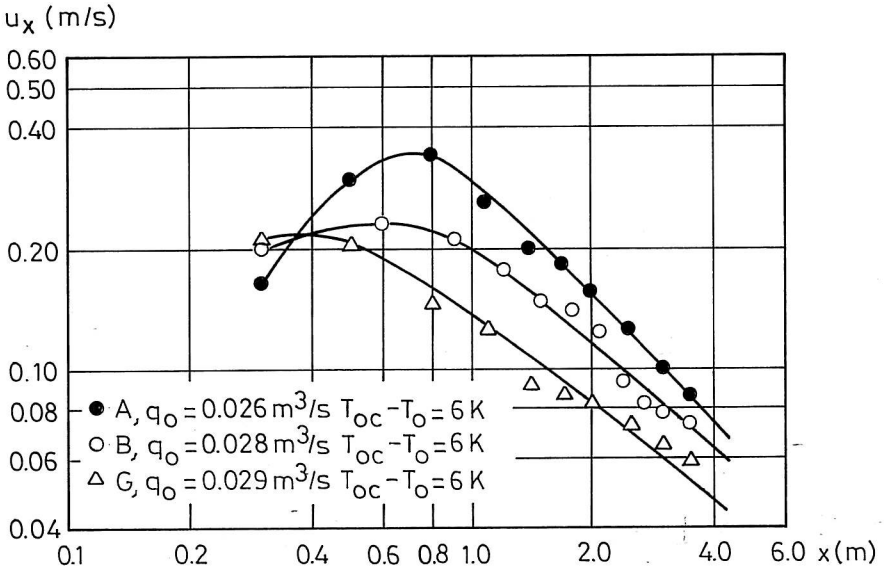

Figure 3. Maximum velocity close to the floor versus distance x. References [1, 2].

The cold air from supply opening A has a high initial acceleration due to buoyancy effect and a velocity of 0.34 m/s is obtained in a distance of 0.8 m from the diffuser. Type B has a larger diffusion of the supply flow, and the gravity will only increase the velocity to 0.23 m/s. The diffuser type G shows an even smaller velocity level although the flow to the room is almost the same in all three situations.

Figure 3 indicates that the maximum velocity in the symmetry plane is proportional to $1/x^n$ where the exponent n is close to 1.0 as pointed out by Nielsen et al. [3].

It is also obvious from figure 3 that different diffuser designs generate a different velocity level at the same flow rate and heat load.

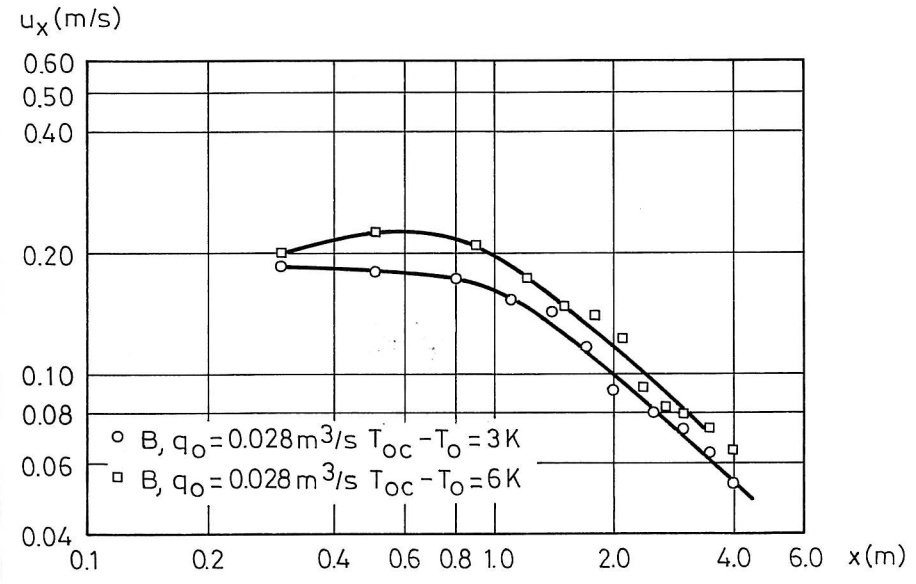

Figure. 4. Velocity decay along the floor at different Archimedes' numbers. Reference [4].

The velocity at the floor is not only influenced by the flow rate to the room and the type of diffuser. Figure 4 shows that the Archimedes number is an important parameter. A 3°C increase in temperature difference will for example increase the velocity from 0.10 m/s to 0.12 m/s in a distance of 2 m from the diffuser. The figure shows that it is the gravity which accelerates the flow close to the diffuser resulting in a higher initial velocity level at higher Archimedes' numbers. This effect is very important for the flow in rooms with displacement ventilation and the outcome can be surprising. The velocity level in a room may for example be uninfluenced although the flow rate is reduced because the heat load in the room requires a reduction of the supply temperature and consequently an increase of the relative velocity level u_x / u_f, see reference [4].

Profile measurements show that the flow in the vicinity of the floor can be characterized by a normalized velocity profile identical to the profile used for the description of wall jet flow, see references [2, 5, 6]. The length scale δ in this profile is defined as the distance from the floor to the height where the velocity has a level which is half of the maximum velocity close to the floor, u_x / 2.

Figure 5 shows the development in δ for three different Archimedes' numbers. It can be seen that the height of the flow region is much smaller than the height of the diffuser, even at a distance of 0.5 m from the diffuser. The cold air from the diffuser accelerates towards the floor due to gravity and it behaves like a stratified flow in its further progress along the floor. δ is rather constant while it is

proportional to x in a wall jet as indicated by the dotted line in figure 5. The length scale or thickness δ is slightly decreased at increasing Archimedes' number.

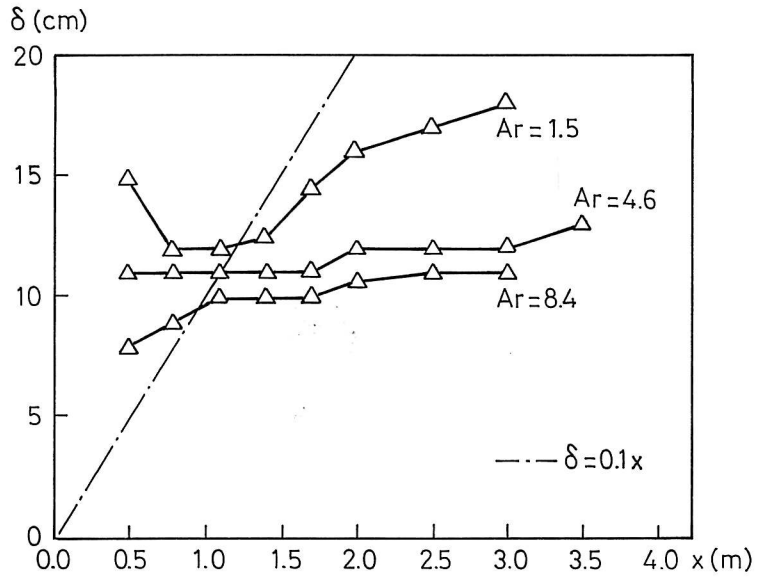

Figure 5. Length scale δ in the flow versus distance from the diffuser. Diffuser type G. Reference [2].

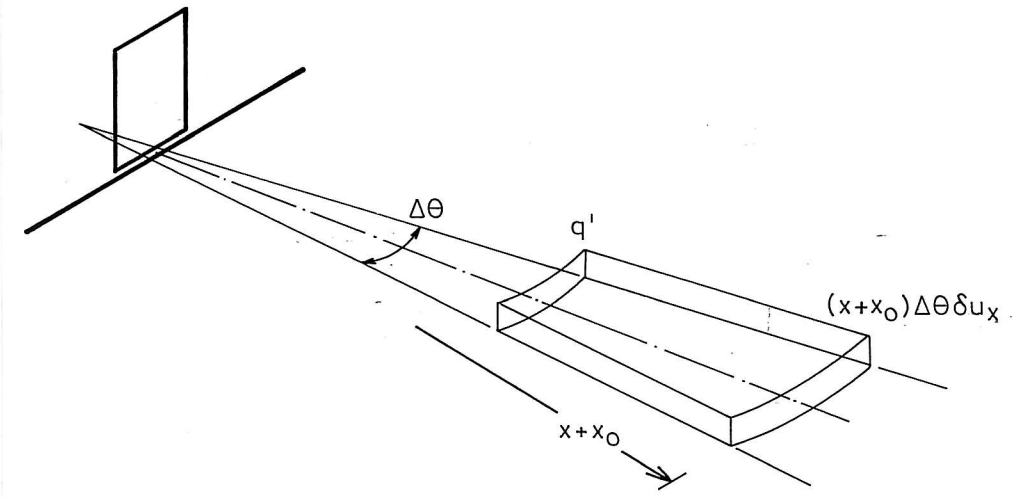

Figure 6. Stratified flow from a wall-mounted diffuser.

The entrainment of air into the flow, or the turbulent mixing process, is diminishing when a vertical temperature gradient is present because the gravity will work against upward movement of heavy fluid and downward movement of light fluid. This is shown in hydraulics by for example Turner [7] and it is shown for

displacement ventilation by Jacobsen and Nielsen [6] and it is also discussed in reference [8].

It is possible to develop an equation for the stratified flow in front of a wall-mounted diffuser, see reference [4]. It is known from measurements that the flow is radial and figure 6 shows a small section $\Delta\theta$ of this flow which has a virtual origin located in a distance x_o from the diffuser. The flow within section $\Delta\theta$ is proportional to $(x + x_o)\Delta\theta\delta u_x$ where $(x + x_o)\Delta\theta$ is the width of the section at distance x, and δ is an expresssion for the height of the section. u_x is an expression for the velocity level in the velocity distribution. The flow is independent of the distance x because the entrainment is small and the following equation can therefore be obtained.

$$\frac{u_x}{q'} \sim \frac{1}{\Delta\theta\delta} \frac{1}{x + x_o} \tag{3}$$

It is also shown by experiments that the normalized velocity distribution is fairly independent of the Reynolds number in areas of practical relevance, see reference [1]. The following equation can therefore be obtained for stratified flow with a constant thickness δ

$$\frac{u_x}{q_o} = K \frac{1}{x + x_o} \tag{4}$$

where K is a function of the Archimedes number as well as an individual function for different types of air terminal devices. Both x and u_x are measured in the middle plane of the room.

The development of equation (4) assumes a high Archimedes number but the structure is also valid for cases where the Archimedes number is very small. In this case the flow will be a part of a potential core or a part of a radial wall jet. The velocity will in most cases be proportional to $1/(x + x_o)$, and equation (4) will therefore be able to predict the velocity u_x when the K-value is adjusted to the situation, see reference [4].

The variables in eqution (4) are easy to measure for a given diffuser and the equation is therefore simple to use in a practical design procedure.

It is possible to obtain a normalized version of the equation for a more general description of the flow. The velocity u_x is normalized by the face velocity u_f and the length x is normalized by the height of the diffuser h

$$\frac{u_x}{u_f} = K_{dr} \frac{h}{x + x_o} \tag{5}$$

where

$$K_{dr} = K \frac{a_f}{h} \tag{6}$$

Velocity distribution in rooms with displacement ventilation is also discussed by Mathisen [5] and by Sandberg and Mattsson [9].

VIRTUAL ORIGIN OF THE FLOW

Some of the tested diffusers discussed in this paper generate a velocity decay of $1/x^n$ where n is slightly different from 1.0. Figure 7 shows an example where the measurements are in agreement with equation (4) for $x > 2.0$ m, while the equation overestimates the velocity closer to the diffuser.

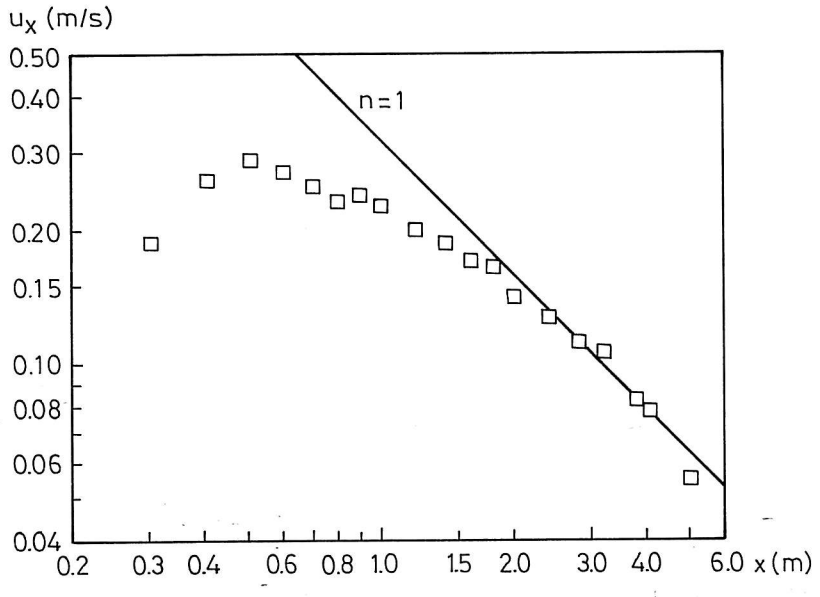

Figure 7. Velocity decay in the flow from a wall-mounted air terminal device type D_1. q_o = 0.028 m^3/s and Ar = 45.8. Reference [10].

The presence of a virtual origin located at some distance x_o behind the diffuser can explain the velocity decay shown in figure 7, but deviations of the same type will also take place if the flow is influenced by entrainment, by non-radial flow or by negative growth in the lenght scale δ. More detailed measurements are therefore necessary to determine if the influence especially is from the presence of a virtual origin located in some distance from the diffuser.

Figure 8 shows the flow direction measured with smoke close to the floor. The conditions for the experiment are close to the conditions in figure 7. It can be seen from the figure that the flow close to the symmetry line has a virtual origin x_o which is about 0.5 m, although the measurements are rather scattered. It is also obvious from the figure that the general flow is radial, even rather close to the side walls.

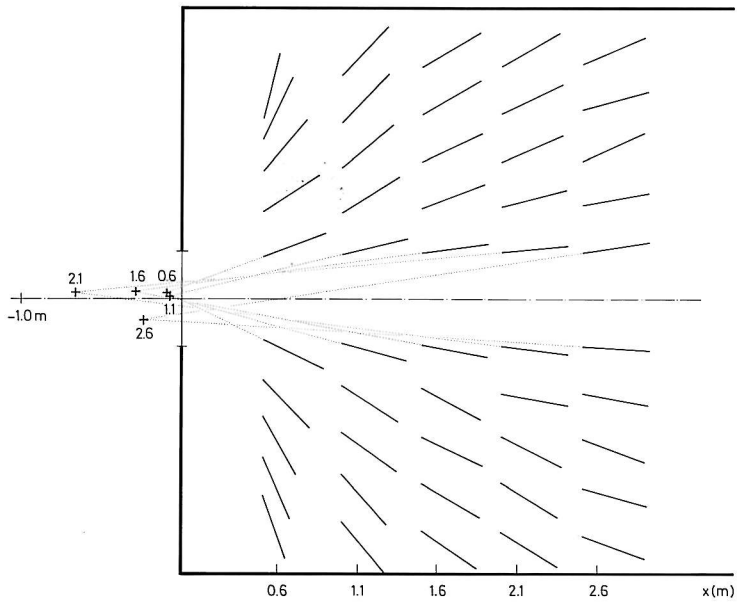

Figure 8. Flow directions at the floor. Diffuser type D_1. q_o = 0.028 m^3/s and Ar = 47. Reference [10].

Figure 9 shows the earlier measured velocity u_x versus $x + x_o$ where x_o = 0.5 m. It can be seen that the velocity decay is close to $1/(x + x_o)$ for $x > 1.5$ m which indicates that the measurement of a virtual origin will improve the presentation of the results close to the diffuser.

Many measurements show, however, that most of the diffusers have virtual origins which are located very close to the surfaces of the diffusers, which leads to small x_0. The influence of a small x_o is only important close to the diffuser and it is therefore ignored in the presentation in this paper, also because it is very difficult to measure in practice.

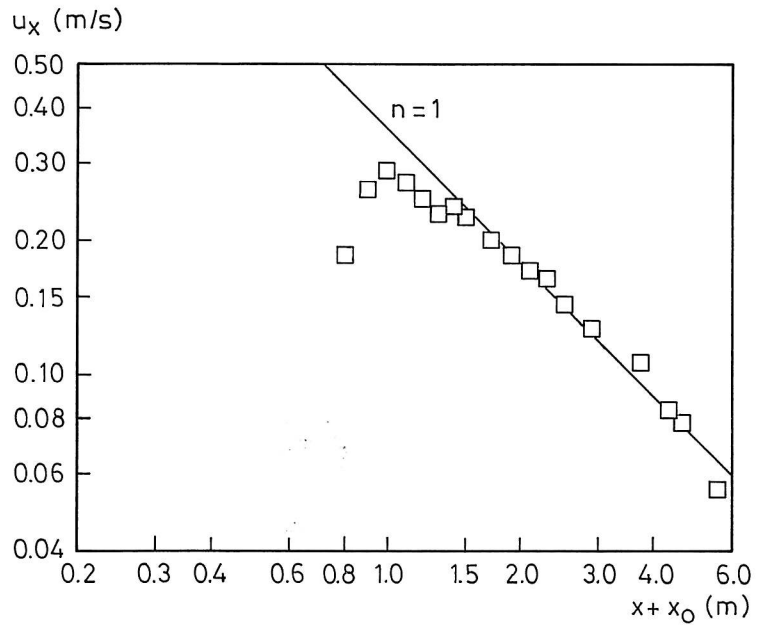

Figure 9. Velocity decay in the flow from diffuser D_1 versus$(x + x_o)$. q_o = 0.028 m^3/s, Ar = 45.8 and x_o = 0.5 m.

MAXIMUM VELOCITY IN THE FLOW CLOSE TO THE FLOOR

Equation (4) gives the description of the flow along the middle plane in a room with displacement ventilation. The equation is easy to use in practice because the variables are the primary variables in a design procedure.

The variable K is a product dependent variable which is also a function of the Archimedes number. A large number of experiments have been made to establish this variable and the results are shown in figure 10.

Figure 10 shows that K may be very different for different products as it varies from 5 to 12 m^{-1} at high Arhcimedes' numbers.

The figure shows that K increases with increasing Archimedes' number. This is due to the fact that gravity will accelerate the vertical flow close to the opening and generate a stratified air movement in a relatively thin layer along the floor where the obtained velocity level will be retained. This effect is also shown in figure 4. Diffuser A shows an increase in velocity at small Archimedes' number. This increase could be explained by the increase in radial flow which takes place for this diffuser at high Archimedes' number.

The high level of K for the diffuser D_2 can be explained by the induction unit used in this product.

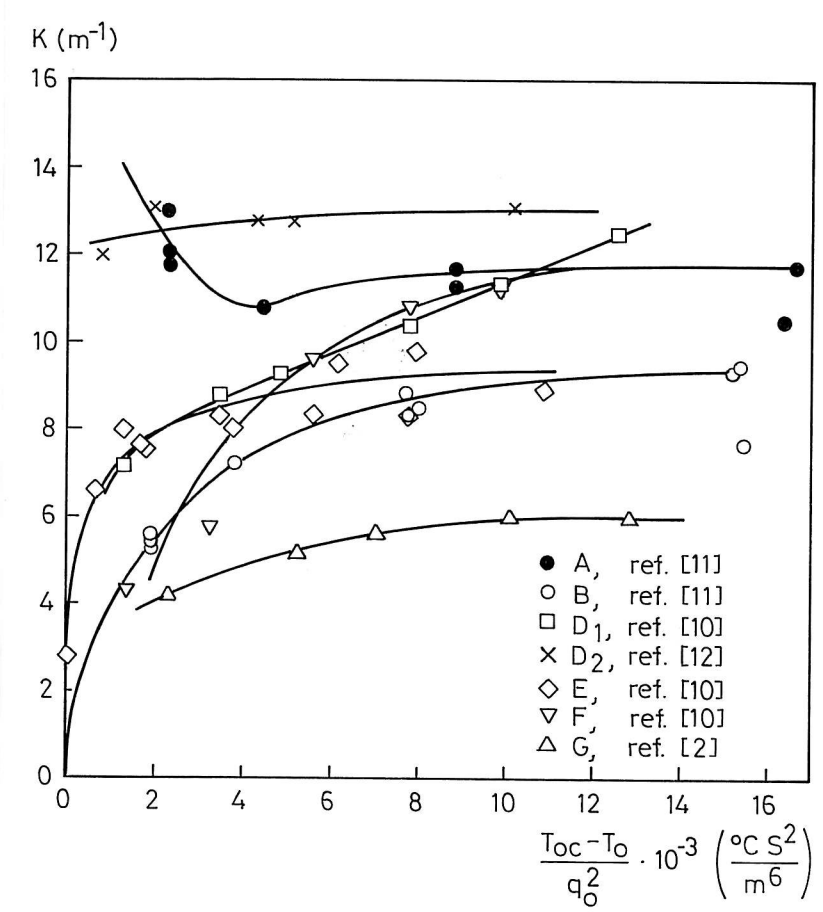

Figure 10. K versus temperature difference and supply flow rate for seven different wall-mounted air terminal devices. x_o = 0.0.

Equation (4) can only be used at some distance from the diffuser as it appears from the figures 3, 4 and 7 . This distance is 1.0 m to 1.5 m for most of the diffusers. The diffuser D_2 with an induction unit generates a flow which follows equation (4) for x > 1.5 m at high Archimedes' numbers, while the measurements show that x should be larger than 2 - 3 m for small Archimedes' number. Equation (4) will in any case give a velocity equal to or higher than the actual velocity and therefore a value which is suitable for a design procedure.

It is known from stratified flow in hydraulics that obstacles located downstream may influence the length scale δ of the flow, see references [7, 8]. Most of the measurements are made in test rooms of equal size, so it is difficult to determine the influence from the end wall and the side walls, but practical experience from the ventilation industry indicates that room dimensions are of minor importance, see reference [13].

It is typical that all diffusers, except diffuser F, have reasonable sizes compared to the test rooms. It might therefore be concluded that the diffusers are tested under conditions and dimensions close to the conditions which they are meant to cover in practice, and the velocity level given by the variable K, in figure 10, is therefore typical of a practical application.

The K-values in figure 10 are from measurements of flow in the middle plane. Measurements by Jacobsen and Nielsen [6] show that K is also a variable of the direction θ.

Equation (5) is a normalized version of the velocity decay formula. The face velocity u_f and the height of the individual diffusers h are reference values in this equation. Figure 11 shows that the dimensionless variable K_{dr} in equation (5) takes different values for different products. A normalization with the geometrical length scale h does not give a continuous description of the K_{dr}-values and it may therefore be concluded that the design details in the diffuser have a large influence on the K_{dr}-value.

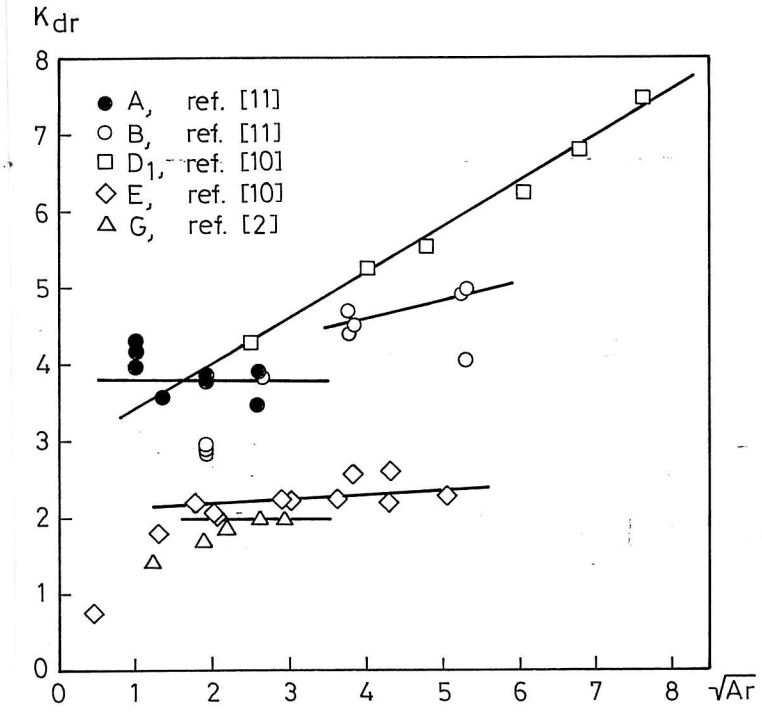

Figure 11. K_{dr} versus Archimedes' number for five different wall-mounted air terminal devices. x_o = 0.0.

Mathisen [5] has shown that the maximum velocity in the flow from a wall-mounted diffuser can be described as a linear function of $\sqrt{Ar}$. Figure 11 does confirm this

assumption for large Archimedes' numbers, but deviations take place at smaller Archimedes' numbers.

FLOW BETWEEN OBSTACLES

The flow in the vicinity of the floor may be influenced by furniture and by other obstacles in the occupied zone. The maximum velocity in the flow is located rather close to the floor (between 1 to 5 cm above the floor), and a great deal of the air movement will therefore take place in this region. Conventional furniture will only have a small influence on the air movement while obstacles placed directly on the floor will block the flow. An opening between this type of obstacles will work as new supply opening because the flow in the room is stratified. Figure 12 shows an example from a room with short movable walls.

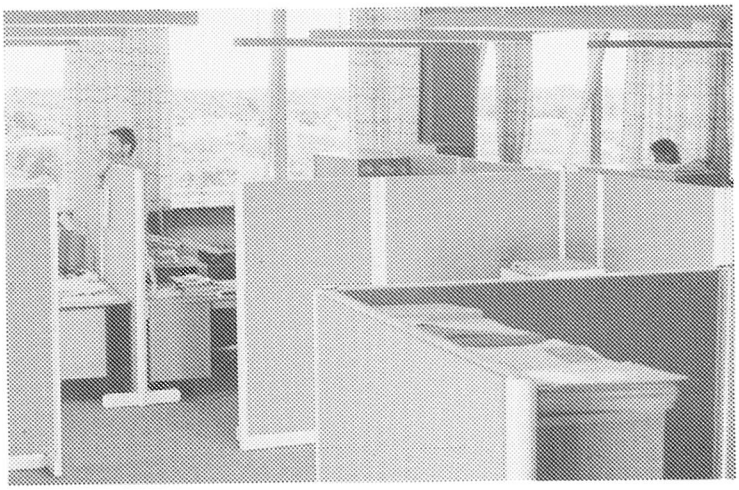

Figure 12. Room with short movable walls.

Experiments have shown that the flow from an opening between obstacles can be described as a semi-radial flow like the air movement from a wall-mounted supply opening. The velocity decay can be described by the equation

$$\frac{u_x}{q_o} = K_{ob} \frac{1}{x} \tag{7}$$

u_x is maximum velocity in distance x from the opening and q_o is the excess air supplied on the other side. u_x is measured in the symmetry plane.

Figure 13 shows the measurements of K_{ob} in equation (7). The structure of equation (7) and the distribution of K_{ob}-values are equivalent to the structure of

equation (4) and the structure of K-values. The temperature difference $T_{oc} - T_{ob}$ is the difference between the temperature in the height 1.1. m in front of the opening and the lowest temperature in the opening between the obstacles.

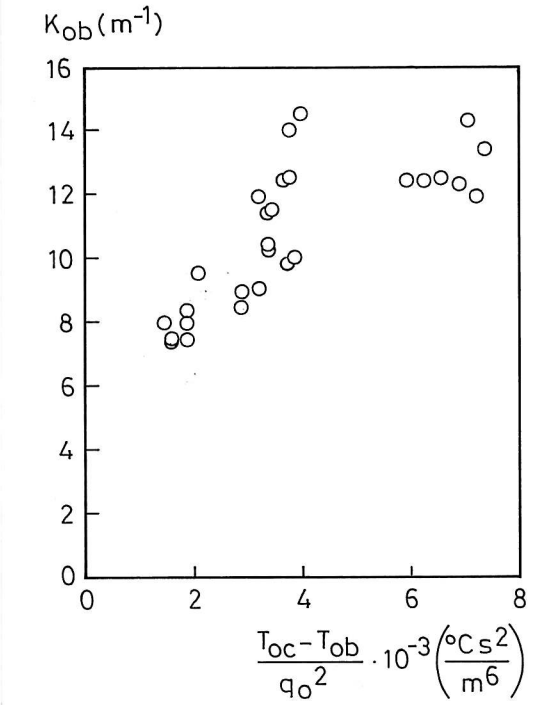

Figure 13. K_{ob} versus flow rate and temperature difference. Reference [14].

It is interesting to see that the level of the variable K_{ob} is only slightly larger than the level of K.

The width of the opening is varying from 0.1 m to 1.5 m in the experiment. Measurements show that the importance of the width is less obvious and results for different widths are given in figure 13.

CONCLUSIONS

Wall-mounted air terminal devices are often used in displacement ventilation. The flow from a device will accelerate in a vertical movement close to the opening due to the gravity effect when inlet air is colder than room air. The airflow will then move along the floor in a radial pattern and behave like a stratified flow. The airflow will influence the thermal comfort of the occupants and it is therefore important to develop an expression for the flow for design proposals.

Measurements show that the velocity at the floor is not only influenced by the flow rate to the room. It is also influenced by the temperature difference - or by the Archimedes number - and the velocity level may vary for different types of diffusers.

The flow is stratified at large temperature differences. This is indicated by a constant height of the cold flow independent of the distance from the supply opening. It is shown that the radial flow has a virtual origin close to the front of the diffuser. The velocity level in the flow along the floor is inversely proportional to the distance from the diffuser. The velocity decay can be described individually for each type of diffuser by a single equation and a variable which is a function of the Archimedes number. It is further shown that the maximum velocity can be described as a linear function of the square root of the Archimedes number.

The influence of side walls and the end wall has not been studied but it is known from stratified flow in hydraulics that obstacles located downstream may influence the height of the cold flow. Practical experience indicates that the room dimensions are of minor importance, but more work in this area is necessary.

Openings between obstacles placed directly on the floor will generate a flow similar to the air movement in front of a diffuser. It is shown that the velocity distribution can be described with an equation system with the same structure as the system describing the stratified flow from wall-mounted diffusers.

REFERENCES

[1] Nielsen, P.V. **"Displacement Ventilation in a Room with Low-Level Diffusers"**. DKV-Tagungsbericht, ISBN 3-922-429-63-7, Deutscher Kälte- und Klimatechnischer Verein e.V., Stuttgart, 1988.

[2] Brohus, H, Bøgh, B.-O., Mogensen, F. and Thomsen, T. **Private communication**, Aalborg University, 1992.

[3] Nielsen, P.V., Hoff, L. and Pedersen, L.G. **"Displacement Ventilation by Different Types of Diffusers"**. Proc. of the 9th AIVC Conference, ISBN 0 946075 40 9, AIVC, Warwick, 1988.

[4] Nielsen, P.V. **"Air Velocity at the Floor in a Room with Wall-Mounted Air Terminal Device and Displacement Ventilation"** (in Danish). Internal report, Nordic Ventilation Group, ISSN 0902-7513 R9004, Aalborg University, Aalborg, 1990.

[5] Mathisen, H.M. **"Analysis and Evaluation of Displacement Ventilation"**. Ph.D.-thesis, Technical University of Norway, 1989.

[6] Jacobsen, T.V. and Nielsen, P.V. **"Velocity and Temperature Distribution in Flow from an Inlet Device in Rooms with Displacement Ventilation"**. Proc. of Roomvent '92, Third International Conference on Air Distribution in Rooms, DANVAK, Copenhagen, 1992.

[7] Turner, J.S. **"Buoyancy Effects in Fluids"**. Cambridge University Press, Cambridge, 1979.

[8] Nielsen, P.V. **"Velocity Distribution in Rooms with Displacement Ventilation and Low Level Diffusers"**. Internal report, International Energy Agency, Energy Conservations in Buildings and Community Systems, Annex 20, 1992.

[9] Sandberg, M. and Mattsson M. **"The Mechanism of Spread of Negatively Buoyant Air from Low Velocity Air Terminals"**. IV Seminar on "Application of Fluid Mechanics in Environmental Protection 91", Gliwice, 1991.

[10] Berg, S.-R. and Larsen, H.H. **Private communication**, Aalborg University, 1991.

[11] Hoff, L. and Pedersen, L.G. **Private communication**, Aalborg University, 1987.

[12] Eskildsen, L.J., Jensen, J.O., Bakmann, U., Jespersen, C. and Bukh, B. **Private communication**, Aalborg University, 1990.

[13] Laurikainen, J. **Private communication**, Halton, Kausala, 1990.

[14] Gorgin, A.R. and Tang J.S. **Private communication**, Aalborg University, 1992.

Appendix D

Velocity and Temperature Distribution in Flow from an Inlet Device in Rooms with Displacement Ventilation

Torsten V. Jacobsen and Peter V. Nielsen

VELOCITY AND TEMPERATURE DISTRIBUTION IN FLOW FROM AN INLET DEVICE IN ROOMS WITH DISPLACEMENT VENTILATION

T.V.Jacobsen and P.V.Nielsen
Aalborg University, Denmark

INTRODUCTION

The extended use of the displacement principle in room ventilation has been the incentive to a number of investigations concerning the restrictions on inlet flow and heat load with respect to human comfort. The recommendations which have been put forward are essential in the design phase but they do not explain the physical processes in details. An improved understanding of the underlying physical phenomena is important for the development of design tools and the recommendations which are offered today.
Displacement ventilation is characterized by a flow field which is driven mainly by buoyancy forces. Cool air is supplied at floor level and upward directed thermal plumes from heat sources give rise to a vertical temperature gradient. The stratification diminishes vertical air movement and diffusion and apart from the region above heat sources the flow field is divided into more or less distinct horizontal layers. The outlet is located in the upper part of the room ,e.g. at the ceiling, and it ensures a relatively efficient removal of excess heat.
One of the main comfort problems in a room with displacement ventilation is the relatively high velocities in front of the inlet device. To compensate an increasing heat load it is necessary to increase the cooling capacity either by increasing the inlet flow or by increasing the temperature difference between inlet and outlet. Both adjustments will tend to increase the maximum velocities which are found a few centimeters above floor level.
An altered relation between momentum and buoyancy forces at the inlet has a profound effect on the magnitude of the initial acceleration due to gravity, the rate of entrainment and the flow field in general. Provided that a specific inlet device is considered and that the variation in the volumetric expansion coefficient and in the gravitational acceleration is negligible, a reduced Archimedes number can be defined to describe this relation.

$$Ar_r = \frac{\Delta T_0}{U_o^2} \qquad (1)$$

ΔT_0 is the temperature difference between the occupied zone (y=1.10 m) and the inlet, $\Delta T_0 = T_{1.10m} - T_{inlet}$ and U_0 is the velocity at the surface of the inlet device calculated from the inlet flow and the area of the inlet device.
It is the objective of the experimental work presented here to show how Ar_r affects not only the maximum velocities but also the initial spread as well as the velocity distribution in front of the inlet device.

TEST ROOM AND MEASUREMENTS

The air supply device, exhaust openings and heat sources are arranged in such a way that the middle plane of the room coincides with the middle plane of the inlet device constituting a symmetry plane for all boundary conditions.

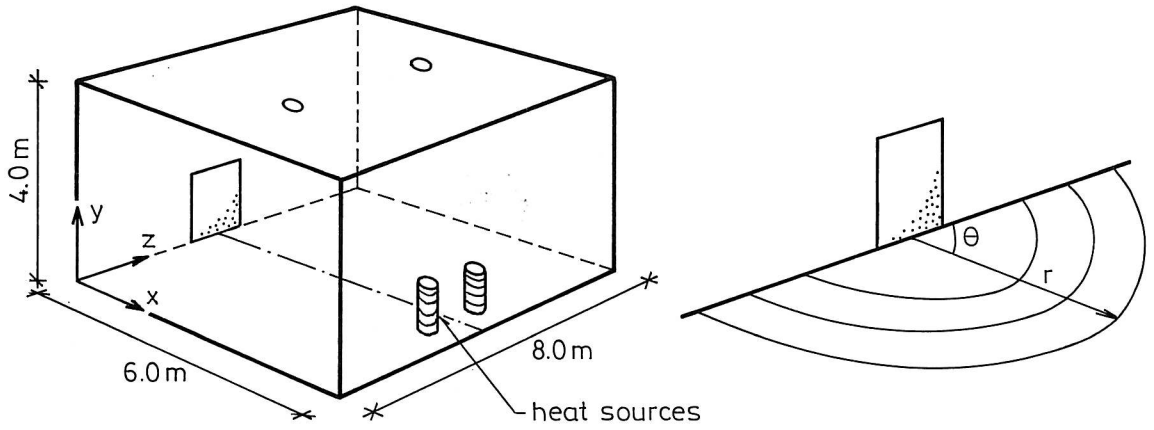

Fig.1 Test room arrangement and illustration of radial flow pattern in front of inlet device.

Smoke is added to the inlet in order to visualize the flow pattern and choose a suitable line of procedure for the measurements. The smoke experiments reveal important features of the flow pattern. Under isothermal conditions it is observed that the flow from the diffuser penetrates horizontally about 1 m into the room where the smoke is dissolved due to entrainment. Even at small temperature gradients ($Ar_r \approx 300$ °Cs^2/m^6) the inlet air drops to the floor where it is deflected and it spreads out radially in a thin layer which flows to the surrounding walls. At $Ar_r > 500$ °Cs^2/m^6 the transition between the cool layer at the floor and the room air becomes even more distinct - presumably because of a more stable stratification. The apparently fully radial flow along the floor has a layer thickness of 20-30 cm with a slight decrement for increasing Ar_r.
Observations show that the streamlines are emanating from a centre point in front of the inlet device and that they are straight lines corresponding to a radial flow along the floor. The vertical velocity and temperature profiles are consequently measured along the stream-lines (given θ-values, 1.0m ≤ r ≤ 3.5m), see fig. 1.
The measurements are made at steady state conditions using hot sphere anemometers for the velocities and thermocouples for the temperatures.

DECAY OF MAXIMUM VELOCITIES

The maximum velocities are located 2-5 cm above the floor. The decay of maximum velocities with distance from the air terminal device has earlier been described by *Sandberg et al. 1991* and *Nielsen 1990.* A simple expression suggesting exponential decay (*Nielsen 1990*) is suitable in the following form:

$$\frac{U_{max}(r)}{q_0} = K\,(\theta, Ar_r)\,\frac{1}{r} \qquad (2)$$

$K(\theta,Ar_r)$ is a factor of proportionality, θ and r are angle and radius respectively and q_0 is the inlet flow.

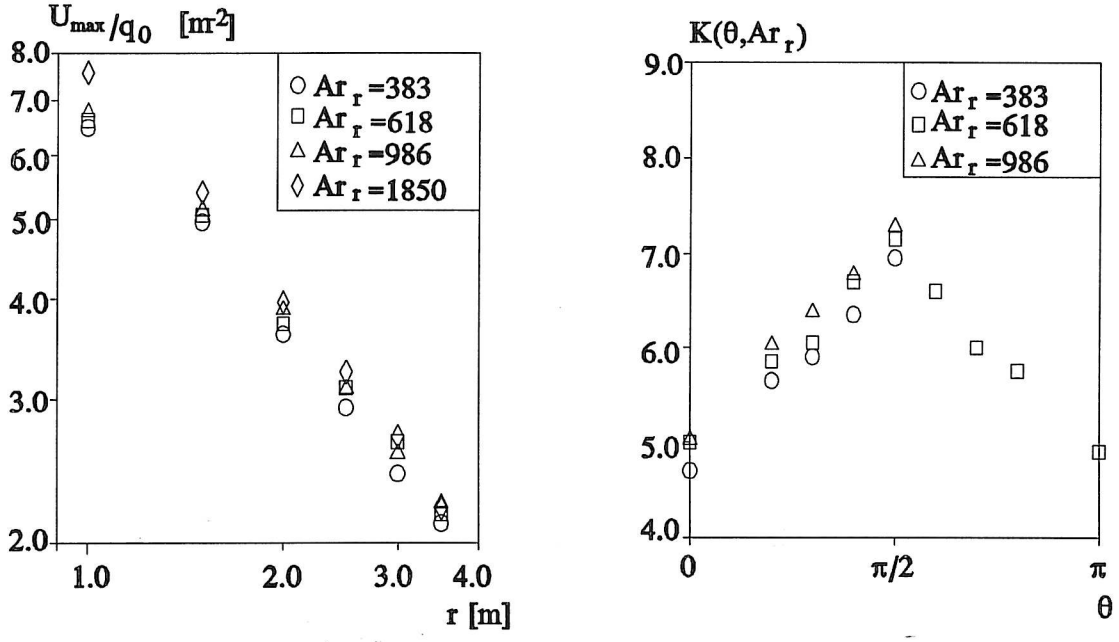

Fig.2 Measured velocity variation in the centre line ($\theta=\pi/2$) with distance from inlet for different Ar_r-numbers and $K(\theta,Ar_r)$ variation with streamline angle for different Ar_r-numbers.

Fig. 2 shows that eq.2 is a good approximation to the velocity decay for a given Ar_r-number. The velocity level is highest in the centre line and it is seen that an increment in Ar_r-number will increase the velocity level slightly.
Furthermore, fig. 2 shows that the K-values calculated for each streamline are distributed symmetrically around the centre line of the inlet device and vary with the direction. The distribution of K-values with streamline direction is approximately similar for the chosen Ar_r-numbers. This might change for larger Ar-numbers where the initial spread of inlet air is different from the cases of the current study.

VELOCITY AND TEMPERATURE PROFILES

In the field of turbulent jets velocity profiles are often assumed to be similar. The measured velocity profiles in front of the inlet device shows not only similarity in shape but they are also much like the profiles for a wall jet. This opens up the prospect of applying a similarity function of the jet type.
Mathisen 1990 applies a similarity function for half a free jet but here a wall jet expression is preferred. Verhoff's (*Verhoff 1963*) solution takes into account the bondary layer occuring near the surface and the free jet boundary to the surrounding fluid.

$$\frac{U(y)}{U_{max}} = A\left(\frac{y}{b}\right)^{\frac{1}{7}}\left[1-erf\left(B\left(\frac{y}{b}\right)\right)\right] \qquad (3)$$

where the constants A and B equals 1.48 and 0.68, repectively, erf is the error function and b is the height of the profile defined as the level where the velocity is 0.5 U_{max}.
Relations for heat transfer can often be deduced from the momentum transport. For turbulent jets a ratio between temperature profile and velocity profile can be applied. It is confirmed by regression that using the second power in eq.4 actually gives the best obtainable fit when all T-profiles are included.

$$\frac{U(y)}{U_{max}} = \left(\frac{\Delta T(y)}{\Delta T_{max}}\right)^2 \qquad (4)$$

$\Delta T(y)$ is the temperature difference between room air and a point at y distance from the ΔT_{max} location.

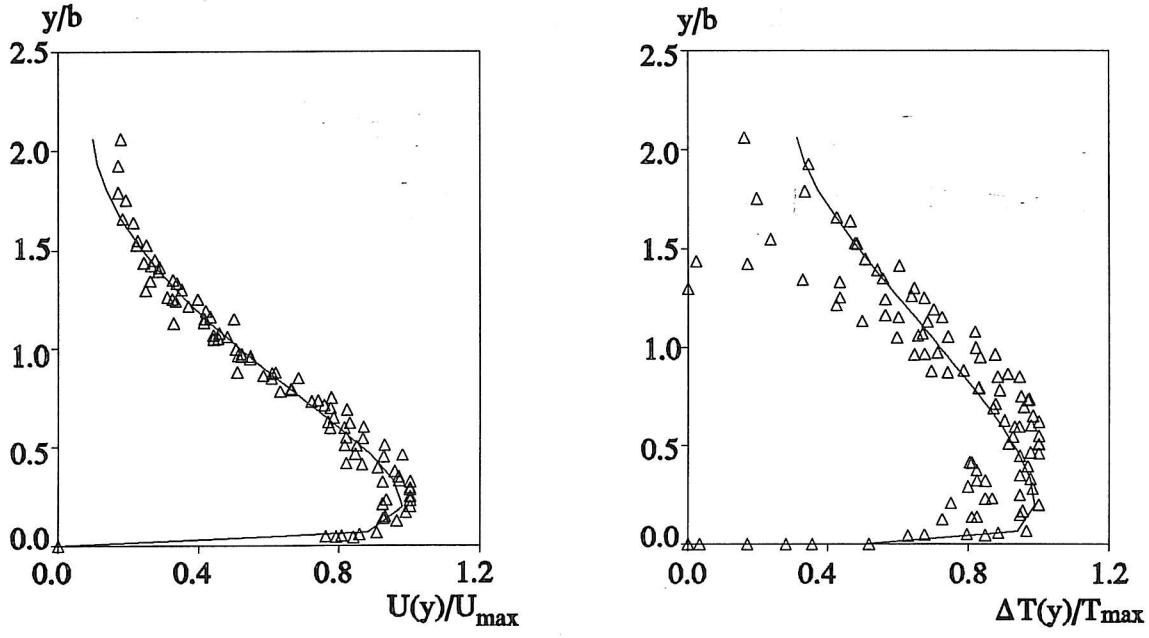

Fig.3 Measured velocities and temperatures compared with theoretical profiles, eq.(3) and eq.(4),(Ar_r=618 °Cs^2/m^6).

The agreement between eq.3 and the measured velocities in fig.3 is obvious and the slight divergence at y > 1.5 y/b is probably caused by the recirculating flow in the domain above the inlet flow.
The temperatures have a more scattered distribution and they do not fit into the theoretical expression in the same convincing way as the velocities.
The divergence does not occur solely at single points but also the entire profile shape is altered which implies caution in using eq.4 as an approximation. A closer study reveals a slowly increasing discrepancy with distance from the inlet device. The heat flux at the floor and the heat sources distort the temperature distribution and make the approach of universal profiles less obvious.
The conclusions based in fig.3 can be extended to the Ar_r-number range which is considered (~300-1900 $°Cs^2/m^6$). The measured values of velocity and temperature become relatively more scattered as the angle between the centre axis of the inlet and streamline increases where the flow is influenced by the sidewalls. The use of equations (2),(3) and (4) is therefore restricted to the area outside the initial zone where the profiles are not yet developed, and outside the zones near to the walls where deceleration occurs.

EFFECTS OF STRATIFICATION

As mentioned earlier buoyancy forces are important to the overall flow pattern. The stratification effects generate an interface between the layer of supplied cool air close to the floor and the surrounding room air. The flow development in the dense current along the floor is strongly influenced by the interfacial mixing. On microscale the entrainment rate of light air into the dense layer is closely connected to the interfacial turbulence and on macroscale it is highly dependent on density and velocity profiles. The density difference at the interface tends to counteract the diffusion at the interface while the velocity gradient tends to increase it.
Sandberg et al. 1991 elaborate the subject and suggest that the flow field in front of the inlet device should be considered as divided into a sub- and supercritical flow domain. The concept of a sub- and supercritical domain has its origin in the field of hydraulics where the transition between the two domains is defined by the densimetric Froude number, F_Δ, but here it is more convenient to use a local Arkimedes number, Ar.

$$Ar = \frac{1}{\sqrt{F_\Delta}} = \frac{g\beta\Delta Tl}{U^2} \qquad (5)$$

$Ar < 1 \Rightarrow$ *supercrit.*
$Ar > 1 \Rightarrow$ *subcrit.*

In this case a local Archimedes number Ar_l is used.

$$Ar_l = \frac{g\beta\Delta T_{max} l}{U_{max}^2} \qquad (6)$$

It is possible to calculate entrainment rates for the flow as the increment of volume flow through sections of the cool air layer. Provided that the flow from the inlet device

can be regarded as being fully radial and that the air is entrained through the face, A_e, an entrainment velocity can be estimated as shown in fig.4.

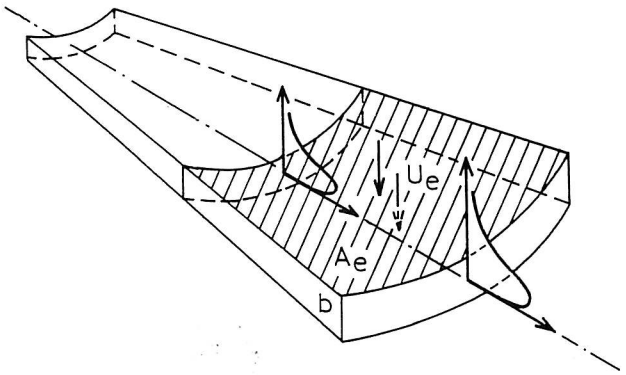

Fig.4 Entrainment velocity in radial flow from inlet device.

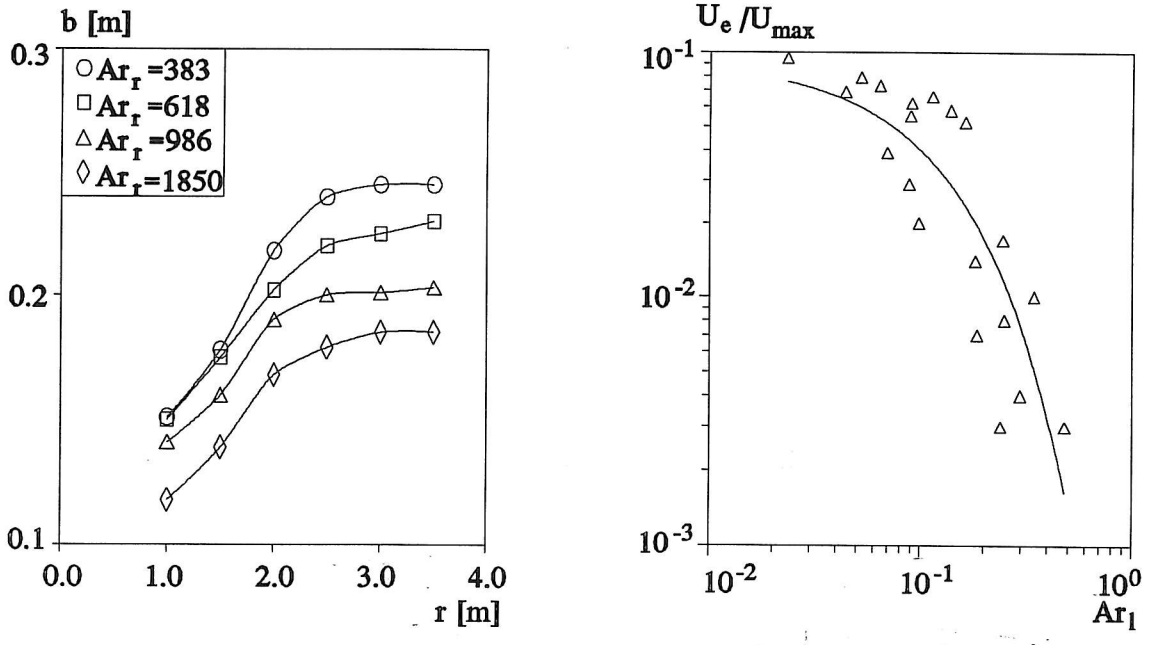

Fig.5 Growth of cool layer thickness with distance from inlet device and decay of entrainment velocities with local Archimedes number.

In the zone close to the inlet device the entrainment velocities are of the same order of magnitude as an isothermal jet. As the inlet flow mixes and spreads out the Ar_l increases and the entrainment velocity falls rapidly as it is seen in fig. 5. The entrainment velocity becomes extremely small for $Ar_l > 0.1$ ($r > 2.0$-3.0 m). *Pedersen (1986)* and *Turner (1979)* describe a similar abrupt decrement of entrainment rate as the flow becomes subcritical for dense bottom currents in the field of hydraulics. The measurements seem to support the theory on a two domain approach.
It should be kept in mind that the room geometry might play an important role in the flow development along the floor. Theoretically two flow domains still occur when the room geometry is altered but the location of the transition between flow domains will probably be displaced.

NUMERICAL MODELLING

This section presents the introductory considerations which are made for modelling displacement ventilation and it shows the results achieved up to now.
The reliability of predictions made by a turbulence model depends on the theory itself in terms of a mathematical description, the precision of the computer algorithm and the boundary conditions employed.
For example *Skovgaard and Nielsen 1991* show that provided a proper method for describing especially inlet boundaries is applied the predictions made with the k-ϵ model in case of a isothermal jet in a room agree to a large extent with the experimental reality. Even though the k-ϵ model is less reliable than more advanced models it is widely accepted as applicable in room air simulation.
If acceptable predictions shall be expected by extending the use to the non-isothermal field and in this case displacement ventilated rooms, the measurements suggest that additional properties are to be implemented. It is of crucial importance that *buoyancy forces, stratification effects and heat flux at boundaries* are included. The influence of *radiation* is essential to the temperature distribution in particular. In the process of building a model which complies with these demands the first step is to include buoyancy forces by adding a term to the momentum equation of the vertical velocity component U_2.

$$U_2\frac{\partial U_i}{\partial x_i} = -\frac{1}{\rho}\frac{\partial P}{\partial x_i} + (\nu_l+\nu_t)\left(\frac{\partial^2 U_2}{\partial x_i^2}\right) - g\beta\Delta T \qquad i\in[1..3] \tag{7}$$

P, ρ, β, g, ν_l and ν_t are pressure, density, volumetric expansion factor, gravitational acceleration, laminar and turbulent kinematic viscosity, respectively.
The turbulent quantities are also modified due to buoyancy thus the k- and ϵ equations are extended by a generation term. This extension results in lower turbulent kinetic energy, k, higher dissipation, ϵ, and a reduced turbulent viscosity, ν_t when the flow is stratified.
Equations for U_1, U_3-momentum,continuity,temperature and turbulent quantities can be found in *Chen 1988* or *Davidson 1989.*
At the boundaries the dependent variables and the heat transfer are predicted by means of empirical logarithmic wall functions.
The surface radiation in the room causes a net heat flux to take place from the warmer upper part of the room to the colder lower part. The vertical temperature gradients are approximately linear except close to the floor and close to the ceiling. An advanced radiation model e.g. a discret transfer model, can be used but in this case a simple approach based on experimental results is applied. A linear vertical temperature variation is prescribed at the walls :

$$T(y) = \frac{y}{H}(T_e - T_f) + T_f \tag{8}$$

where T_e is the exhaust temperature and $T_f = 0.55(T_i + T_e)$ is the floor temperature.

When a simple inlet profile is applied it it possible to obtain a solution for the flow domain which has the characteristic velocity decay in a region in front of the inlet device, and a radial spreading.

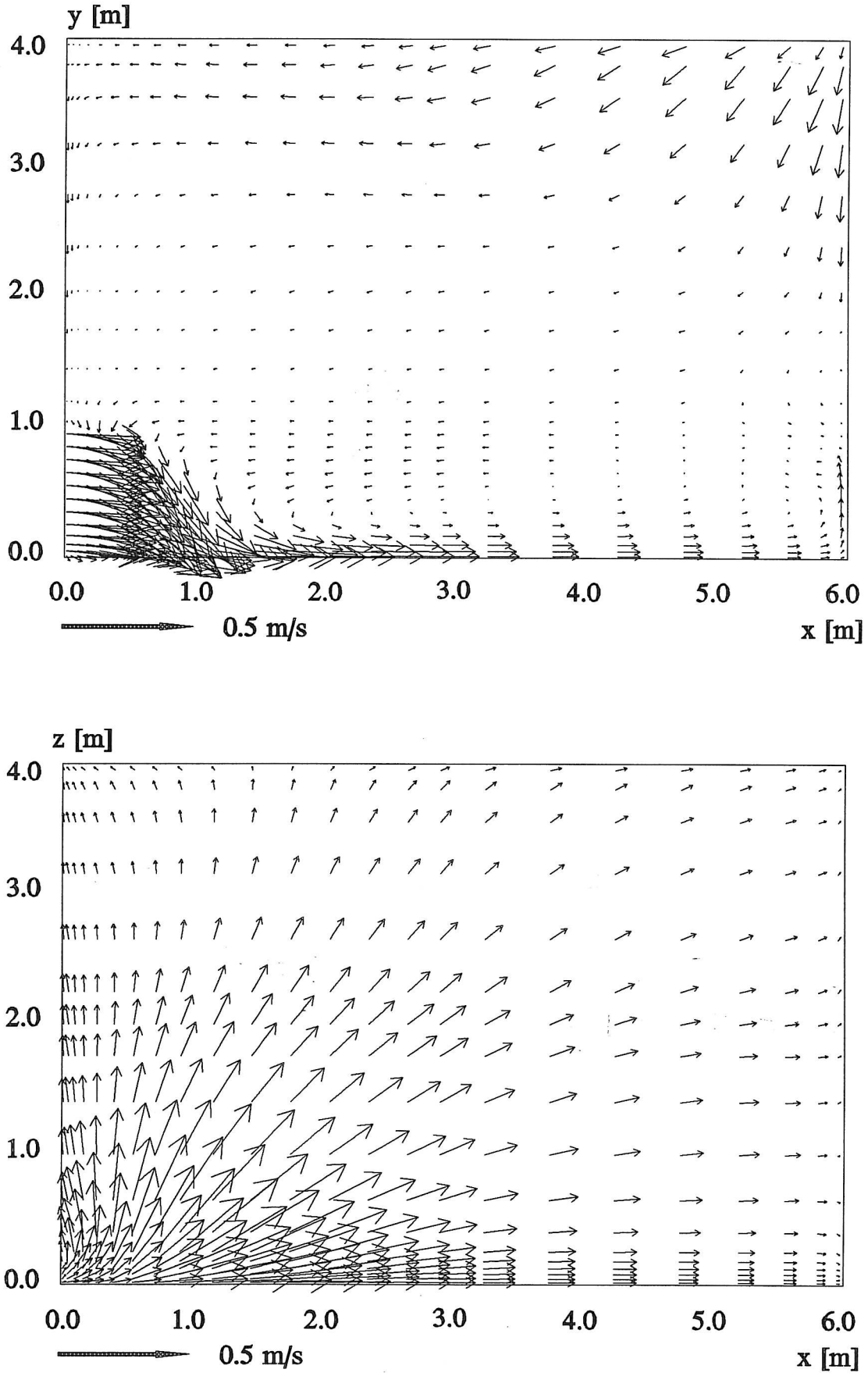

Fig. 5 Velocity vectors in an xy-plane (z=0.0 m) and in an xz-plane (y=0.03 m).

A realistic flow pattern is predicted but the heat flux at the surfaces described by logarithmic wall law and eq.8 results in a net heat removal from the room. The Ar_r-numbers in the measurements are larger than the Ar_r-numbers obtained in the numerical simulation and this causes a reduction in the predicted initial acceleration and consequently too low maximum velocities along the floor.
To avoid this discrepancy it is necessary to improve the calculation of heat flux at the walls and to obtain qualified estimates of the internal heat exchange by radiation. Furthermore it is probably required to apply a more advanced inlet boundary condition. This will be the scope of future development of the model.

CONCLUSION

This paper deals with aspects of the air flow in rooms with displacement ventilation with reference to detailed full-scale measurements. The results show that it is possible to describe the decay of maximum velocities along the floor by relatively few parameters, and that theories concerning the vertical temperature and velocity profiles for turbulent jets can be applied in displacement ventilation as well. While the similarity of profiles is obvious for the measured velocities it can be regarded as an acceptable approximation in case of temperature profiles.
Even though the measured velocity and temperature profiles show resemblance to isothermal wall jet profiles the flow is clearly stratified. This is illustrated by the variation of entrainment velocities which indicates that the flow in front of the inlet device can be divided into two different flow regimes.
The application of numerical modelling for displacement ventilation seems promising with respect to simulating the fundamental characteristics. A further refinement of the CFD method in terms of improved handling of heat flux at walls, radiation and inlet boundary conditions can contribute to the introduction of numerical modelling of displacement ventilation in the design phase.

REFERENCES

Chen, Q.
Indoor Airflow, Air Quality and Energy Consumption of Buildings, Ph.D thesis, Technicsche Universiteit Delft, Delft 1988.

Davidson, L.
Numerical Simulation of Turbulent Flow in Ventilated Rooms, Ph.D.-thesis, Chalmers University of Technology, Göteborg 1989.

Mathisen, H.M.
Displacement Ventilation - the Influence of the characteristics of the Supply Air Terminal Device on the Airflow Pattern, Indoor Air, Danish Technical Press,Copenhagen 1990.

Nielsen, P.V.
Air Velocity at the Floor in a Room with Wall Mounted Air Terminal Device and Displacement Ventilation (in danish), Nordic Ventilation Group, Oslo 1990.

Pedersen, F.B.
Environmental Hydraulics - Stratified Flows, Lecture Notes on Coastal and Estaurine Studies, Springer Verlag 1986.

Sandberg, M., Mattson, M.
The Mechanism of Spread of Negatively Buoyant Air from Low Velocity Air Terminals, Application of Fluid Mechanichs in Environment Protection 91, Wisla 1991.

Skovgaard, M., Nielsen, P.V.
Modelling Complex Inlet Geometries in CFD - Applied to Air Flow in Ventilated Rooms, Proc. of the 12th AIVC conference, Warwick 1991.

Turner, J.S.
Buoyancy effects in fluids, Cambridge University Press, Cambridge 1979.

Verhoff, A.
The two-dimensional, Turbulent Wall Jet with and without an External Free Stream, Report no. 626, Princeton University 1963.

Appendix E

Stratified Flow in a Room with Displacement Ventilation
and Wall-Mounted Air Terminal Devices

Peter V. Nielsen

Stratified Flow in a Room with Displacement Ventilation and Wall-Mounted Air Terminal Devices

Peter V. Nielsen
Aalborg University

Abstract

The paper describes experiments with wall-mounted air terminal devices. The stratified flow in the room is analysed and the influence of stratification and the influence of room dimensions on the velocity level and on the length scale are proved. The paper shows that the velocity level in the occupied zone can be described by a single equation based partly on stratified flow theory and partly on measurements.

A radial stratified flow will be obtained if the room is ventilated by a single diffuser, or if the diffusers are placed in large distance to each other.

A two-dimensional stratified flow will be obtained if the room is ventilated by a number of diffusers placed close to each other on one sidewall. The velocity will have a slight tendency to be constant in an area along the floor.

Introduction

For many years ventilation systems with vertical displacement flow have been used in industrial areas with high thermal loads. Quite recently the vertical displacement flow systems have grown popular as comfort ventilation in rooms with thermal loads, e. g. offices.

The air is supplied direct into the occupied zone at low velocity from wall-mounted diffusers. The plumes from hot surfaces, from equipment and from persons entrain air into the occupied zone and create a natural convection flow upwards in the room, see figure 1.

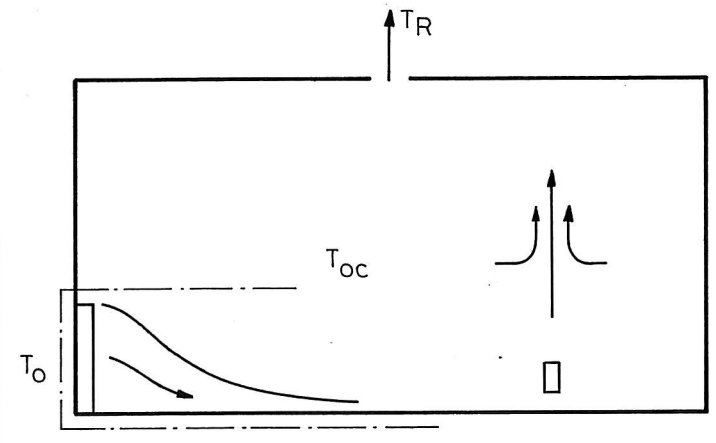

Figure 1. Room with low-level diffuser, heat source and displacement flow.

The displacement flow systems have two advantages compared with traditional mixing systems.

- An efficient use of energy. It is possible to remove exhaust air from the room where the temperature is several degrees above the temperature in the occupied zone which allows a higher air inlet temperature at the same load.

- An appropriate distribution of contaminated air. The vertical temperature gradient (or stratification) implies that fresh air and contaminated air are separated and the most contaminated air can be found above the occupied zone.

It is important to examine the flow in front of an air terminal device and to investigate if this flow can be treated unconnected with parameters as room geometry (generally speaking), heat source location and location of exhaust opening, etc., as indicated in figure 1. The design procedure is simplified if the flow only depends on some main parameters as e.g. type of diffuser, obstacles on the floor, flow rate and Archimedes' number of the flow.

The theories of both wall jet flow and stratified flow are used for a discussion of the measurements shown in this paper. The discussion will be divided into two cases according to geometry and the number of diffusers. The first case will be a radial flow from a single diffuser in situations where the air movement is not influenced by the sidewalls. The second case will be a flow from a number of diffusers placed close to each other on the end wall. The flow will merge into a two-dimensional flow with a velocity characteristic different from the situation in radial flow.

The radial flow is characterized as a flow close to the floor which has an virtual origin at the diffuser, and the two-dimensional flow is characterized as a plane flow at the floor parallel to the sidewalls of the room.

Isothermal wall jets and stratified flow theory

This chapter will discuss two different models which may have some relevance to the actual flow in the vicinity of the floor.

The wall jet description is relevant to mixing ventilation, see Nielsen (1991), and it may also be relevant to the flow in rooms with displacement ventilation in cases where the temperature differences are very small because it shows the type of flow which may be approached when the heat load goes to zero.

Stratified flow is the type of flow which is generally relevant to displacement ventilation. The theory behind stratified flow has been used in hydraulic models as for example models of water with density difference discharged into a pond, and it has also been used to describe processes in the atmosphere as the Föhn winds.

Recently stratified flow theory has been used in room air motion by for example Lane-Serff et al. (1987), Sandberg and Holmberg (1990), Sandberg and Mattsson (1991) and Nielsen (1992).

Wall jet model

The flow from a low velocity diffuser may contain some elements of wall jet flow in situations where the temperature difference is very small. The height of the diffuser h will often be fairly large compared with other dimensions in the room, meaning that an initial flow region may cover a large part of the room.

The initial region of the flow in front of the diffuser may be described as a "constant velocity core". The velocity in the core is obtained at the distance where all the small jets from the openings in the surface of the diffuser have merged into a coherent flow. Figure 2 shows how a shear layer between this flow and the surrounding air volume reduces the constant velocity core at increasing distance. The maximum velocity in the initial region is constant when the flow is two-dimensional or three-dimensional, while the velocity is inversely proportional to the distance x when the flow from the diffuser is radial.

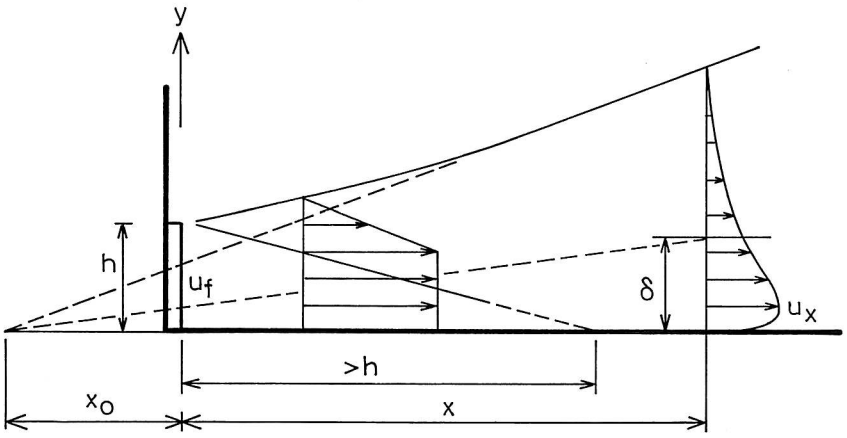

Figure 2. Idealized wall jet flow from an opening. The figure shows the initial flow region close to the opening and a fully developed flow in the right side of the figure. $T_{oc} - T_o \sim 0.0$.

Two-dimensional or three-dimensional flow gives the relation

$$u_x \sim const \tag{1}$$

and radial flow gives the following relation

$$u_x \sim \frac{1}{x} \tag{2}$$

Two-dimensional flow will only take place when the opening covers the whole width of the room or when a number of openings are located very close to each other. Three-dimensional flow takes place when the velocity is perpendicular to the surface at the supply opening. Even a small temperature difference will change a three-dimensional wall jet into a radial stratified flow because the buoyancy effect will accelerate the flow towards the floor and therefore introduce a spreading of the flow field.

Radial flow at the diffuser is very common and it is generated by blades in the diffuser in such a way that the velocity will obtain a radial distribution at the surface.

A wall jet flow will develop into a self-preserving flow further downstream, see for example Rajaratnam (1976). The normalized velocity profile u/u_x will be self-semilar and given as a function of y/δ. u_x is the maximum velocity in distance x, and δ is the y-direction height to a velocity which is half of the maximum velocity, $u_x/2$, see figure 2.

The velocity distribution in the vicinity of the floor may be described by the decay of the maximum velocity u_x as a function of the distance x. The velocity decay will be given by the following equation in the case of a three-dimensional wall jet or in the case of a radial wall jet, Rajaratnam (1976)

$$\frac{u_x}{u_f} \sim \frac{h}{x + x_o} \tag{3}$$

and it will be given by expression (4) in the case of a two-dimensional wall jet.

$$\frac{u_x}{u_f} \sim \sqrt{\frac{h}{x + x_o}} \tag{4}$$

h is the height of the diffuser in the case of a radial or a three-dimensional flow, and h is the height of the equivalent face area in the case of two-dimensional boundary conditions and two-dimensional flow. x_o is the distance to a virtual origin for the self-preserving flow as shown on figure 2. This distance may either be positive or negative but it is often a small distance compared with other distances in a room and it is therefore ignored in mixing ventilation.

The face velocity u_f is given as supply flow rate divided by the face area a_f of the diffuser in the case of radial and three-dimensional flow, and it is given as supply flow rate divided by the total face area of all diffusers in the case of two-dimensional flow.

The thickness δ is proportional to the distance $x + x_o$ in all types of wall jet assuming the flow is self-preserving.

$$\delta = D(x + x_o) \tag{5}$$

The growth rate D is a constant for each diffuser and it takes values between 0.06 and 0.10, Rajaratnam (1976).

Stratified flow

Stratified flow theory may describe the flow from wall-mounted low velocity diffusers in cases where the temperature differences are very large.

Flow in water with a density current has the features shown on figure 3. The flow close to the opening entrains water with lower density and the process is similar to the flow in a wall jet. There will be a roller region and a density jump in a certain distance. The entrainment will disappear in the flow further downstream from the density jump, and this is especially characteristic of stratified flow. The location of the density jump is dependent on the height of a weir located downstream in the flow, see Wilkinson and Wood (1971). The density jump moves towards the opening if the weir is increased, resulting in decreasing entrainment into the density current. Further increase of weir height at this stage will cause the jump to flood so that the upstream end of the jump becomes submerged in dense fluid. There is no entrainment into a flooded jump.

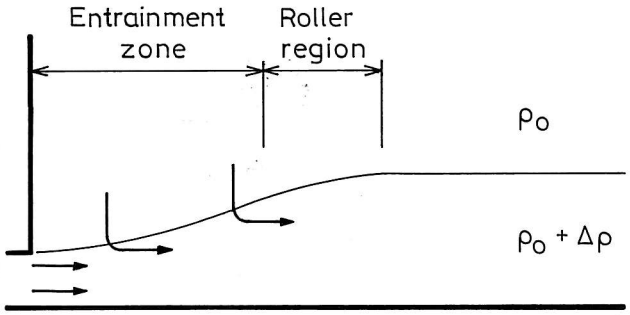

Figure 3. Stratified flow in water with both an entrainment zone and a zone with very little mixing between the two layers.

Stratified surroundings will damp the entrainment in a horizontal flow. The turbulence in the shear layer will decrease because vertical movements in a fluid with a temperature gradient are damped by the buoyancy effect on the movement.

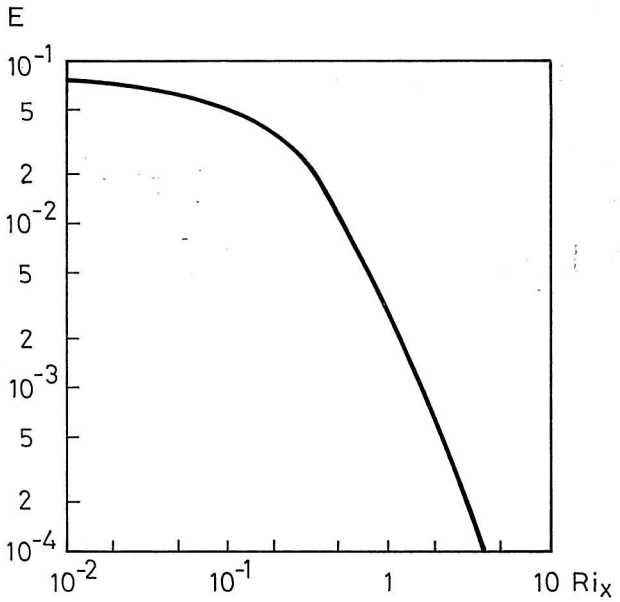

Figure 4. Rate of entrainment into a turbulent stratified flow as a function of overall Richardson' number.

The entrainment, or lack of entrainment, is obviously an important parameter in stratified flow. Turner (1979) has shown that the rate of entrainment E can be given as a function of the overall Richardson number Ri_x as shown on figure 4. The entrainment function assumes that the entrainment into the horizontal flow is proportional to the local velocity U. The Richardson number is defined as

$$Ri_x = \frac{g \cdot \Delta\rho \; l}{\rho \cdot U^2} \tag{6}$$

g is gravitational acceleration and l and U are characteristic length and characteristic velocity, respectively. l and U may correspond to the height of the flow δ and the maximum velocity u_x in the flow at the location x for the overall Richardson number. ρ is the density of the heavy fluid and $\Delta\rho$ is the local density increase. (In a two-layer system the layer with the standard density ρ_o may be regarded as weightless, compared with the layer with density $\rho = \rho_o + \Delta\rho$. The heavy layer will flow as if it is influenced by a reduced gravitational acceleration $g\Delta\rho/\rho$, see Prandtl (1952)).

The most important feature of figure 4 is the rapid fall of E with increasing Ri_x. The flow will act as a wall jet with entrainment if it is initiated with a high velocity and a low Ri_x. The Richardson number will increase downstream in the flow and figure 4 shows that the entrainment will decrease and change the flow to a stratified flow without entrainment. This process is shown on figure 3 where entrainment takes place in the left side of the figure but disappears in the right side after the roller zone. Flow with high entrainment is called supercritical and it moves to a subcritical state with increasing Ri_x as it passes the roller zone.

The velocity distribution in a stratified radial flow with constant thickness, small entrainment and self-similar velocity distribution is given by the following equation, Nielsen (1992)

$$u_x \sim \frac{1}{x} \tag{7}$$

The corresponding velocity distribution in a stratified two-dimensional flow is given by

$$u_x \sim const \tag{8}$$

The self-similar profiles measured in stratified flow in a room are often identical to the universal wall jet profile and this paper will therefore define the length scale δ as the height to the velocity $u_x/2$.

Profiles measured in hydraulics may also have a form different from a wall jet profile. Measurements by Lofquist (1960) show a profile with a high location of the maximum velocity. The high density $\rho_o + \Delta\rho$ is constant in the whole flow except a very thin layer with a gradient up to the ρ_o-layer. The density gradient in the flow is caused by different salt concentrations, and the problem cannot be compared with stratified flow in rooms where

radiant heating of the floor plays an important role. Velocity profiles shown in the measurements of Wilkinson and Wood (1971) look more like a universal profile in a wall jet.

It is possible to show that the rate of entrainment E is proportional to the growth rate D or

$$\frac{d\delta}{dx} \sim E \tag{9}$$

The radial flow is described by equation (3) in the supercritical stage and equation (7) in the subcritical stage. The plane flow is described by equation (4) in the supercritical stage and equation (8) in the subcritical stage as shown by Turner (1979) and Rodi (1982).

Velocity distribution in the radial flow from a wall-mounted diffuser

The primary flow in a room with displacement ventilation expresses the similarity which is typical of fully turbulent flow. Vertical temperature gradients, velocity level in stratified flow at the floor, stratification level and ventilation effectiveness can all be described by an Archimedes number independent of the velocity level in the room as shown by Nielsen (1988). The Archimedes number is defined as

$$Ar = \frac{\beta g h (T_{oc} - T_o)}{u_f^2} \tag{10}$$

where β, g and $(T_{oc} - T_o)$ are volume expansion coefficient, gravitational acceleration and temperature difference between the temperature in the height 1.1 m and the supply temperature, respectively.

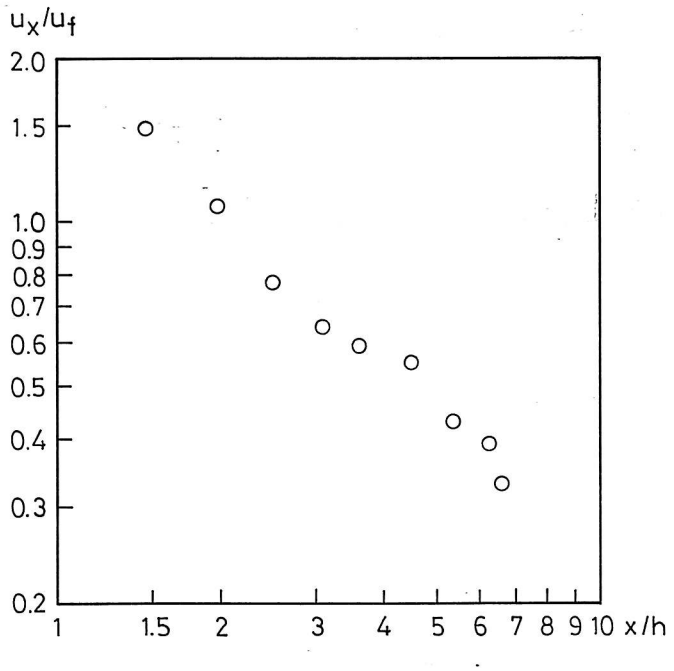

Figure 5. Maximum velocity close to the floor versus distance from the diffuser. Diffuser type G. Ar = 7.4 and q_o = 0.028 m^3/s.

The flow from a wall-mounted diffuser is shown on figure 5. The velocity ratio u_x/u_f is given as a function of the dimensionless distance x/h. The cold air from the supply opening has a high initial acceleration due to gravity, and a relative velocity of 1.49 will be obtained in some distance from the diffuser. (u_x is the maximum velocity in the flow and it is located close to the floor (1 - 4 cm)).

Figure 5 indicates that the maximum velocity in the symmetry plane is proportional to $1/x^{\alpha}$ where the exponent α is close to 1.0 as pointed out by Nielsen et al. (1988). This type of velocity decay is typical of radial stratified flow (equation (7)).

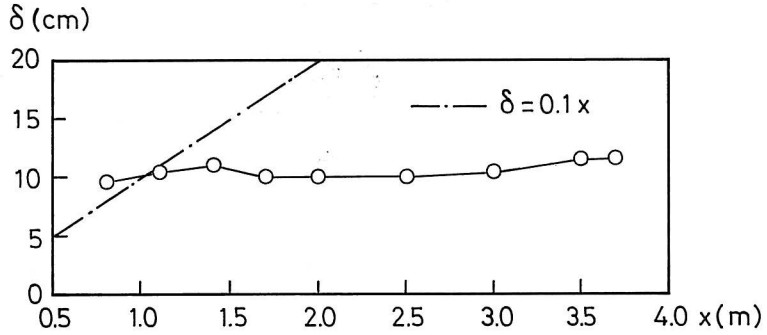

Figure 6. Length scale δ in the flow versus distance from the diffuser. Diffuser type G. $Ar \sim 5$.

The length scale or the thickness δ is rather constant and independent of the distance from the diffuser at an Archimedes number of 5, as shown on figure 6, and this is a strong indication of stratified flow. The dotted line on the figure indicates a progress which could be expected in a wall jet (equation (5)).

It can be seen that the height of the flow region is much smaller than the height of the diffuser ($h = 0.56$ m) even very close to the diffuser. This shows that the cold air from the diffuser will reach the floor very close to the opening and at least within half a metre from the diffuser.

The maximum velocity u_x in different distances x from the opening can be given by the following equation, Nielsen (1992).

$$\frac{u_x}{u_f} = K_{dr} \frac{h}{x} \tag{11}$$

h is the height of the diffuser and u_f is the face velocity defined as flow rate q_o divided by the face area a_f of the diffuser. K_{dr} is a function of the Archimedes number as well as an individual function for different types of air terminal devices. Both x and u_x are measured in the centre plane of the room.

The equation is valid for very small as well as large Archimedes' numbers. The velocity will in both cases be proportional to $1/x$ (see equations (2), (3) and (7)), and the equation will therefore be able to predict the velocity u_x when the K_{dr}-value is adjusted to the situation.

The variables in equation (11) are easy to measure for a given diffuser and the equation is therefore simple to use in a practical design procedure.

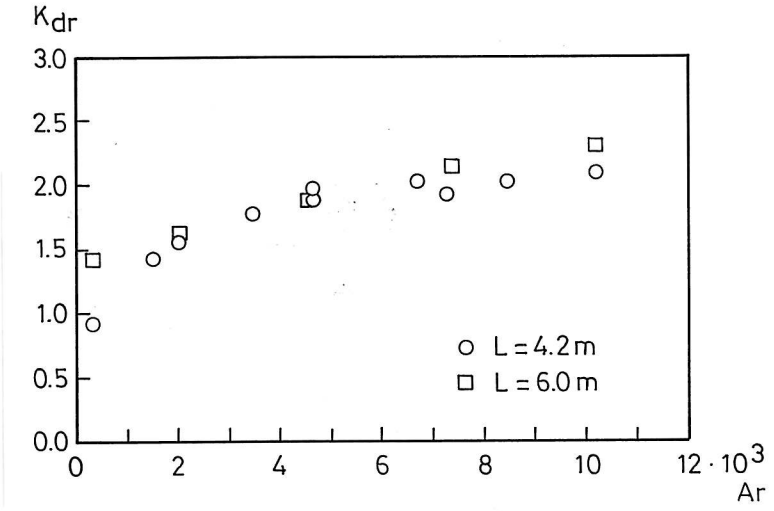

Figure 7. K_{dr} measured in the middle plane versus Archimedes' number for a wall-mounted air terminal device (type G).

Figure 7 shows that K_{dr} increases with increasing Archimedes' number for the given diffuser (type G). This is due to the fact that gravity will accelerate the vertical flow close to the opening and generate a stratified air movement in a relatively thin layer along the floor. Increased Arhcimedes' number will decrease δ and increase the maximum velocity in the layer.

It is known from stratified flow in hydraulics that obstacles located downstream may influence the length scale δ of the flow, see Wilkinson and Wood (1971). The measurements on figure 7 show that K_{dr} is independent of the room length and the corresponding room width within the variation indicated on the figure. Practical experience does also indicate that room dimensions are of minor importance, Nielsen (1992).

The entrainment process in the stratified flow will now be discussed in more details. A local Archimedes number is defined by the expression

$$Ar_x = \frac{\beta g \delta \Delta T_x}{u_x^2} \tag{12}$$

where δ, u_x and $\Delta T_x = (T_{oc} - T_x)$ all are local reference values. T_x is the minimum temperature in the flow and it is located close to maximum velocity u_x. It is assumed that the

following expression can be used for an estimate of ΔT_x in case of high entrainment.

$$\frac{T_{oc} - T_x}{T_{oc} - T_o} \sim \frac{u_x}{u_f} \tag{13}$$

The length scale δ will be proportional to x in the supercritical stage and ΔT_x will be proportional to $1/x$ (equation (11) and (13)). u_x^2 is proportional to $1/x^2$. The total effect is that Ar_x is proportional to x^2 in the supercritical stage and it will therefore increase with the distance x. It is also possible that the local Archimedes number will increase with the distance x in the subcritical stage due to decreasing velocity.

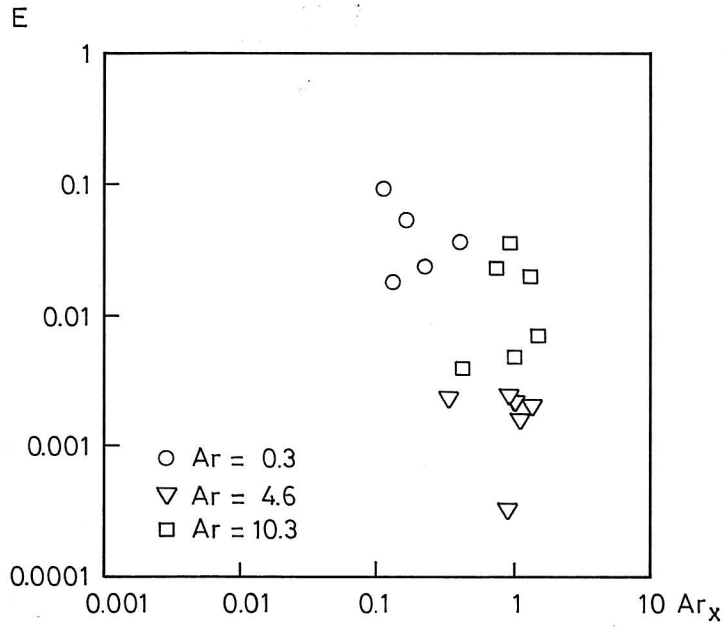

Figure 8. Rate of entrainment versus the local Archimedes number Ar_x for the diffuser type G.

The rate of entrainment E is measured at different positions in the flow, and figure 8 shows a variation which is similar to the result indicated on figure 4. The stratified flow moves from a supercritical stage to a subcritical stage with an abrupt decrement of the entrainment rate. A similar variation of the entrainment function has also been shown by Jacobsen and Nielsen (1992).

The theory has been discussed by Sandberg and Mattsson (1991) and they suggest that the flow field in front of the diffuser should be divided into a super- and a subcritical flow domain.

Velocity distribution in plane flow from wall-mounted diffusers

The flow from a number of diffusers placed close to each other on the wall will merge to a two-dimensional stratified flow in the downstream direction. The same effect will take place when the room is large in the x-direction compared with the width.

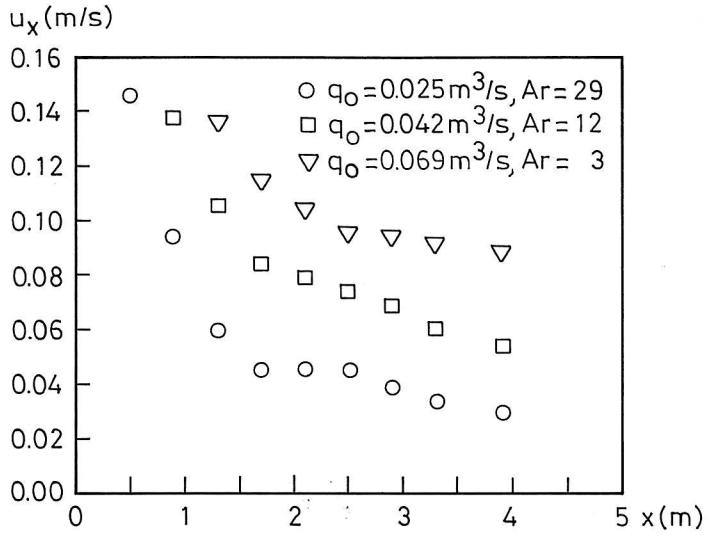

Figure 9. Maximum velocity u_x versus distance x from the end wall at three different flow rates and three different Archimedes' numbers. Plane flow.

Figure 9 shows some measurements of the flow. There is a high velocity decay for $x < 1.5$ m and this is mainly due to a radial flow from the diffusers. The flow will merge into a two-dimensional air movement for $x > 1.5$ m but there will still be some velocity decay. The velocity level seems to be strongly dependent on the flow rate.

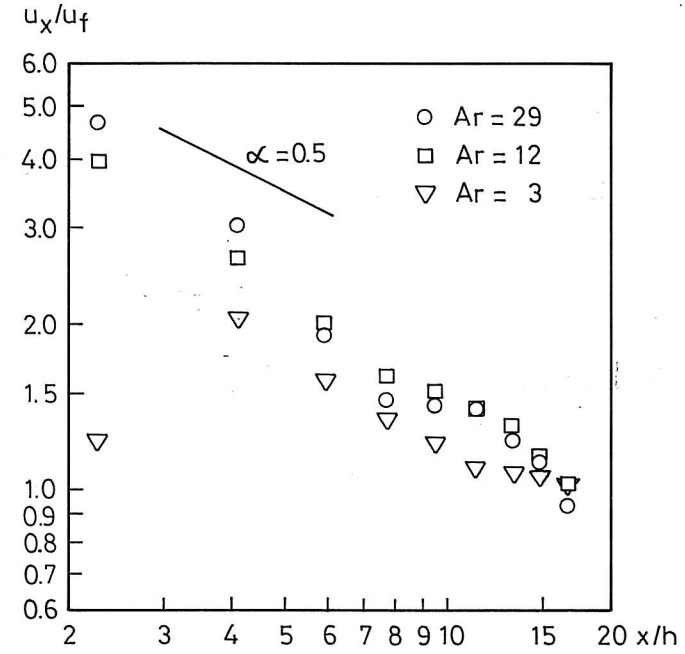

Figure 10. Relative velocity u_x/u_f versus relative x/h for three different Archimedes' numbers. Plane flow.

The relative velocity level u_x/u_f is shown on figure 10 for the same set of measurements as shown on figure 9. It is possible to see that the velocity level is slightly influenced by the

Archimedes number with an increase of the velocity level at increasing Archimedes' number. The velocity u_x is proportional to the face velocity u_f or the flow rate q_o at a given distance x. The measurements are made in a room with three diffusers of the type E distributed over a width of 3.6 m. q_o is the total flow rate to the room and h is the equivalent height of a two-dimensional diffuser covering the whole width of the room. The Archimedes number in this chapter is consequently based on this definition.

It is indicated on the figure that the velocity decay is proportional to $1/x^{0.5}$ in certain areas. This is also the velocity decay which should be expected in a flow of the wall jet type (equation (4)), but it might also be the transition from radial flow to stratified plane flow. It is possible to observe some areas with a constant velocity level which is typical of a stratified plane flow, see equation (8).

The plane stratified flow may be described by the equation

$$\frac{u_x}{u_f} = K_{d\rho} \tag{14}$$

where K_{dp} is equal to 1.1 for $Ar = 3$ and equal to 1.4 for $Ar = 29$. K_{dp} is a function of the diffusers and the geometry around the diffusers as well as the Archimedes number. Equation (14) can only describe the flow in a narrow range of distances as shown by the measurement on figure 10.

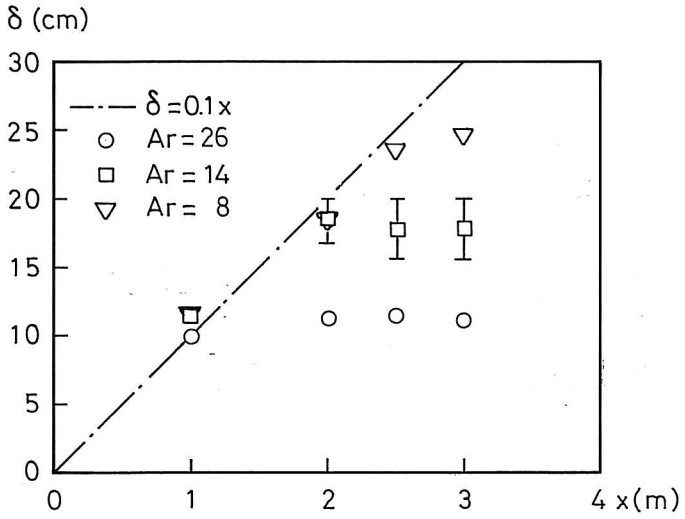

Figure 11. Length scale variation in plane flow at three different Archimedes' numbers.

The plane flow can be further analysed from measurements of the length scale δ. Figure 11 shows that the length scale has an initial increase which is rather similar to the growth of a wall jet which is the type of flow that can be found in the supercritical stage. The flow will change from increasing δ to constant δ downstream in the air movement at all three Archimedes' numbers and this is very typical of a stratified flow.

It has not been possible to make a prediction of the entrainment function E but equation (9) shows that constant length scale δ is equivalent to zero entrainment.

Figure 11 shows that increasing Archimedes' number will give a decreasing thickness δ. This effect may explain the increase in relative velocity u_x/u_f in case of a large Archimedes number as discussed in connection with figure 10.

The heat load per diffuser is reduced when more diffusers are used in a room. It is therefore possible to reduce the velocity level close to the diffusers when more diffusers are used, and it is possible to obtain a two-dimensional flow with a velocity in the main part of the occupied zone which is lower than the velocity close to a single diffuser giving a radial flow.

Conclusion

Isothermal wall jets and stratified flow theory is discussed generally.

It is shown that the velocity level in the occupied zone can be described by a single equation based on stratified flow theory and measurements.

A two-dimensional stratified flow will be obtained if the room is ventilated by a number of diffusers placed close to each other on a single wall. The velocity level in a room with two-dimensional flow may be lower than the velocity in the vicinity of a single diffuser at a given heat load.

It is necessary to make more measurements in two-dimensional flow to obtain a complete description of the general air movement, but it is shown that the velocity will be constant in an area in front of the diffusers in case of stratified flow.

References

Nielsen, P.V. 1991. Models for the Prediction of Room Air Distribution, 12th AIVC conference, Ottawa, Canada, ISBN 0 946075 53 0.

Lane-Serff, G.F., P.F. Linden and J.E. Simpson.1987. Transient Flow through Doorways Produced by Temperature Difference, ROOMVENT '87, International Conference on Air Distribution in Ventilated Spaces, Stockholm.

Sandberg, M. and S. Holmberg. 1990. Spread of Supply Air from Low-Velocity Air Terminals, ROOMVENT '90, Oslo.

Sandberg, M., and M. Mattsson. 1991. The Mechanism of Spread of Negatively Buoyant Air from Low Velocity Air Terminals, "Application of Fluid Mechanics in Environment Protection 91", Gliwice.

Rajaratnam, N. 1976. Turbulent Jets, Elsevier, Amsterdam.

Wilkinson, D.L., and I.R. Wood. 1971. A Rapidly Varied Flow Phenomenon in a Two-Layer Flow, J. Fluid Mech., Vol. 47, part 2, pp. 241-256.

Turner, J.S. 1979. Buoyancy Effects in Fluids, Cambridge University Press, Cambridge.

Prandtl, L. 1952. Essentials of Fluid Dynamics, Blackie, London.

Nielsen, P.V.. 1992. Velocity Distribution in the Flow from a Wall-Mounted Diffuser in Rooms with Displacement Ventilation, Proc. of the Third International Conference on Air Distribution in Rooms, ROOMVENT '92, ISBN 87-982652-6-1, Copenhagen.

Lofquist, K. 1960, Flow and Stress near an Interface between Stratified Liquids, Physics of Fluids, Vol. 3.

Rodi, W. 1982. Turbulent Buoyant Jets and Plumes, HMT: The Science and Applications of Heat and Mass Transfer, Pergamon Press.

Nielsen, P.V. 1988. Displacement Ventilation in a Room with Low-Level Diffusers, DKV-Tagungsbericht, ISBN 3-922-429-63-7, Deutscher Kälte- und Klimatechnischer Verein e.V., Stuttgart.

Nielsen, P.V., L. Hoff and L.G. Pedersen. 1988. Displacement Ventilation by Different Types of Diffusers, Proc. of the 9th AIVC Conference, ISBN 0 946075 40 9, AIVC, Warwick.

Jacobsen, T.V. and P.V. Nielsen, 1992. Velocity and Temperature Distribution in Flow from an Inlet Device in Rooms with Displacement Ventilation, Proc. of ROOMVENT '92, Third International Conferenc on Air Distribution in Rooms, DANVAK, Copenhagen.